

**AN ASSESSMENT OF SOME POSSIBLE
NEUROLOGICAL APPLICATIONS OF ELECTRICAL
IMPEDANCE TOMOGRAPHY.**

A thesis submitted for the degree of

Doctor of Philosophy

in the University of London

by

DAVID SIMON HOLDER,

Department of Physiology,

University College London.

March 1991

ProQuest Number: 10609846

All rights reserved

INFORMATION TO ALL USERS

The quality of this reproduction is dependent upon the quality of the copy submitted.

In the unlikely event that the author did not send a complete manuscript and there are missing pages, these will be noted. Also, if material had to be removed, a note will indicate the deletion.



ProQuest 10609846

Published by ProQuest LLC (2017). Copyright of the Dissertation is held by the Author.

All rights reserved.

This work is protected against unauthorized copying under Title 17, United States Code
Microform Edition © ProQuest LLC.

ProQuest LLC.
789 East Eisenhower Parkway
P.O. Box 1346
Ann Arbor, MI 48106 – 1346

ABSTRACT

Electrical impedance tomography (EIT) is a recently developed technique which produces reconstructed images of the internal distribution of the impedance of an object from measurement with external electrodes. It was assessed for its possible application in imaging intra-cranial disorders non-invasively with the use of scalp electrodes.

Cerebral impedance increases of 12-55% were measured by a four electrode method at 50 kHz during global cerebral ischaemia or cortical spreading depression (CSD) in anaesthetized rats. Measured with scalp electrodes in two pairs 2 - 26 mm apart, impedance increased by 1.8-5.9% during global cerebral ischaemia for 5 or 15 min ; the changes correlated in duration with cortical impedance changes, but increased more gradually. Increases of about 2% still were observed when the effects of variations in temperature and local scalp impedance were excluded. A finite element model was used to predict the attenuation of a signal due to cerebral anoxic depolarization by the extracerebral layers. These residual impedance changes were compatible with this, but their cause by other mechanisms related to the method of production of cerebral ischaemia could not be ruled out. An unexpected decrease of 0.8% was observed during CSD with electrodes 0.5mm apart on the scalp. This became undetectable when scalp temperature was kept constant. The model predicted that impedance changes of about 1% could be measured during CSD with scalp electrodes spaced further apart.

Images were then collected using a prototype EIT system operating at 51 kHz during the same model of cerebral ischaemia. Test objects in a medium of constant resistivity could be accurately localized, but spatial resolution of intracranial impedance changes was substantially degraded when recorded with scalp electrodes. EIT has the potential for imaging various cerebral physiological or pathological changes, but improvements to the reconstruction algorithm are needed if regional intracerebral changes are to be discriminated during recording with scalp electrodes.

ACKNOWLEDGMENTS.

I am most grateful to Dr. A.R. Gardner-Medwin for the use of the facilities in his laboratory, and for many hours of penetrating discussion. Professor B. Brown of the Department of Medical Physics, Royal Hallamshire Hospital, Sheffield, very kindly loaned both the single channel impedance measuring device and the EIT system and has encouraged this work over several years. Dr. S. Arridge and Dr. D. Delpy of the Department of Medical Physics generously gave their time to discussion of quantitative issues. I am very grateful to Professor T.J. Biscoe, whose support led to the initiation of this work at U.C.L., and who has encouraged it ever since.

Mr. N. Todd gave invaluable advice as a result of his own experience with the four vessel model of cerebral ischaemia. Professor J.B. Davies of the Department of Electrical Engineering kindly advised on aspects of the finite element model.

I should also like to thank my wife, Amanda, for her patience, understanding and support, and my mother for her encouragement over many years.

This work was supported by a Medical Research Council Training Fellowship and a Royal Society University Research Fellowship.

TABLE OF CONTENTS

1. INTRODUCTION.		9
1.1. REASONS FOR INTEREST IN IMPEDANCE IMAGING, YET ANOTHER IMAGING MODALITY.		9
1.2. ELECTRICAL IMPEDANCE TOMOGRAPHY		12
1.3. BACKGROUND : IMPEDANCE MEASUREMENTS IN THE BRAIN DURING ANOXIC DEPOLARIZATION		20
1.4. RATIONALE FOR THE EXPERIMENTS IN THIS WORK		33
1.5. SOME PRACTICAL DETAILS REGARDING THE EXPERIMENTS.		39
2. METHODS		40
2.1. IMPEDANCE CHANGES DURING CEREBRAL ISCHAEMIA IN THE ANAESTHETIZED RAT		40
2.2. IMPEDANCE CHANGES DURING SPREADING DEPRESSION IN THE ANAESTHETIZED RAT		50
2.3. MEASUREMENT OF SINGLE CHANNEL IMPEDANCE AT 50 kHz		55
2.4. IMPEDANCE IMAGING OF CEREBRAL ISCHAEMIA IN THE ANAESTHETIZED RAT		59
3. RESULTS		66
3.1. IMPEDANCE CHANGES DURING CEREBRAL ISCHAEMIA IN THE ANAESTHETIZED RAT		66
3.2. IMPEDANCE CHANGES DURING SPREADING DEPRESSION IN THE ANAESTHETIZED RAT		83
3.3. IMPEDANCE IMAGING DURING CEREBRAL ISCHAEMIA IN THE ANAESTHETIZED RAT		95
4. DISCUSSION (1) : SIMPLE MATHEMATICAL MODELS OF SOME OF THE EXPERIMENTAL SITUATIONS DESCRIBED ABOVE		113
4.1. INTRODUCTION		113
4.2. MODEL TO ESTIMATE THE DEPTH OF THE CORTICAL IMPEDANCE CHANGE DURING SPREADING DEPRESSION		113
4.3. FINITE ELEMENT MODEL OF IMPEDANCE CHANGES MEASURED IN THE SCALP DURING CEREBRAL ISCHAEMIA OR SPREADING DEPRESSION		116

5. DISCUSSION (2) : INTERPRETATION OF RESULTS	127
5.1. IMPEDANCE CHANGES DURING CEREBRAL ISCHAEMIA	127
5.2. IMPEDANCE CHANGES DURING SPREADING DEPRESSION	150
5.3. EIT IMAGES TAKEN DURING CEREBRAL ISCHAEMIA	157
5.4. POSSIBLE APPLICATIONS OF EIT IN NEUROSCIENCE	169
5.5. CONCLUSIONS	173
REFERENCES	176
GLOSSARY OF ABBREVIATIONS	188

LIST OF FIGURES

Figure 1.1. The Sheffield EIT system reconstruction algorithm	13
Figure 2.1. Clasp used to occlude the common or internal carotid arteries	42
Figure 2.2. Experimental arrangement for measuring impedance	44
Figure 2.3. Positions of electrodes on the rat's head	46
Figure 2.4. Diagram of the impedance measuring device	54
Figure 2.5. Calibration curve for impedance measuring device	56
Figure 2.6. Block diagram of EIT data collection system	62
Figure 2.7. Physical dimensions of the Sheffield EIT system	62
Figure 3.1. Rat survival and blood pressure with different anaesthetic regimes	67
Figure 3.2. Summary of impedance changes during cerebral ischaemia	71
Figure 3.3. Examples of impedance and temperature changes measured on the cortex or in the scalp during episodes of carotid occlusion of varying duration	72
Figure 3.4. Comparison of the duration (FWHM) of impedance changes during cerebral ischaemia	74
Figure 3.5. Example of the variation of scalp impedance with temperature	76
Figure 3.6. Impedance and temperature changes during cerebral ischaemia when scalp temperature was controlled artificially	77
Figure 3.7. Illustration of the correspondence of the time course of scalp and cortical impedance changes	79
Figure 3.8. Example of impedance change in surgically isolated scalp during cerebral ischaemia	80
Figure 3.9. Examples of impedance changes during cerebral ischaemia in surgically and electrically isolated scalp	81
Figure 3.10. Typical examples of cortical impedance and D.C. potential changes during spreading depression	82
Figure 3.11. Baseline impedance changes observed under resting conditions	84
Figure 3.12. Impedance measured with scalp electrodes, averaged with respect to the ECG or respiratory cycle	86
Figure 3.13. Scalp impedance changes during spreading depression initiated on the ipsilateral or contralateral side of the head	88
Figure 3.14. Comparison of scalp impedance changes <i>ante-</i> and 10 <i>min post-mortem</i>	89
Figure 3.15. Propagation of the scalp impedance change during spreading depression	90
Figure 3.16. Effect of external warming on changes in scalp impedance	92
Figure 3.17. Impedance measurements during spreading depression with R2 earthed to provide data for modelling of the impedance	

change	93
Figure 3.18. Calibration curve for EIT system	96
Figure 3.19. Sensitivity of EIT measured with scalp electrodes to replacement of cranial contents by air	98
Figure 3.20. EIT images taken during changes in scalp temperature <i>in vivo</i>	99
Figure 3.21. Localization of a polythene rod by EIT	101
Figure 3.22. Discrimination of two polythene rods by EIT	102
Figure 3.23. Imaging of intracranial polythene rods by EIT with scalp electrodes	103
Figure 3.24. Detection of small localised impedance changes by EIT	104
Figure 3.25. Effects of impedance changes out of the plane of the electrode ring on the EIT image	106
Figure 3.26. Averaged EIT measurements in the rat made with either cortical or scalp electrodes during cerebral ischaemia or <i>post-mortem</i>	107
Figure 4.1. Matrices used in finite element models of impedance measurement	115
Figure 4.2. Results of models of impedance measurement during cerebral ischaemia or SD with translational projection	121
Figure 4.3. Results of a model of impedance measurement during cerebral ischaemia with rotational projection	122
Figure 4.4. Predicted impedance changes for different spacings of electrodes on the scalp during cortical spreading depression	124
Figure 5.1. Comparison of the frequency dependence of the peak resistance change during CSD, and the resistances of bone or skin below the <i>stratum corneum</i>	147

LIST OF TABLES

Table 2.1. Two way analysis of variance of the impedance change (δZ) measured at 5 or 15 min between successive ischaemic episodes in one animal and between animals.	49
Table 2.2. Comparison of impedance changes during : a) Anaesthesia with inspired halothane or intravenous alphaxolone /alphadolone. b) Ligation of either the internal or common carotid arteries.	50
Table 2.3. Analysis for trends in measurements during successive episodes of spreading depression within one experiment	55
Table 3.1. Arterial blood gases in different anaesthetic regimes	69
Table 3.2. Changes in impedance during global cerebral ischaemia	73
Table 3.3. Impedance measurements during cortical spreading depression.	83
Table 3.4. Measurements with further electrode arrangements during cortical spreading depression	85
Table 3.5. Baseline scalp impedance variations under resting conditions	87
Table 3.6. Scalp impedance changes with superfusing cup ipsi- or contra-lateral to the araldite recording array.	87
Table 3.7. Scalp impedance variation during warming of the scalp by a lamp	91
Table 3.8. Effect of external warming on scalp impedance changes	94
Table 4.1. Results of finite element model	121

1. INTRODUCTION.

1.1. REASONS FOR INTEREST IN IMPEDANCE IMAGING, YET ANOTHER IMAGING MODALITY.

1.1.1. Background : existing imaging methods.

Since the invention of X-ray computerised tomography (CT) in the early 1970's, there has been a rapid development of various imaging methods for use in clinical diagnosis and, to a lesser extent, in physiology. The principle of all such methods is that the internal distribution of a specified variable can be mapped with the use of external measurements alone. They are non-invasive in the sense that no surgical intrusion into the subject is needed; they are therefore ideal for clinical diagnosis or scientific experiments in which data need to be accumulated repeatedly in the same preparation.

The quantities that can be imaged have been limited by the spectroscopic modalities used. The sole use of CT is in imaging anatomical structures, on the basis that different tissues attenuate X-rays to different extents. Magnetic resonance imaging has the potential to be more flexible, as any one of a variety of elements could, in principle, be detected. In practice, however, clinical use is largely restricted to the imaging of protons in body water, because the technique is insensitive and protons are the only nuclear particles present in sufficient concentration. This, like CT, gives information on anatomical structures.

From a physiological point of view, images of changes in function would be important. At present, NMR is used in one of two basic ways : either for imaging of a single element (as above) or as a spectroscopic method to give unlocalized measurements of the concentration of a variety of metabolites in a single sample. In principle, these could be combined to yield reconstructed images of several selected metabolites in a subject. Unfortunately, the poor sensitivity of the technique leads to excessively long data acquisition times or unacceptable reductions in spatial resolution. For example, it took 34 min to acquire images with a voxel size of 27 cm^3 (3 cm along each axis) of high energy phosphates in the human head (Troop et al, 1988). Positron emission

tomography (PET) has great sensitivity, but has the requirement that a suitable radioisotope is physically present in the tissue of interest, and that data acquisition takes place for a period of the order of the half life of the isotope, so that exposure to ionising radiation is kept to a minimum. In practice, this means acquisition times are of the order of tens of minutes. The technique is very flexible, as a positron emitting isotope can generally be attached to a metabolite or ligand of interest. In this way, blood flow and glucose utilization in the brain during various pathological conditions have been imaged with a spatial resolution of 8mm or so along each axis in the plane of the imaged slice (see (Jolles et al, 1989) for a recent review). Single photon emission computed tomography (SPECT) is similar in principle to PET, except that it has a poorer spatial resolution. All the above techniques cost many hundreds of thousands of pounds. There is usually a large demand for the services of a device, so that access may be difficult to obtain, and a subject has to be brought physically to the apparatus.

1.1.2. Continuous inexpensive portable recording of changes related to cerebral anoxic depolarization.

There are several circumstances in clinical medicine or physiological experimentation when neurones outrun their energy supply. There is then a cellular depolarization and shift of fluid from the extracellular to the intracellular space as a result of the failure of the sodium pump to maintain ionic gradients. This has been termed "anoxic" depolarization, but the same process occurs with other causes, such as ischaemia. This occurs in cerebral ischaemia, spreading depression (SD) and epilepsy (see Bures et al, 1974, Van Harreveld and Schadé, 1962, Van Harreveld, 1972). It would be useful to be able to localize these changes non-invasively, principally for diagnosis in clinical medicine.

Such events can at present be detected by imaging changes in blood flow with techniques such as PET, but there is a poor temporal resolution, and there are logistical problems in obtaining rapid access to scarce facilities. Tissue impedance increases by tens of per cent in the above conditions, and so it should be possible to image the changes with the recently developed

technique of impedance imaging (Electrical Impedance Tomography, EIT). (It is also termed Applied Potential Tomography, APT, but "EIT" will be used throughout this work). A current prototype EIT device (see sections 1.2 and 2.4.2.1) is physically small - about the size of a video recorder, attached to a microcomputer (Fig. 2.7), and costs about £11,000. It therefore could be placed adjacent to a clinical or experimental subject and be used for continuous monitoring over extended periods. These are important, albeit practical, advantages over other methods. It could also have a temporal resolution of seconds which would be a great advantage if rapid events, such as epilepsy or spreading depression, are to be characterized. Its principal disadvantage at present is a poor spatial resolution (see below).

Examples of its possible application in diagnosis include the assessment of the extent of damage after a cerebrovascular infarction in humans, or localization of an epileptic focus. A postulated cause of migraine is spreading depression, but one objection is that this has never been recorded in human subjects. Cerebral blood flow changes have been measured extensively during migraine but the techniques used have insufficient spatial or temporal resolution to identify the restricted blood flow disturbances of SD (see Gardner-Medwin and Mutch, 1984, Lauritzen and Olesen, 1987). EIT could provide crucial evidence one way or the other as it would be suitable practically and theoretically for imaging changes related to SD in an elusive migraine attack.

1.1.3. Outline of introduction.

It is therefore proposed that impedance imaging could constitute an important advance in neuroscientific technology. A description of the technique and its current development is presented in section 1.2. In section 1.3, the physiological problems involved in imaging the above changes, current state of knowledge, and the rationale and purpose of the experiments performed in this work are discussed.

1.2. ELECTRICAL IMPEDANCE TOMOGRAPHY.

1.2.1. The four electrode method of impedance measurement.

Impedance measurements in biological samples may be inaccurate if electrode impedances are not taken into account. This problem is minimized by a method in which four electrodes are used (Brown, 1983). It was employed in both the single channel impedance and the EIT device used in this work. A constant alternating current is applied to two "drive" electrodes (D1 and D2), and the impedance is taken to be proportional to the in-phase component of the potential difference between two other "recording" electrodes (R1 and R2) (according to Ohm's law). In this way, the effects of changes in electrode impedance are minimized because : 1) The current which passes through the tissue is constant. 2) The input impedance of the buffer amplifiers is sufficiently high (10 meg Ω) that negligible current is drawn, and so the recording electrode impedances become immaterial. 3) A substantial potential difference (PD) may develop between R1 and R2 because of capacitive coupling between the electrode leads, which would be affected by changes in electrode impedance. However, this PD has a phase shift, and is substantially eliminated by the use of a phase sensitive detector, set to pass only the in-phase component of the signal. In practice, capacitive coupling to earth of the leads to the recording electrodes can produce a lower input impedance. This may lead to artefacts, because current is then drawn through the recording electrodes, and the size of the input capacitance may vary between the two inputs in an unpredictable way. These effects may be minimized by reducing the input capacitance. Available methods include reduction of the length of leads from the subject to the input amplifiers in the impedance measuring hardware, and the use of buffer amplifiers placed close to the animal.

All impedance measurements in this study were made with this technique. As a result, all impedance measurements are of the resistive component of impedance (also termed the "real" or "in-phase" component). Unless otherwise stated, "impedance" will refer to this resistive component (which, in practice, is close to the resistance for measurements in tissue below

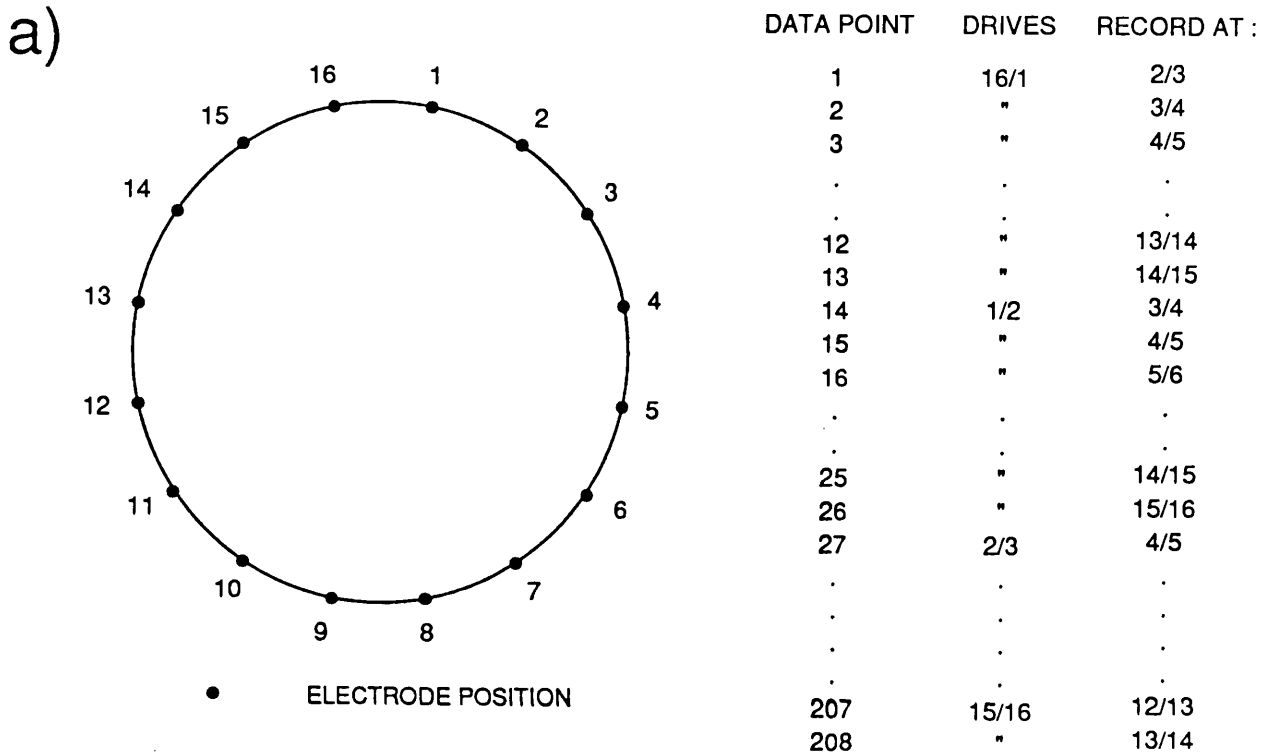


Figure 1.1. The Sheffield EIT system reconstruction algorithm. a) Data collection procedure. Constant current is initially applied to electrodes 16 and 1. The in-phase component of the potential difference between electrodes 2 and 3 is measured. This is repeated in turn for electrodes 3 and 4, 4 and 5, and so on around to electrodes 14 and 15. This sequence is then repeated for all 16 electrode current drive pairs.

100 kHz (see section 1.3.2)). In some relevant published studies, which are discussed below, both the real and imaginary components of impedance were measured. In these cases, "complex impedance", "resistance" or "capacitance" will be used to refer to the complex impedance, and its real or imaginary components respectively. In some cases, published results are presented in terms of conductivity. For consistency, these have all been converted to their reciprocal, resistivity.

1.2.2. Principle of EIT.

The principle of EIT is that a large number of impedance measurements are made from electrodes on the boundary of an object. These are processed by computer to produce a reconstructed two-dimensional image of the impedance in the plane of the electrodes. Whilst there are many ways of achieving this in theory, the following description refers to the only commercially available working prototype device - the "Sheffield EIT system", which was used in this study.

a) Data collection. Sixteen electrodes are equally spaced around the subject. A current of 5 mA peak-to-peak at 51 kHz is passed between two adjacent electrodes, and the in phase component of the potential difference is then recorded from each of the thirteen adjacent pairs of other available electrodes. Potential is not measured from drive electrodes, as this can introduce errors related to variations in electrode impedance. This is repeated for each possible drive electrode pair, giving a total of 208 measurements (Fig. 1.1a; Brown and Seagar, 1987). The measurement from any set of one drive and one recording pair will be the same as that measured when the drive and recording pairs are reversed (i.e. there is reciprocity). As a result there are $N(N-1)/2$ independent measurements in one minimum data set (where N is the number of electrodes; this yields 104 measurements for 16 electrodes). Multiple sets of data may be averaged in order to reduce noise. The minimum data set (104 readings) may be collected in 40 msec. In addition, the system only measures differences in impedance between a reference and subsequent images. This results in a method which is more robust with respect to inaccuracies in electrode placement and stray capacitance between leads

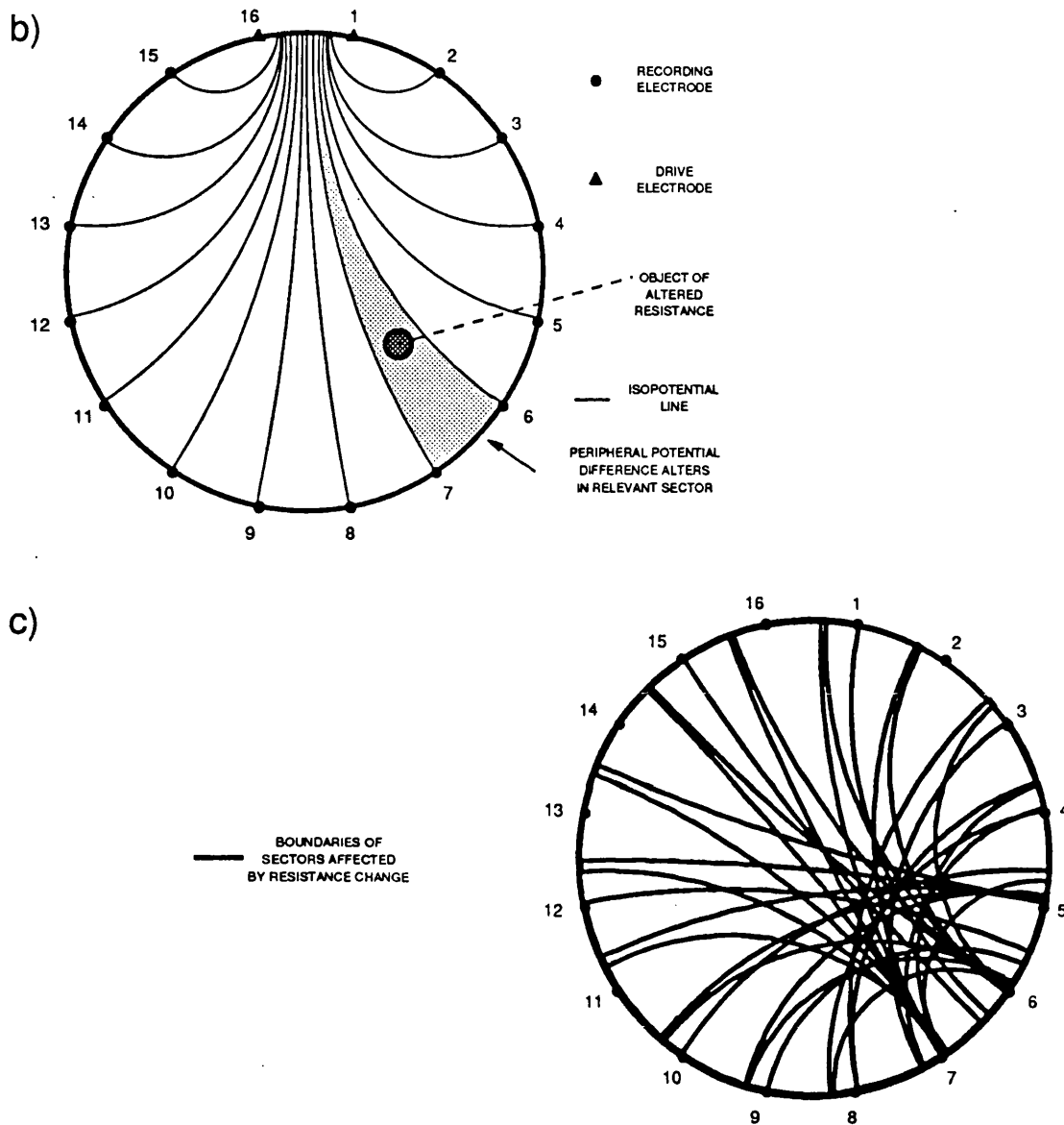


Figure 1.1. The reconstruction algorithm (continued). b) It is assumed that the object has an initially constant resistivity. The current applied to an adjacent electrode pair is equivalent to a dipole, and produces the illustrated lines of isopotential. (These are calculated in advance and included in the algorithm). The algorithm is based on the empirically supported principle that a change in the potential difference (PD) recorded between two adjacent electrodes is proportional to the natural logarithm of the resistivity change of the sector enclosed by isopotential lines ending on the recording electrodes. A resistance change within such a sector should therefore produce an equivalent change on the boundary PD corresponding to that sector. This is illustrated for a circular resistance change in the sector ending at electrodes 6 & 7 when current was applied to electrodes 16 and 1. c) Reconstruction is performed by back-projecting each change in PD along its corresponding sector, and then adding all the resulting changes. This produces a blurred reconstructed image, which is improved by an empirically designed filtering algorithm. This is illustrated for the object in (b). Each sector containing altered resistance is bounded by a heavy line.

(Barber and Brown, 1988). The potential difference between each set of recording electrodes is normalized and stored on a microcomputer as a change relative to its equivalent value during the reference image.

b) The reconstruction algorithm. It may be shown empirically that reasonable reconstructions may be obtained by treating this value as proportional to the natural logarithm of the impedance change in a sector of tissue stretching along isopotential lines which end at the recording electrodes. This simplification seems not to introduce serious artefacts, providing that the impedance disturbance is relatively small. It is assumed that the object has an initial constant resistivity. The isopotentials are then calculated in advance and stored on a microcomputer. The recorded potential difference for each sector is then back projected over the area of the sector using a computer program, and all 208 resulting images are added together. This produces a blurred reconstructed image, which is improved by weighting the contribution of each pixel, and with the use of an empirical de-blurring filtering function (see Fig. 1.1 b & c; Barber and Seagar, 1987). This "filtered back-projection" algorithm is not theoretically optimum, but is rapid and practicable. (See Brown et al, 1987, Brown et al, 1988, Webster, 1990 for two symposium volumes and a book review regarding further details of EIT design).

1.2.3. Current status and applications of EIT.

At present, impedance imaging is in its infancy. About twenty medical physics or engineering groups worldwide are working on its technical improvement, and about thirty of the Sheffield EIT systems have been produced by one of these groups for research purposes. To the author's knowledge, it is not in routine clinical use for any purpose, but is used in clinical research for monitoring gastric emptying (Mangnall et al, 1987, Lamont et al, 1988). Preliminary examples of EIT images of the thoracic impedance gated to the ECG (Eyuboglu et al, 1987, Eyuboglu and Brown, 1988) or respiration (Harris et al, 1987, Harris et al, 1988), and the upper arm during fracture healing (Kulkarni et al, 1990) have been published. There has been some interest in imaging vascular changes in the neonatal (McArdle et al, 1988). Preliminary images of intraventricular haemorrhage in the neonate

(Murphy et al, 1987), or ECG gated changes in the adult head (McArdle et al, 1989) have been published, but are single examples and their accuracy has not been validated.

1.2.4. Limitations of EIT.

The Sheffield EIT system used in this study is a prototype device and has several specific limitations as a result of its design :

1) Spatial resolution. The spatial resolution of the Sheffield EIT system has a maximum limit determined by the number of electrodes. The number of pixels in the image is limited to the number of independent measurements made, which is 104 with the data collection system described above (Barber and Brown, 1984). This suggests that the maximum possible resolution is about 10% of the image diameter, which is the length of one side of a pixel. The images are presented as a 32 x 32 matrix by interpolation between pixels, but this does not alter the underlying limit on resolution.

For the algorithm chosen, the method of data collection is optimal; driving non-adjacent electrode pairs would not add information, as all profiles can be obtained by superposition of those obtained from adjacent drive pairs (Barber and Brown, 1984). However, the disadvantage of imaging with electrical current, as opposed to a modality such as X-rays in which the rays travel in straight lines, is that the current spreads out away from the electrodes. Spatial resolution would therefore be expected to be least in the centre of the imaged object, where current density would be lowest. The spatial resolution of the Sheffield EIT system was investigated by Eyuboglu et al (1989), using an insulating ball, whose diameter was 10% of the diameter of a saline containing tank, 17 cm across. 35% of the tank diameter away from the centre and in the plane of the electrodes, the peak impedance change was 4.7 times greater than at the centre. At the same position, the Full Width at Half Maximum (FWHM) was 14.5% of the tank diameter in the radial direction and 22% in the tangential direction; at the centre the FWHM was 24%. This indicates that, for a spherical object under these conditions, the spatial resolution is, as expected, worse centrally in the image, and becomes less in an asymmetric fashion nearer the edge. In the present study, two objects are

defined to be distinguishable when the impedance profile between their peaks falls to less than $1/e$ (36.8%) of the mean of the peaks. For equal peaks, this is equivalent to a separation of the peaks of 2 standard deviations (S.D.) if the impedance profiles are gaussian. For a gaussian curve, the FWHM is 1.67 times the S.D., so the spatial resolution would be $2 \times \text{S.D.} = 1.19 \times \text{FWHM}$. On this basis, the above figures correspond approximately to a spatial resolution of about 29% of the tank diameter at the centre, and 17-26% at 35% of the tank diameter from the centre. However, the object was itself 10% of the tank diameter across, so the spatial resolution for a point disturbance might be expected to be roughly 20% of the tank diameter at the centre or 10-16% near the edge.

2) Off-plane impedance changes. Impedance changes out of the plane of the electrodes ("off-plane") would be expected to produce changes in the image, as current will spread in all directions. In the same test preparation as above, Eyuboglu (1989) found that the radial impedance profile of off-plane impedance disturbances was not the same as that in the electrode plane. It also varied with distance away from the electrode plane. For example, the peak impedance change fell by 50% and 86% as the ball was moved 70% of the tank diameter off-plane from positions respectively at the centre or 35% of the tank diameter from the centre. In general, impedance changes from a progressively smaller central area were represented in the image, as an impedance disturbance progressively moved off-plane. Therefore an impedance change which was actually the full diameter of the electrode array, but off-plane, would appear in the image as a central impedance disturbance.

3) Distortion due to assumption of initial constant resistivity. Any inhomogeneity in the resting resistivity of the subject will produce greater inaccuracy, as the program used assumes homogeneous resistivity in calculating the equipotential lines on which back projection is based. In the case of the adult head, this can produce serious distortion, as the skull has a high resistivity relative to the scalp and brain. McArdle et al (1989) produced a concentric three layer analytic model to assess this effect, and found that the diameter of the brain in the resulting image was about 55% of its original diameter in the model.

4) Imaging of impedance differences only. The imaging procedure has

been designed to image only the difference between a specified reference image and subsequent images. In the experiments in this work, this was not a disadvantage, as a clear control condition could be defined before a disturbance (spreading depression or cerebral ischaemia) was initiated. However, in clinical subjects, this could produce problems if imaging were initiated after a sought disturbance had already commenced.

5) Assumption of a circular electrode array. It is assumed that the electrodes are equally spaced and form a circle. Any deviation from this will result in a distortion in the image.

However, whilst these limitations may pose problems for current research with the Sheffield EIT system, there are good grounds for anticipating substantial technical improvements in the future. Spatial resolution should improve with better reconstruction algorithms and computer processing power, and with a greater number of electrodes. Barber and Brown (1984) estimated that a spatial resolution of 1% of the electrode array diameter could be achieved with a circular ring of 128 electrodes. The equipotential lines used to form the reconstruction matrix could be modified if prior knowledge of the resistivity of the subject was available. This could be achieved, for instance, by the use of potentials measured from known current sources in a physical model of the human head (*cf.* McArdle et al, 1988). The program is currently being modified to allow for irregular electrode spacing, and, it should be possible to extend the 2-D reconstruction algorithm to permit 3-D imaging (Liu et al, 1988).

On the other hand, the Sheffield EIT system has a contrast resolution of about 0.1% change in impedance, and a minimum data set can be collected in 40 msec (Brown et al, 1985, Brown and Seagar, 1987). One image can be reconstructed in about 5 sec on the recommended IBM compatible microcomputer with an Intel 80186 processor. The Sheffield system should therefore be most useful in imaging rapid small changes in impedance in a subject of initial homogeneous resistivity.

1.3. BACKGROUND : IMPEDANCE MEASUREMENTS IN THE BRAIN DURING ANOXIC DEPOLARIZATION.

1.3.1. Changes in the extracellular space during anoxic depolarization.

When cerebral grey matter outruns its energy supply, a characteristic sequence of events takes place. These are termed "anoxic depolarization", because they occur during pure hypoxia, but the term has been extended to include the similar events which occur in ischaemia, spreading depression or epilepsy (see Bures et al, 1974 for a review). These events have been most studied in the cerebral cortex, but also occur in other areas of grey matter in the brain (Bures et al, 1974). When measured in the cerebral cortex, the characteristic event is that spontaneous electrical activity ceases and a sustained negative shift of tens of millivolts is recorded with an electrode on the cortical surface. The underlying biochemical events have recently been reviewed (Siesjö, 1990) : 1) Extracellular potassium rises, and there is an influx of sodium, chloride and calcium into cells. In the case of cerebral ischaemia, this starts gradually, and is probably due to inhibition of sodium-potassium exchange by the sodium pump and activation of potassium channels due to influx of calcium; both processes occur because of low ATP levels. In SD, these changes occur suddenly, and are due either to initiation of SD by the application of extracellular KCl, or intense neural activity. 2) Excitatory amino-acids, particularly glutamate, are released as a result of the depolarization. This further increases calcium influx by activating NMDA channels, and further depolarization occurs due to activation of kainate and quisqualate glutamate channels. 3) Recovery from these events depends on the availability of ATP. In cerebral ischaemia, ATP is deficient, and lasting cellular damage may be caused (see Nedergaard, 1988). In spreading depression ATP levels are adequate and there is no histological evidence of damage under normal conditions (Nedergaard and Hansen, 1988). Anoxic depolarization therefore will continue in ischaemic tissue for the duration of the ischaemia, but SD recovers spontaneously over 2 min or so.

These events are accompanied by a substantial movement of ions and water. Maintenance of animal cellular volume may be described by the "double

Donnan" hypothesis (MacKnight and Leaf, 1977), according to which the excess intracellular osmotic pressure is balanced by the continuous extrusion of sodium ions. When this fails, water follows sodium and chloride into cells (Van Harreveld, 1972, MacKnight and Leaf, 1977), so that the extracellular space shrinks. Determination of the relative size of the extracellular space in the CNS may be made with the use of extracellular markers such as inulin, electron microscopy, or impedance measurements but each of these is subject to inaccuracies. Taking results from various different studies Van Harreveld (1972) concluded that the resting extracellular space in the mammalian cerebral cortex is about 15% of the tissue volume. During either cerebral ischaemia or spreading depression in the rat, careful study with the extracellular markers choline or trimethyltris(hydroxymethyl)methyl ammonium ion indicated that the extracellular space in the cerebral cortex decreased by about 50% (Hansen and Olsen, 1980).

1.3.2. Impedance measurements in resting brain.

Current applied to the brain passes via two main routes: 1) At frequencies up to 100 kHz, the majority passes through the extracellular fluid. This component of current will be resistive. 2) Other current may cross cell membranes, enter the cytoplasm, and leave by crossing the cell membrane again. The cells across which this happens are neurones and glia in roughly equivalent amounts (Ranck, 1963b). The cell membranes may be considered as a resistance and capacitance in parallel (Hodgkin and Rushton, 1946). As a result, the amount of current passing through this second route will depend on the frequency of applied current. In addition, the orientation of cells or their processes becomes important. The impedance of an area of membrane decreases with increasing surface area, so that current which passes longitudinally towards a cell process will meet a lower impedance than that which is applied to the process transversely.

The situation in cerebral grey or white matter is very complex, as impedance will be affected by a wide spectrum of cell shapes and sizes at all orientations. Some authors have employed a simplified approach, by using or modifying Maxwell's equations for the resistivity of a suspension of spheres (to

represent cells) in a medium of different resistivity (Cole and Curtis, 1936; discussed in (Van Harreveld, 1972)). An approximate idea of the effect of frequency on tissue impedance may be illustrated by considering the equation for spheres in a uniform medium (Van Harreveld, 1972, p.463). The effective resistivity of a spherical "balloon", R_s , of radius a consisting of an inner fluid of resistivity R_i , and outer shell with resistance of unit area R_m , is given by :

$$R_s = R_i + \left(\frac{R_m}{a}\right) \quad (1)$$

Taking a lower bound for the resistance of nerve or neuroglia membrane as $1000 \Omega \cdot \text{cm}^2$ (Coombs et al, 1955; Kuffler and Potter, 1964), spheres of radius of $10 \mu\text{m}$, and R_i as $60 \Omega \cdot \text{cm}$ (Ranck, 1963b), R_s is $1 \text{ meg}\Omega \cdot \text{cm}$. The equation for the resistivity of the whole suspension, R , simplifies to

$$\frac{1 - \left(\frac{R_o}{R}\right)}{2 + \left(\frac{R_o}{R}\right)} = \frac{\alpha}{2} \quad (2)$$

where R_o is resistivity of the medium, and α is the volume concentration of the spheres, providing the resistivity of the particles is much greater than that of the medium. Taking α as 0.85 (see above) and R_o as $20 \Omega \cdot \text{cm}$ (Hodgkin, 1947), then $R_s \gg R_o$, and R is $190 \Omega \cdot \text{cm}$. This figure only takes resistance into account, and is therefore for DC measurement. With AC measurement, the capacitance of the cell membrane will have an effect. Taking the capacitance of cell membrane per unit area, C_m , as $1 \mu\text{F} \cdot \text{cm}^{-2}$ (Hodgkin, 1947), the impedance of the cell membrane, Z_m , will be given by

$$Z_m = \frac{R_m}{(1 + 2\pi f R_m C_m)} \quad (3)$$

where f is the frequency of applied current in Hz. At 100 kHz , Z_m is about 2

Ω .cm. Whilst this is much smaller than with DC measurement, R_s will still be much larger than R_o .

For spherical cells, therefore, the great majority of current applied below 100 kHz passes in the extracellular space. However, the use of Maxwell's equations requires that the cells be uniformly spherical in a dilute medium (Van Harreveld, 1972). In the brain, this is not the case; in particular, cells are many different sizes, and there are numerous cylindrical cell processes, which may be millimetres long in grey matter, and centimetres in white matter. As a result substantial amounts of current may pass into the process if the direction of current flow is along the process. This may be discussed in terms of the space constant, λ , which is the distance along a membrane at which potential arising from an injected current falls to 1/e of its value at the site of injection. Current may therefore be considered to have crossed a membrane within several space constants of the site of injection. For DC measurement,

$$\lambda = \sqrt{\frac{r_m}{(r_o + r_i)}} \quad (4)$$

(Hodgkin and Rushton, 1946) where

$$r_m = \frac{R_m}{\pi d} \quad (5) \quad \text{and} \quad r_i = \frac{R_i}{\pi (d/2)^2} \quad (6)$$

r and c (used below) refer respectively to the resistance or capacitance of a unit length of cell process. Suffices are used as previously: "i", "o" and "m" refer to intracellular, extracellular or membrane quantities. d is the diameter of a process. For the purposes of illustration, r_o will be ignored, as, for small processes, $r_i \gg r_o$. For AC measurement, the membrane capacitance must be taken into account. Then the equivalent of the space constant is the attenuation constant, λ^* , which is defined as the length at which the peak value of the sinusoidal transmembrane potential falls to 1/e of its value close

to the site of injected current. If the membrane impedance is almost entirely determined by the capacitance, the following approximation may be used (Equation III.1-15, Eisenberg and Johnson, 1970) :

$$\lambda^* = \sqrt{\frac{1}{\pi f c_m r_i}} \quad (7)$$

where f is the applied frequency in Hz and c_m is given by

$$c_m = C_m \pi d \quad (8)$$

where C_m is membrane capacitance for a unit area.

To illustrate this point, consider a cell process 1 μm in diameter, with other properties as in the idealized cell mentioned above. Then λ is about 200 μm , and λ^* at 50 kHz (the frequency used in this study (see below), when the assumption that membrane impedance is almost entirely capacitive should be valid) is about 16 μm . In this case, it may be seen that, with direct applied current, most will cross into processes which are millimetres long when applied longitudinally, but a negligible fraction will enter processes if applied transversely. At higher frequencies, more current will enter shorter processes when applied longitudinally, but still a very small proportion will enter when applied transversely.

The resting impedance of cerebral grey matter in various sites and species has been reported to be in the range of about 200 to 500 $\Omega\cdot\text{cm}$ at frequencies up to 5 kHz (see Geddes and Baker, 1967; Van Harreveld, 1972). In agreement with the arguments proposed above, white matter in the cat internal capsule was reported to be anisotropic : resistivity was 800 $\Omega\cdot\text{cm}$ across fibres and one-ninth of this along fibres (Nicholson, 1965). Ranck (1963a, 1963b) measured cortical impedance in the rabbit at frequencies from 5 Hz to 50 kHz. The resistive component of the impedance measured at 50 kHz ($\approx 210 \Omega\cdot\text{cm}$) was about two-thirds of that measured at 5 Hz ($\approx 320 \Omega\cdot\text{cm}$). This difference was attributed mainly to increased longitudinal current passage in neurons and their processes. Above 50 kHz, he proposed that resistivity would

fall further because of transverse current flow in neurones and glia and their processes.

A quantitative analysis is outside the scope of this work. Qualitatively, it appears that, with measurement with direct current, some current will enter cell processes which are oriented along the direction of current flow, and also are of the order of millimetres in length. These will form a small proportion of the tissue, most of which will consist of cell bodies and cell processes not orientated longitudinally with respect to the current flow. Current will not enter these to any great degree, so that DC brain impedance will be mainly determined by the size of the extracellular space. At 50 kHz, the resting impedance is lower, because a higher proportion of current will pass into cells. This will mainly be due to longitudinal current flow along neuronal processes.

1.3.3. Impedance changes during anoxic depolarization.

During anoxic depolarization, there are two main ways in which it might be expected that tissue impedance would change : 1) The main effect would be an *increase* due to shrinkage of the extracellular space, as most current travels in it. 2) As some current appears to cross into cells, a smaller impedance *decrease* might be expected to occur due to the fall in membrane resistance concomitant with the transfer of ions. Both effects would be smaller at higher frequencies. As the impedance increase would predominate, measurement at higher frequencies during anoxic depolarization might be expected to produce a smaller impedance increase.

1) Spreading depression. Ranck (1964) performed a similar detailed study of cortical impedance changes during CSD in the rabbit. At 5, 50, 500, 5,000 and 50,000 Hz, the peak resistivity increase was 73, 73, 77, 64 and 43 % respectively (from Fig. 2, Ranck, 1964). These increases were attributed mainly to a decrease in the size of the extracellular space and in the membrane resistance of neurones. He concluded that, at 50 kHz, little current flowed transversely through cells or their processes, and longitudinal current flow was largely independent of membrane resistance. The larger impedance increase at lower frequencies included a decrease due to changes in membrane resistance. The net impedance increase was larger than at 50 kHz, because the shunting of current through intracellular fluid in cell processes at 50 kHz had been excluded.

There are likely to be species differences in the magnitude of the impedance change during SD, as this will depend on cell size and distribution. In the rat, the animal used in the present study, cortical impedance increased by a maximum of 34% during CSD, when measured at 1kHz (Weiss et al, 1966). However, this employed a two electrode impedance measuring method. No compensation was made for the inclusion of the impedance of the electrodes in the current path, so the tissue impedance change would have been larger to an undetermined degree. Hoffman et al (1973) measured cortical impedance during CSD in the rat with a microelectrode, 20 μm in diameter at the tip, which was implanted in rat cerebral cortex. Resistance increases of about 310% and 280% were recorded at frequencies of 400 and 3200 Hz respectively. The large size of the changes was attributed to measurement by the microelectrode of a small sample of cortex, entirely affected by CSD. Measurements with surface electrodes might yield lower impedance changes because some inactive cortex was included at any one time, but the cause of the discrepancy between these results, and other results with or without surface electrodes, is not clear. Cortical resistance in the rabbit, measured at 1 kHz with a two electrode system, increased by 17% during CSD (Van Harreveld and Ochs, 1957). In the cat, measured with square waves lasting 0.3-0.7 ms and a four electrode system placed perpendicular to the cortical surface, cortical resistance increased by 13% during CSD (Freygang and Landau, 1955).

On the basis of indirect evidence available from other studies, two other factors would be expected to play a minor role in the impedance changes during SD : i) Blood volume. By diluting the blood of rabbits with solutions of known conductivity Van Harreveld and Ochs (1956) estimated that blood contributed about 10 % of brain resistivity. The relative volume of blood in various cerebral tissues in the rat has been estimated by comparing the tissue content of albumin labelled with iodine-131 with that of whole blood (Nair et al, 1960). It varied between 11% in cerebral cortex and 4% in the hypothalamus. From measurement with a microelectrode on rabbit cortex, Ranck (1963a) estimated that pial vessel walls had a negligible resistance in comparison to that of blood, which has a resistivity in the rabbit of about 130 $\Omega\cdot\text{cm}$ (Van Harreveld and Ochs, 1956). Since this is approximately half of cerebral resistivity as a whole (see section 1.3.2), these figures suggest that the contribution of blood to cerebral resistance is about 5%. Blood flow during CSD has recently been reviewed in detail (Lauritzen, 1987). Immediately prior to CSD, a variable

vasoconstriction has been observed in some studies. During CSD, and following it for about 5-10 min, there is a vasodilatation. This is also variable, and appears to be dependent on the anaesthetic used. It was present with barbiturate, but not ether, anaesthesia. With halothane, the cortical blood flow appeared to depend on the state of the vasculature prior to the initiation of CSD. In measurements in normal rats, it increased by about 40%. It may therefore be estimated that changes in blood flow during CSD may cause an initial increase in impedance prior to the DC potential shift, and then a subsequent decrease lasting 5-10 min (in halothane anaesthetized rats), but these are unlikely to be more than a few per cent in size.

ii) Temperature. Cortical temperature has been observed to increase by about 0.5 °C during CSD, measured with external infra-red thermography (Shevelev et al, 1986) or a thermocouple thin film thermistor inserted 0.7 mm into the cerebral cortex (LaManna et al, 1987). This is likely to be due to a combination of increased cerebral blood flow and metabolism. The precise contributions in CSD have not been assessed. In a similar situation, during and following nitrogen-induced hypoxia in the rat, LaManna et al (1987) estimated that each of these factors contributed an approximately equal amount to the observed temperature increase of 0.8 °C. The variation of the resistivity of brain tissue with temperature does not appear to have been investigated. Li et al (1968) observed that the resistivity of brain tissue was similar to that of 0.09% saline, whose resistivity varied by -1.3% per °C. It is therefore unlikely that temperature effects will cause a cortical impedance decrease of more than one per cent during CSD.

In summary, available evidence suggests that four main factors are likely to affect cortical impedance during CSD. Cell swelling will *increase* impedance by tens of per cent. A fall in membrane resistance, increase in blood flow, and predominant temperature increase will all cause impedance, in contrast, to *decrease*, but these effects are all likely to be at least one or two orders of magnitude smaller. The net effect should therefore be an impedance increase of tens of per cent.

In the rat, local cortical resistance was measured with a microelectrode during CSD. It increased by 220 - 300% at all depths down to 1.3 mm. The largest increase was observed at about 0.3 mm below the surface. Other increases below this were similar; the smallest occurred in the lowest cortical layer (Hoffman et al, 1973). In the cat, an impedance decrease of about 5%

was observed in sub-cortical white matter during CSD (Freygang and Landau, 1955). SD is thought to be confined to grey matter; DC potential changes during SD in the rat were not observed in subcortical white matter (Monakhov, Fifkova and Bures, 1962). The absence of an impedance *increase* in white matter is not unexpected, but the explanation for the impedance *decrease* is not clear.

2) Cerebral ischaemia. Similar changes may be observed in cerebral ischaemia, except that the condition is not self-limiting as in SD. The impedance changes will depend on the method of production of ischaemia, its duration, and the species. Impedance was measured at 1 kHz in the rat during forebrain ischaemia induced by bilateral carotid artery occlusion and hypotension for 15 min. The impedance changes were not reported directly, but expressed as a change in extracellular space, calculated with Maxwell's equations. The maximum decrease in extracellular space was estimated to be 55% (Von Hanwehr, Smith and Siesjö, 1986). In the cat, ischaemia was produced by clamping the innominate, left subclavian and mammary arteries. Cortical impedance was measured with pulses 3 ms in duration. It increased by 37, 65, and 113% at 5, 10 and 30 min respectively. It returned to the baseline level over 60 min or less (Hossman, 1971). In the cat, the impedance in left parietal cortex, measured with a square wave pulse 1ms in duration, increased by 66% and 89% at 15 min and 1 hr following middle cerebral artery occlusion (Matsuoka and Hossman, 1982). In monkeys, cortical impedance measured at 1kHz increased by 7% and 27% during systemic hypotension for 15 and 30 min respectively. Impedance returned to baseline within 5 min of the end of hypotension in most animals (Gamache et al, 1975). All the above studies used a four electrode impedance measuring method.

There do not appear to be any published studies of impedance measurement made with the species and procedure for cerebral ischaemia employed in this work. It seems likely, from the above reports, that cortical impedance increases of several tens of per cent, much as during SD, might be expected during cerebral ischaemia of 5 - 30 min. The mechanisms are likely to be similar to that of SD, except that blood flow and temperature will fall as a result of ischaemia and, in contrast to SD, would cause an additional *increase* in impedance. The magnitude of the impedance increase will depend on several factors, including the degree of ischaemia. In the "four vessel" model of cerebral ischaemia employed in this study (see below), cerebral blood flow

generally fell to 5 - 8% of its resting value after 15 min of ischaemia (Todd et al, 1986). This is thought to be because flow persists in small cervical vessels, which may be occluded if desired by tightening a snare around the neck (Pulsinelli and Buchan, 1988). Cerebral impedance changes following circulatory arrest due to cutting of the aorta in the rabbit have been analyzed (Van Harreveld and Ochs, 1956). This differs from cerebral ischaemia in that blood flow ceases absolutely, but the mechanisms should otherwise be similar. An analysis of the various contributing factors was achieved by a combination of theoretical and experimental approaches; emptying of blood vessels was examined by diluting the blood, and anoxic depolarization by the use of ether or cyanide, which abolish SD or destroy grey matter respectively. The impedance increased by 155% after 25 min, and about 380% four hours after death. The responsible factors (percentage contribution in parentheses) were estimated to be : 1) Cooling of the brain to room temperature (20%), 2) Draining of cerebrospinal and extracellular fluid (15-20%), 3) Emptying of blood vessels (10%), 4) Anoxic depolarization (30-35%).

3) Other conditions. Cortical impedance increases of 3-5% were observed during measurement at 1 kHz with a two electrode system during epileptic episodes in the rabbit or cat (Van Harreveld and Schadé, 1962). Cortical impedance measured at 1 kHz increased by 86%, 117% and 138% during hypoglycaemia for 5, 15 or 30 min in the rat (Pelligrino et al, 1981).

1.3.4. Problems arising from impedance measurement of cerebral events by scalp electrodes.

In laboratory studies on experimental animals, it is conceivable that EIT could provide useful information if recorded with electrodes placed directly on the brain. There are also some clinical situations in which this might be useful : for instance, epileptic foci might be localized with subdural electrodes implanted anyway for EEG monitoring prior to neurosurgery for epilepsy. However, for most clinical and scientific purposes, it would be far preferable if imaging of impedance changes related to anoxic depolarization could be performed non-invasively with scalp electrodes.

Unfortunately, the scalp has a relatively low resistance, and the skull has a high one. This will increase the tendency for current applied to the scalp to be diverted through the scalp rather than enter the brain. There are no

published reports of the resistivity of the relevant tissues in the rat, but values may be estimated from the literature. 1) Skull. The resistivity of fresh cortical bone of the rat femur measured at 50 kHz was about 14,000 $\Omega\cdot\text{cm}$ (Kosterich et al, 1983), which is in reasonable agreement with a value determined experimentally for rat skull in this work (section 4.3). 2) Scalp. In the present work, scalp measurements were made after the skin was abraded, or needle electrodes were used, so the relevant resistivity will be that of dermis and connective tissue in the subcutaneous scalp. Figures for this were not directly available, but are likely to be comparable to those for mammalian skeletal muscle. This has been reported to have a resistivity between 435 and 1130 $\Omega\cdot\text{cm}$ measured at 10 - 100 kHz in several species (see Geddes and Baker, 1967). 3) Meninges. The resistance of the arachnoid membrane in the cat was about 50-100 $\Omega\cdot\text{cm}^2$ (Bennett, 1969). It is therefore unlikely to contribute significantly to the high resistance of the skull. No experimental measurements of the resistance of the dura mater appear to have been published. Because it too is a thin membrane, it seems likely that its resistance will also be small compared to that of the adjacent skull.

These figures indicate that the brain and scalp have a roughly comparable resistivity, but are separated by the skull, which has a resistivity approximately 20 times greater. This will create three types of problem for impedance imaging in the head with scalp electrodes :

1) The magnitude of an impedance change measured on the scalp, compared to the same measurement made in the same way on underlying cortex, will be considerably reduced. This is because i) The fraction of current which passes through the cerebral structures of interest is diminished and ii) For any given amount of current which does pass through cerebral structures, the amplitude of the signal recorded on the scalp will be decreased. The extent of this reduction will depend on the resistivities of the intervening tissue layers, their geometry, and the relative positions of the electrodes. Of these three factors, electrode position is the only one which could be varied during non-invasive recording conditions. The factors which are likely to influence the relationship between electrode position and size of impedance change recorded with scalp electrodes may be considered as follows : For imaging, electrode separation in a fronto-occipital ring will be constrained by the dimensions of the head. For detection of intracranial events by single channel impedance measurement, the largest signals would be expected when the volume of

intracranial tissue in which impedance is changing occupies the largest proportion of the tissue through which current is passing. In practice, this will be a complicated issue : greater electrode separation might increase the proportion of current passing through the brain, but current would not flow equally through all areas. In the case of CSD, the measured impedance change would only increase if additional current flowed through the cortex; current passing through subcortical white matter in which impedance decreases (see above) would decrease signal size. In addition, the disturbance in CSD travels at about $3 \text{ mm}\cdot\text{min}^{-1}$, and lasts about 1 min (see section 3.2), and so is about 3 mm wide. Current passage through a wider volume of brain would then lead to a lesser signal as only part of the cortex would be active at any one time. It might therefore be expected that there would be an optimum electrode separation. In the case of cerebral ischaemia, the same arguments regarding electrode separation would apply, except that it is likely that the impedance of a much larger volume of brain would increase. It is unclear how the impedance of white matter would change, compared to that of grey matter, but anoxic depolarization has only been observed in grey matter (see Bures et al, 1974). Again, the impedance increase measured might be expected to be greatest when electrode separation was such that the greatest proportion of grey matter was included in the current path. This might either occur when current only flowed through the cortex, or when electrodes were widely spaced on either side of the head and so included sub-cortical grey matter.

There do not appear to be any previous reports which have investigated these issues with respect to impedance measurement during anoxic depolarization in any species, or to current flow in the head of the rat. In the cat, Rayport et al (1966) constructed a simple model of the extracerebral layers in the cat from *in vivo* measurements at 100 Hz. They estimated that the potential difference measured by two drive electrodes placed 1 cm apart subdurally would be attenuated by 99% when measured above the drive electrodes on the scalp. Rush and Driscoll (1968) measured current densities in the cranium when constant current was applied to two electrodes on the scalp in a physical model of the human skull in a tank of saline, and compared the results with a mathematical model. They observed that 45% of the current applied to electrodes on the occipital and frontal bones passed through the cranial cavity. They also found that current density in the cortex was greatest when the drive electrodes were 5 cm apart. Similar models of the extracerebral

layers have been created, in particular for the purpose of analyzing the effect of the extracerebral layers on the EEG (e.g. Cuffin and Cohen, 1979; Hosek et al, 1978).

2) An attenuated signal arising from the brain might be difficult to distinguish from variations in scalp impedance. The effects of variations in scalp impedance will be exaggerated because the presence of the skull will tend to cause current to pass preferentially through the scalp. The skin is richly innervated and vascular, and large changes in impedance measured with superficial electrodes occur as a result of changes in autonomic activity. These appear to be epidermal in origin (Edelberg, 1971), and so should be minimized by the use of subcutaneous needle electrodes, or preliminary skin abrasion. It is well recognized that cephalic impedance measured with scalp electrodes varies by about 0.05% in concert with the pulse (Jenkner, 1962). This forms the basis of the technique of rheoencephalography (see below). By applying pressure with the aid of a tourniquet, Weindling et al (1982) reduced the pulse related impedance change by 20%. This was attributed to occlusion of blood flow in the scalp. The variability in scalp baseline impedance due to pulse related blood flow is therefore likely to be only a small fraction of one per cent. The way in which the scalp impedance baseline might vary over tens of minutes, the measurement period used in this study, has not been reported.

3) The presence of the skull is likely to degrade spatial resolution of EIT, because the algorithm assumes initial constant resistivity. This has been investigated in a model of the neonatal skull, which was surrounded by an agar film and filled with agar, to simulate the scalp and brain respectively. Saline solutions of varying conductivities were placed in a cylindrical cavity cut in the agar near the centre of the skull. EIT images were obtained with the Sheffield EIT system. It was estimated that the resistivity change in this area in the EIT image was under-represented by about 70% (McArdle et al, 1988). In a further study, an analytic model of the head was constructed on a computer in order to examine the effect of the adult skull and scalp (McArdle et al, 1989). The scalp, skull and brain were represented as concentric spheres. Radii of the spheres were 80, 85 and 92 mm. and resistivities were 160, 14000 and 230 Ω .cm, for brain, skull and scalp respectively. These were estimated so that the model agreed with measurements made with scalp electrodes in adult human subjects. Boundary values were then calculated, and reconstruction was performed on them using the algorithm employed in the Sheffield EIT system.

It was found that the skull and scalp comprised 61% of the diameter of the EIT image, whereas they only comprised 13% of the diameter of the model. This effect may have been overestimated, because the ratio of skull to brain resistivity employed was high. However, it indicates the probability that intracranial events will be compressed into a small central area in EIT images recorded with scalp electrodes. The skull will be represented by an area with a similar *total* resistance to that of the skull; because it is assumed that its resistivity is the same as that of the brain and scalp, this area will be much larger than in reality.

1.3.5. Previous reports of the measurement of impedance changes during cerebral ischaemia or spreading depression measured with scalp electrodes.

Several channels of impedance were measured across the head of clinical subjects with the technique of rheoencephalography, which is now largely of historical interest. Measurements were typically made at about 20 kHz with two electrodes per channel and a Wheatstone bridge. The resulting records are dominated by pulse related changes of about 0.05%. They were considered to be mainly due to intracerebral vascular changes, as they were substantially reduced by occlusion of the internal but not the external carotid arteries in both guinea pigs and human subjects (Jenkner, 1962). The fluctuations were considered mainly to be due to variations in the proportions of cerebrospinal fluid and blood in the cranium as a result of the pulse (Bostem et al, 1982). Variations in these pulse-related signals were claimed to be diagnostic of certain clinical conditions, but the technique never achieved wide clinical acceptance. To the author's knowledge, there have been no reports (other than those described above) of measurement with scalp electrodes of impedance changes directly related to anoxic depolarization.

1.4. RATIONALE FOR THE EXPERIMENTS IN THIS WORK.

1.4.1. General purpose of experiments in this work.

The overall purpose of the experiments in this work was to assess the application of EIT to imaging intracranial events non-invasively with scalp electrodes. Previous experimental results, reviewed above, indicate that

substantial impedance changes of the order of tens of per cent can be recorded during anoxic depolarization with electrodes on the cortex, at frequencies below 100 kHz. However, no data exists concerning the detection of such events by impedance measurement with scalp electrodes. Recording with scalp electrodes would be preferable, for both clinical and scientific use, as it would be non-invasive. Impedance measurements or EIT images were therefore collected with scalp electrodes during conditions in which anoxic depolarization occurred. These were compared with equivalent measurements made with cortical electrodes. The extent to which the scalp measurements may be attributed to intracerebral events, and the implications of this for the future use of EIT, are considered in the discussion section.

The difference in measurements made with cortical or overlying scalp electrodes was assessed in three different situations. The first two studies were intended to assess if clearly defined cortical impedance disturbances could be measured distinctly and reliably with scalp electrodes in an equivalent overlying position. The two critical features examined were : 1) Could the scalp impedance changes be clearly distinguished from baseline variability ?, and 2) Did any reproducible changes appear to be direct manifestations of the intracranial impedance change, or could they be attributed to artefacts or epiphenomena (such as local changes in the scalp) ? To assess these issues, single channel (non-imaging) impedance measurements were made with up to four electrode configurations. This approach was chosen because the technical problems of attaching 16 electrodes (needed for EIT) could be avoided, events at a single site could be recorded with high sensitivity and continuously, and, if necessary, controls could be performed in one animal with differing conditions in different parts of the head. Measurements were made during the conditions of global cerebral ischaemia or cortical spreading depression, selected because they represented a widespread or localized disturbance of cerebral impedance respectively.

The results of these first two studies were intended to be used for two purposes : 1) To assess if the conditions studied seemed suitable for attempting to image the observed scalp impedance changes with EIT, and 2) To test and refine a general model of the extracerebral layers in terms of their passive electrical properties. This could then be used to interpret or assess other applications of EIT in the head.

In the third study, EIT images were made during global cerebral

ischaemia, with cortical or scalp electrodes. The purpose of this study was to examine the effect of the extracerebral layers on the spatial resolution of EIT images collected with the Sheffield system.

There are other possible applications of EIT in neuroscience. One of these, imaging of neuronal depolarization with a high temporal resolution, has been investigated by the author prior to and during the studies presented in this work (Holder, 1989a, Holder, 1989b). These studies indicated that such changes are unmeasurable or small and difficult to distinguish from artefacts or epiphenomena. As a result, the major part of the studies concentrated on the much larger impedance changes during anoxic depolarization, and this work is restricted to these findings. Possible broader applications of EIT in neuroscience, and the implications of the results of this work in this respect, are discussed in section 5.4.

1.4.2. Rationale for choice of recording at 50 kHz.

In medical applications in which impedance measurement is employed, a frequency of several tens of kHz is used (see Webster, 1990). The reasons for this are : 1) An important problem in impedance recording is that variations in electrode impedance may introduce artefacts. In practice, electrode capacitance tends to be more constant than electrode resistance (Barber and Brown, 1984), so this favours high frequency measurement. 2) The amount of current that may be applied to tissue is restricted by safety considerations. At frequencies up to 100 kHz, the main concern is to avoid stimulation of nervous tissue; this is particularly true if measurements are to be made in the brain. British standards are not specifically set for electrodes on the brain, but a similar situation exists for impedance measurement with intracardiac electrodes. A maximum of 10 μA r.m.s. is permitted at frequencies below 1 kHz. Above this, the limit is 10 μA multiplied by the frequency in kHz. Therefore, 500 μA is permitted at 50 kHz (BS, 1982). It is desirable to use as high a recording current as possible, in order to improve the ratio of signal arising from the injected frequency to the noise which occurs in the electronic recording circuits. This is especially true in the case of EIT imaging, when the voltages arising at a pair of adjacent electrodes diametrically opposed to the drive pair may be very small (see Brown and Seagar, 1987). For both these reasons, the Sheffield EIT system, and the single channel impedance

measuring device used in the other studies, were constructed to operate at about 50 kHz. In this work, the single channel device applied currents of 22-56 μA peak-to-peak (8-20 μA r.m.s.). With the EIT system, applied currents were about 2 mA peak-to-peak (about 700 μA r.m.s.). This was slightly greater than the BS specification for normal use for equipment connected directly to heart muscle. However, it was within the higher limit (2.5 mA r.m.s. at 50 kHz) accepted for a single fault condition for heart muscle recording. A much higher limit (5 mA at 50 kHz) is permitted for skin recording for impedance measurements, so the EIT measurements made with scalp electrodes would have met this. Both devices were kindly loaned by Prof. B. Brown.

The evidence discussed in section 1.3 indicates that larger impedance changes during anoxic depolarization might have been expected at lower frequencies. The main concern of the studies in this work was to establish if reproducible and distinguishable scalp impedance signals could be measured. For this purpose, there is likely to be an optimum frequency at which the conflicting factors of size of biological signal, biological baseline variability, electronic noise, and safety considerations, combine to give the greatest sensitivity. Determining this frequency is likely to be a time-consuming matter. It was clear from previous work (see section 1.3) that a substantial cerebral impedance change could be recorded with cortical electrodes at 50 kHz, and so 50 kHz was chosen for these studies as a reasonable initial compromise.

1.4.3. Rationale for experimental design of impedance measurements during cerebral ischaemia with scalp electrodes.

In order to obtain global cerebral ischaemia, the model chosen was that of temporary occlusion of all four main cerebral vessels in the unanaesthetized rat (Pulsinelli and Brierly, 1979). This method produces a profound global cerebral ischaemia and, unlike other models, does not directly compromise the systemic circulation. In the original procedure, the vertebral arteries were occluded by diathermy and loose carotid ties were inserted at a preliminary operation under anaesthesia. After a recovery period of 24 hr, the carotid ties were occluded in unanaesthetized animals to produce ischaemia.

In order to simplify the procedure for the present study, the original protocol was modified. All procedures were performed at the same operation

under terminal anaesthesia. It subsequently transpired that a similar procedure had been successfully employed in similar experiments (Todd et al, 1986). The anaesthetic used initially was intraperitoneal urethane. Its anaesthetic effects last 10-12 hr (Flecknell, 1987), and so its use has the advantage that it is usually only necessary to give one dose at the outset of the experiment. In the event, this regime was found to be unsatisfactory, and four regimes were tried in all.

A single channel impedance measuring device was employed, but was multiplexed so that up to four electrode configurations could be measured concurrently. Measurements were made during cerebral ischaemia with various electrode spacings intended to measure the impedance of different amounts of brain. Measurements were made either on the cortex, or, in different animals, with electrodes in equivalent positions in the scalp. Further measurements were made with different durations of ischaemia, and with the scalp excised and then replaced, in order to investigate if the observed changes could be attributed to events other than intracranial impedance changes.

1.4.4. Rationale for experimental design of impedance measurements during spreading depression with scalp electrodes.

The animal model chosen was that of CSD initiated by perfusing the surface of the cerebral cortex with 150 mmol.l⁻¹; this is an established and reliable method (e.g. Gardner-Medwin and Mutch, 1984).

Impedance measurements during CSD were made with a single channel system. They were made with the same electrode configuration either on the cortex or, in different animals, in an equivalent position on the scalp.

Because initial scalp recordings indicated that any impedance changes were of a similar magnitude to baseline fluctuations, a number of different scalp recording arrangements were tested. The best of these was an arrangement in which the electrodes were set in a block, which was pressed firmly onto the scalp.

A priori, it was unclear which electrode spacing would be likely to yield the greatest likelihood of detection of intracranial impedance changes. In the rat, the skull is about 0.5 mm thick, and the compressed scalp is about the same thickness. Electrodes were set into the block at intervals of 0.5 mm. The minimum possible drive electrode separation, 1.5 mm, was therefore selected

for the majority of studies. It seemed plausible that a substantial amount of current would penetrate to the cortex, as the inter-drive electrode distance was slightly greater than presumed distance of the electrodes from the cerebral cortex. It also seemed to be suitable in that the volume of cortex through which most current passed would be likely to be of similar width, 2 mm or so, in the line of the electrodes. It seemed likely that the sensitivity to CSD might be increased because the entire measured area of cortex was likely to have altered impedance at the same time during the passage of CSD. Wider electrode spacing might have yielded less sensitivity if the volume of cortex sampled was greater than the volume whose impedance was altered at one time by the CSD.

1.4.5. Rationale and purpose of EIT recordings during cerebral ischaemia.

The study outlined in section 1.4.3. indicated that impedance increases of a few per cent could be recorded with scalp electrodes during cerebral ischaemia. They were partly caused by temperature changes; the evidence was equivocal with respect to whether an additional component was due to local scalp impedance changes consequent to ischaemia. It seemed likely that the remaining changes were due to cerebral impedance changes related to anoxic depolarization, but the contribution of other causes could not definitely be excluded on the basis of the available evidence.

Measurement with a single impedance channel is inexpensive, and could perhaps be useful in some clinical situations. Imaging of a slice of the brain would give far more information if accurate, and be easier to interpret for the clinician. A study was therefore undertaken with EIT during cerebral ischaemia. An EIT system was kindly loaned by the department of Medical Physics at the Royal Hallamshire Hospital, Sheffield. The measurements were in two stages : First, the performance of the system was assessed in physical phantoms and in rats where the impedance disturbance was controlled artificially. Secondly, a small number of images were collected in the model of cerebral ischaemia described above. The best anaesthetic regime, inspired halothane with neuromuscular blockade and artificial respiration, had been elucidated by then, and so was employed throughout.

The purpose of this was twofold : First, the accuracy of the Sheffield EIT was to be assessed, both in artificial and live situations. This was

intended to enable some assessment, if only qualitative, of its limitations for eventual physiological or clinical use. This information might also be used to suggest technical improvements needed for further use. Secondly, it was hoped that the images might give further information regarding the origin of the impedance changes during anoxic depolarization observed with scalp electrodes.

1.4.6. Mathematical models of the observed changes.

One purpose of the single channel impedance measurement studies was to furnish empirical data that could be used to test a model of the extracerebral layers. This was constructed with the aid of a computer, using parameters from the experiments and literature by the "finite element method" (see chapter 4). No attempt was made to "massage" values in the model in order to improve its fit to experimental data. It was intended that the main value of comparing the experimental data with the predictions of the model was if they disagreed. If so, this would have cast doubt on the interpretation of the data used in the model.

1.5. SOME PRACTICAL DETAILS REGARDING THE EXPERIMENTS.

The nature of the experiments was such that, in each of the three projects described, a new method had to be developed and tested. This included production or modification of electronic equipment, writing of software for data acquisition, display and analysis, and manufacture of experimental equipment. Over half of all the experiments performed during the course of this work are not presented, as they were only instrumental in improving the experimental method. In some cases, only a small number of results are presented; this is because they form a homogeneous group and appeared to demonstrate clear results from a particular new method. (Experiments were only excluded because the method employed differed from that presented, or a technical problem prevented results from being obtained. The results of all experiments performed with a particular cited method are included in the presentation.) Where results are not derived from a homogeneous series of experiments, any unifying assumptions are stated explicitly.

Dr. A.R. Gardner-Medwin produced the analytical model in Fig. 3.17. All other work presented was performed by the author.

2. METHODS.

2.1. IMPEDANCE CHANGES DURING CEREBRAL ISCHAEMIA IN THE ANAESTHETIZED RAT.

2.1.1. Animal preparation.

Male Wistar rats, which weighed 250 - 400 g and were 9 - 14 weeks old, were used. They were of conventional microbiological status; animals used had no nasal discharge or abnormal respiratory sounds. Three animals were kept in each RC1 solid bottom cage (North Kent Plastic, Erith, Kent), dimensions 56 x 38 x 18 cm, on sawdust grade 8 at 20 - 22 °C and 50 - 55% humidity. They received artificial light for 12 hours each day, and were fed on R & M 3 cubed maintenance diet (Special Diet Services, Witham, Kent). Air was filtered and exchanged 15 - 18 times per hour. They were anaesthetized by one of the following methods. 1) 5.1 - 5.7 ml/kg of 25% w/v urethane was injected intraperitoneally. 2) Induction was by intraperitoneal injection of 1 ml/kg body weight of Hypnorm (0.315mg fentanyl citrate and 10 mg fluanisone in 1 ml solution, Crown Chemical Co.) or by inhalation of ethyl chloride. Maintenance was by intravenous infusion of Alphaxolone/alphadolone (Saffan, Glaxomed) at 6 - 12 mg/kg/hr. 3) Induction and maintenance of anaesthesia were obtained respectively by the inhalation of 3% halothane in air, and then halothane 1 - 3% in a nitrous oxide/oxygen mixture of 70/30 or 50/50%. With these three regimes, breathing was spontaneous; artificial ventilation through a tracheal cannula was only used if spontaneous ventilation failed. 4) The anaesthetic was as in regime (3) but pancuronium bromide 2mg/kg was injected intravenously at regular intervals and the animal was ventilated artificially from the outset with a 50/50% mixture of nitrous oxide/oxygen. The anaesthetic dose was increased if heart rate or blood pressure increased above normal levels. Successive doses of pancuronium were delayed until the animal attempted to breathe spontaneously; the anaesthetic dose was increased if there was any withdrawal response to pinching of the toe web. For regimes

2&3, the anaesthetic dose was kept to the minimum at which no withdrawal response to pinching of the toe web was observed. Animals were sacrificed at the conclusion of the experiment without recovery of consciousness.

The right femoral artery and vein were exposed by an incision over the medial aspect of the thigh. They were cannulated with Portex (Hythe, Kent) polythene cannulae (o.d. 0.75 mm) which were inserted for about 4mm. Central venous pressure was measured in some animals by inserting a similar cannula into the right internal jugular vein through an incision in the neck. The tip of the cannula was advanced until it was estimated to lie in the superior vena cava. A tracheal cannula was inserted through a tracheostomy, and was aspirated every hour or so. The ECG was recorded from needle electrodes in one forelimb and one hindlimb. Blood pressure was recorded from the femoral arterial cannula with a Bell and Howell (Basingstoke, Hants) pressure transducer type 4-422-0002. Blood samples of 0.3 ml were withdrawn from the femoral arterial cannula and pO_2 , pCO_2 and pH were measured on a Radiometer (Copenhagen) PHM 72 machine. Each sample was replaced with an equal volume of normal saline. Respiratory rate (in spontaneously respiring animals) was calculated from observation over a 15 sec period. Blood gases, respiratory rate and blood pressure were not measured systematically throughout the entire course of experiments.

Artificial ventilation was performed with a stroke volume of 1 - 3 ml at 100 cycles per min, which was adjusted to produce normal blood gases (Table 3.1). 0.9% saline was infused into the femoral vein at between 0.5 - 1 ml/hr. If blood pressure fell, attempts were made to restore it by slow intravenous injection of 0.5 ml boluses of Dextran 70 (intravenous infusion) or 0.9% saline, or by 1 ml/kg of 1 in 10,000 adrenaline followed if necessary by infusion at 0.5 - 2 ml/hr. Acidosis was corrected by intravenous infusion of 1-2 mMol/kg body weight of 8.4% sodium bicarbonate. Experiments were performed at room temperature. Rectal temperature was maintained at 37 -39 °C by a warming pad placed under the rat.

In some experiments, scalp warming was produced either by a 60 W electric light placed about 10 cm from the scalp, or by passing water at or

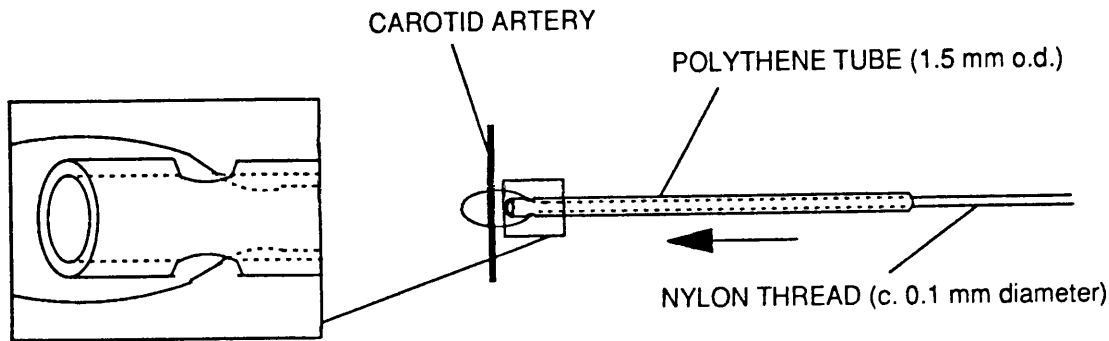


Figure 2.1. Clasp used to occlude the common or internal carotid arteries. A nylon thread approximately 30 cm in length and 0.1mm in diameter was looped around the exposed carotid artery. The free ends of the thread were inserted through the orifices at created at one end of the polythene sleeve and then could be slid to the other end of the sleeve without difficulty. Carotid artery occlusion was achieved by sliding up the sleeve towards the carotid artery. Occlusion was maintained by clamping the free ends of the nylon thread. To enable reperfusion, the sleeve was withdrawn by about 5 cm. The carotid arteries appeared to be patent with a normal flow after repeated periods of occlusion of up to 30 min.

The nylon thread was sufficiently flexible so that no accidental occlusion of the common carotid artery due to twisting or traction occurred. The geometry and size of the internal carotid artery was such that accidental occlusion could occur. It could be avoided if the rat was supine and the clasp was angled laterally and kept under direct vision. The advantage of this method was that common carotid artery occlusion could be reliably performed when the rat was prone and direct surgical occlusion of the arteries was not feasible.

above body temperature through a water jacket which covered the entire scalp including temporal areas. Thermal contact between the water and the scalp was across a latex sheet approximately 0.1 mm in thickness.

2.1.2. Method for production of cerebral ischaemia.

A longitudinal incision was made over the first cervical vertebra, and the alar foraminae were exposed by blunt dissection. The neurovascular bundle was coagulated with the tip of a soldering iron, and then the vertebral arteries were exposed by drilling out the foraminae with a burr 1mm in diameter. The vertebral arteries were coagulated under direct vision by unipolar diathermy with a tapered wire electrode about 0.2 mm in diameter at its tip and an earth pad on the fore-limb. The rat was then turned to a supine position, and a midline longitudinal incision was made in the neck. The common or internal carotid arteries were exposed, and the wound edges were retracted by an Alm's skin retractor. Exposed structures were kept moist by the application of liquid paraffin. Cerebral ischaemia was produced by reversible bilateral occlusion of the arteries for about 5, 15 or 30 min with a clasp (see Fig. 2.1.). Following reperfusion, the arteries were inspected through a binocular microscope (magnification x 20) to ensure patency. Some measurements were made with the rat in the prone position. In this case, the retractor was left expanded in position and carotid artery patency was verified with the aid of a mirror placed underneath the neck.

2.1.3. Measurement of impedance.

Impedance was measured by a four electrode method operating at 50 kHz. Up to four different electrode configurations were recorded simultaneously with the use of a multiplexer (Fig. 2.2, 2.3 and see section 2.3). All electrodes were made of silver with the exposed surface chlorided. Measurements on the cerebral cortex were made with 0.075 mm diameter teflon coated wire formed into balls about 1mm across at one end. These were

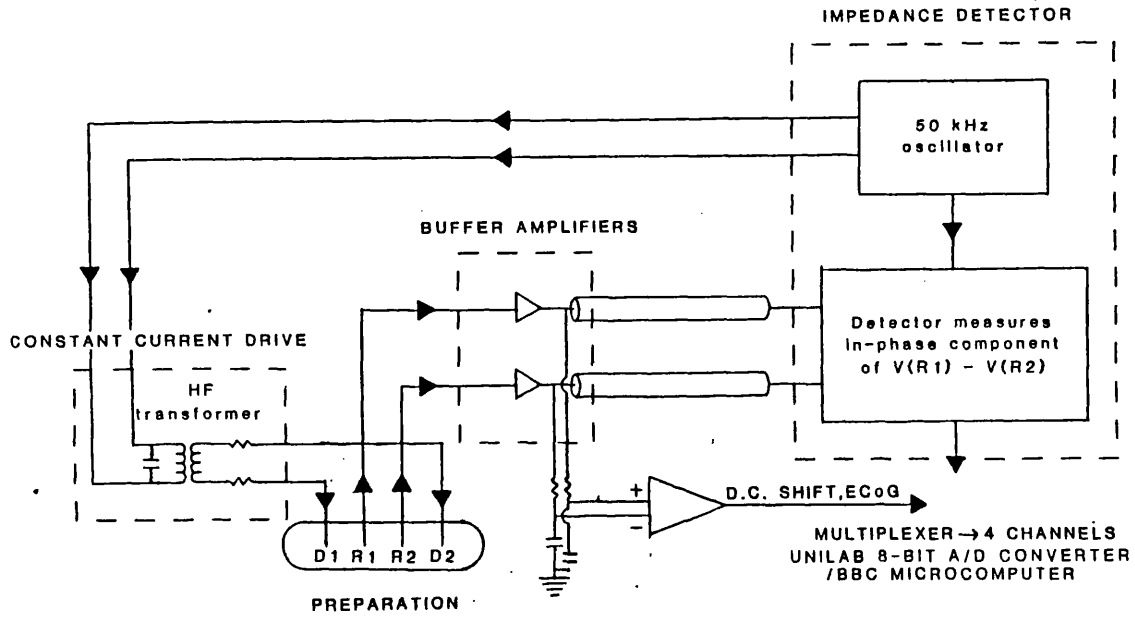


Figure 2.2. Experimental arrangement for measuring impedance. See text for further details.

set into a thin flexible sheet which consisted of epoxy resin (Rapid Araldite, CIBA-Geigy) about 0.5 mm in thickness, sandwiched between two sheets of polyvinylchloride clingfilm. The silver balls initially protruded on one side of this sheet; they were filed flush, which produced a circular exposed area about 1mm in diameter. The sheets were trimmed to a rectangle about 4mm by the appropriate width for the electrode configuration, and were secured by placing two sides of the sheet under the edges of craniotomies made to expose the selected areas of cortex. Scalp measurements were made with wires, 0.5 mm in diameter, and about 4 mm long, which were attached to flexible insulated copper wires.

The animal was earthed with a Ag/AgCl electrode placed in the abdomen or tail.

2.1.4. Preparation of the scalp.

The scalp was depilated with a thioglycollate foam (Immac, Anne French), and covered with a sheet of PVC clingfilm. The electrodes were inserted subcutaneously and secured by gluing the insulated electrode leads to the scalp with cyanoacrylate glue. The electrodes and attached wires were further secured by a lightly applied elastic net (Netelast size B, Roussel medical). This arrangement prevented disturbance of electrode placement if the rat was subsequently turned to the supine position for carotid artery occlusion.

Scalp prepared in the above fashion is termed "normal" below. In some experiments an ellipse of scalp about 2 x 1 cm over either or both parietal regions was excised and then sutured in its former position, in order to interrupt any nervous or vascular connections. In other experiments, similarly excised scalp was placed on a layer of paraffin film about 0.5 mm thick ("Nescofilm") in order to insulate it electrically from underlying tissues. Cyanoacrylate glue was used to secure the paraffin film to the skull, and to replace the excised scalp in its former position. Electrical discontinuity from the animal was checked by verifying that D.C. resistance between the excised

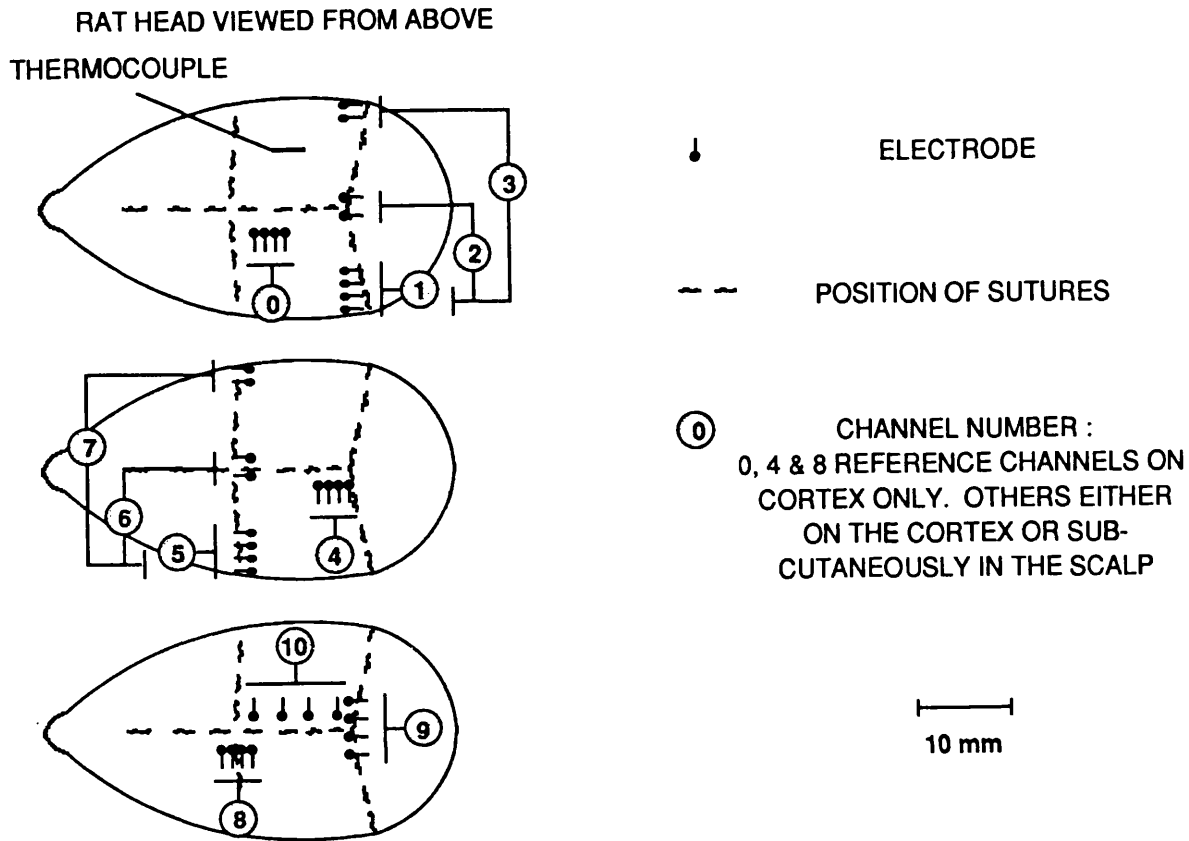


Figure 2.3. Positions of electrodes on the rat's head. Electrode spacings were : 1mm apart - 0, 4 & 8, 2mm apart - 1, 5 & 9, 3mm apart - 10. 2,3,6 and 7 comprised pairs of electrodes 2 mm apart; the pairs were placed about 13 mm (2 & 6) or 26 mm (3 & 7) apart. Simultaneous recording from positions 1) 0-3, 2) 4-7, 3) 1 on the left and right & 8, or 4) 1 & 9 was performed in different experiments.

scalp and the animal was greater than 1 meg Ω . Scalp electrodes were placed subcutaneously in these preparations, which are referred to as "surgically isolated" and "electrically isolated" below.

2.1.5. Measurement of other variables.

The DC potential difference between the two impedance recording electrodes in electrode position 0 was recorded by passing the signal through a low pass filter ($F_c = 1$ kHz). Temperature was recorded with a single Type K (Chromel-Alumel) thermocouple placed subcutaneously or epidurally and a digital thermometer. In some experiments temperature was measured simultaneously from both frontoparietal areas; the difference was 0.1 ± 0.07 °C ($n=18$ in 6 rats), so that temperature measured at one site was taken to be representative of the temperature at any electrode position. The thermocouple was electrically insulated and had an external diameter of about 1 mm. Blood pressure was recorded from a femoral arterial cannula.

Up to four multiplexed impedance channels, DC potential, blood pressure and cortical or scalp temperature were amplified and recorded digitally with the use of a Unilab (Blackburn, U.K.) A/D converter and Acorn "BBC" microcomputer (Fig. 2.2). Data were sampled approximately every 3 s.

2.1.7. Data analysis.

The baseline for impedance and temperature records was defined as the extrapolation of the linear regression of the record during 5 min preceding carotid artery occlusion. The duration of changes was estimated by measuring the full width at half maximum (FWHM). Examples of impedance measurements shown in the figures have been corrected for baseline shift.

The carotid arteries were occluded for approximately 5, 15 or 30 min. Impedance and temperature change (δZ and δT) were measured at 5, 15, or 30 min after the onset of carotid artery occlusion. The figure in parentheses refers to this interval in minutes (*e.g.* $\delta Z(15)$). $T_{\%w}$ is the time taken after the onset

of carotid artery occlusion for δZ to reach half its value at the specified time of measurement. $T_{1/2(d)}$ is the interval between the time at which δZ was maximal and the time at which it returned to half of its maximum value. Generally, the maximum impedance change occurred at, or shortly after, the end of the period of carotid artery occlusion. In some cases, it occurred near the start of the period of ischaemia (see Fig. 3.3 for an example), and to measure it in the same way would have given a misleading result. In these cases, $T_{1/2(d)}$ was taken as the interval between the end of carotid artery occlusion and the time at which δZ returned to half of its value at the end of carotid artery occlusion. After some ischaemic episodes, impedance remained elevated above 50% of its maximum value so that $T_{1/2(d)}$ and FWHM could not be measured.

A varying number of ischaemic episodes were produced in any individual experiment. There was no significant difference in $\delta Z(5)$ or $\delta Z(15)$ measured during successive ischaemic episodes in the same animal with periods of carotid artery occlusion of 5 or 15 min (Table 2.1). Therefore δZ , δT and $T_{1/2(w)}$ measured during longer periods of carotid artery occlusion (*e.g.* measurement at 5 min during a 15 min carotid artery occlusion) have been included in the results presented. Such data were only included from the first of any episodes with carotid occlusion of 30 min, as there were insufficient numbers to establish if measurements in subsequent periods of ischaemia were different.

Equally, the variance of δZ during successive occlusions did not differ significantly to its variance in different animals (Table 2.1). Results from any one ischaemic episode were therefore treated as independent (*i.e.* standard error was calculated taking n as the total number of ischaemic episodes).

$\delta Z(\%)$ measured at :	5 min			15 min	
	0, cort	1, cort	1, scalp	0, cort	1, scalp
n	46	18	24	19	7
N	8	4	8	3	2
F (episode vs experiment)	0.6	1.1	0.7	0.2	0.1
F (episode vs error)	1.6	1.4	1.2	1.1	0.3

Table 2.1. Two way analysis of variance of the impedance change (δZ) measured at 5 or 15 min between successive ischaemic episodes in one animal and between animals. n - total number of ischaemic episodes in different animals. N - maximum number of successive ischaemic episodes in one animal. $p > 0.05$ for all F ratios.

There was no significant difference in $\delta Z(5)$ or $\delta Z(15)$ at the three most measured electrode sites with respect to the use of halothane or alphaxolone/alphadolone (Table 2.2a), or to occlusion of the common or internal carotid arteries (Table 2.2b). Data collected under these different conditions were therefore pooled for analysis. Data from experiments in which the anaesthetic was urethane were not directly comparable, as different electrode positions were used.

a)

δZ measured at:	Electrode site	Anaesthetic	δZ (%) Mean	δZ (%) S.E.	n	p
5 min	Cortex (0)	A/A	18.7	1.9	35	NS
"	"	Hal	16.4	2.5	11	
15 min	Cortex (0)	A/A	17.5	2.0	14	NS
"	"	Hal	26.8	5.9	5	
5 min	Scalp (1)	A/A	2.7	0.2	19	NS
"	"	Hal	2.7	0.3	12	

b)

δZ measured at :	Electrode site	Ligation	δZ (%) Mean	δZ (%) S.E.	n	p
5 min	Cortex (0)	C.C.	18.0	2.2	13	NS
"	"	I.C.	18.2	1.9	33	
15 min	Cortex (0)	C.C.	26.8	5.9	5	NS
"	"	I.C.	17.5	2.0	14	
5 min	Scalp (1)	C.C.	3.0	0.4	8	NS
"	"	I.C.	2.4	0.2	16	

Table 2.2. Comparison of impedance changes (δZ) during : a) Anaesthesia with Hal - inspired halothane or A/A - intravenous alphaxolone/alphadolone. b) Ligation of either the internal (I.C.) or common (C.C.) carotid arteries. Electrode position in parentheses. Measurements at room temperature. NS - $p > 0.05$ (Student's unpaired t test).

2.2. IMPEDANCE CHANGES DURING SPREADING DEPRESSION IN THE ANAESTHETIZED RAT.

2.2.1. Animal preparation.

Male Sprague-Dawley or Wistar rats, weighing about 250g, were kept under the conditions described in section 2.1.1. They were anaesthetized with 5.7 ml/kg of 25% w/v urethane injected intraperitoneally, and breathed spontaneously through a tracheal cannula. The rat's head was held securely by ear bars. A craniotomy was made just large enough to admit an acrylic cup 4mm in diameter which rested on the cortical surface. Cerebral cortex was superfused continuously with artificial CSF (147 mMol/l NaCl, 3mMol/l KCl) flowing in and out of the cup. Liquid paraffin or silicone grease were placed around and on the top edge of the cup in order to produce a high resistance between the surrounding scalp and cortex exposed in the cup. Spreading depression was initiated by changing the superfusing solution to 150 mMol/l KCl for 20 s. Impedance was measured on the cortex or scalp; for measurements on the cortex, the craniotomy was enlarged to admit the

electrode array. The nearest electrode was placed about 4mm away from the cup. Experiments were performed at room temperature. Rectal temperature was maintained at 37 - 39 °C by a warming pad placed under the rat. In some experiments scalp warming was produced by placing a 60W electric light vertically over the scalp at a distance of about 10 cm. Animals were earthed by a Ag/AgCl electrode in the abdomen or tail.

2.2.2. Measurement of impedance.

Impedance was measured at 50 kHz by the method described in section 2.3. All electrodes were made of chlorided silver. Cortical and most scalp impedance measurements were made using a linear array of nine circular electrodes. Each consisted of the cut end of Ag wire, 0.25mm in diameter, set flush in a block of epoxy resin (Araldite, CIBA-Geigy) at intervals of 0.5 mm. The block could be positioned with varying degrees of pressure by a micromanipulator holding twisted stainless steel wires set into it. Unless stated otherwise, measurements were made with four adjacent electrodes selected from this array. This arrangement is termed the "araldite array" below.

Three scalp recording arrangements were compared : 1) The araldite array was pressed firmly onto abraded scalp. 2) Wires, 0.5 mm in diameter, were soldered to insulated flexible copper leads, leaving an exposed length of about 4 mm. These were inserted into the scalp subcutaneously in a coronal direction at intervals of 1mm. Some were lightly secured by an elastic net, others were compressed by a weight of 100g. 3) 3 mm lengths of 1mm diameter polythene tubing were glued to the scalp at intervals of 1.5 mm by collodion. Electrical contact was through balls 0.25 mm in diameter which were placed on 3 Mol/l NaCl - 3% agar introduced into the tubes.

2.2.3. Measurement of other variables.

DC potential was measured from inside the superfusing cup by a ball

about 0.25 mm in diameter placed on the cortical surface, or from one impedance recording electrode by passing the signal through a low pass filter ($F_c = 1$ kHz). In some scalp recording experiments (e.g. Fig. 3.16) a small ball at the end of a teflon-coated wire 0.075 mm in diameter was introduced between the dura and skull so as to lie under the centre of the impedance electrode array. This potential was then recorded in series with DC potential in the cup by passing the signals respectively to the positive and negative inputs of a differential amplifier; signals from the two sites could be distinguished as the cup potential was reversed.

In some scalp measurements, temperature was recorded by insulated copper-constantin thermocouples and digital thermometers. Epidural temperature was recorded with thermocouple wire 0.1 mm in diameter whose tip lay under the araldite array. Scalp temperature was recorded with wire 0.5 mm in diameter, whose tip lay sub-cutaneously about 2 mm lateral to the centre of the araldite array.

The ECG was recorded from the fore-limbs. The respiratory cycle was monitored by measuring temperature at the outlet of the tracheal cannula with a thermocouple and digital thermometer.

2.2.4. Data acquisition.

Impedance and DC potential were amplified and recorded on a chart recorder. Some scalp records, and all records in which the ECG, respiration or temperature were measured, were digitized on a Unilab (Blackburn, U.K.) A/D converter and Acorn "BBC" microcomputer and stored on disc. Quantitative analysis on other records was performed by manual sampling of records at intervals of 1 min.

In one experiment (Fig. 3.12) averaging of scalp impedance was performed by triggering acquisition on the A/D converter from either the ECG or the respiratory cycle.

2.2.5. Data analysis.

Baseline analysis (Fig. 3.11, Table 3.5) was performed on representative periods of 15 min per experiment. The gradient was calculated from a best-fit linear regression. "Minute-to-minute variation" was calculated as the standard deviation of data points around the linear regression.

In records collected during spreading depression, analysis was performed on a period of 12 min centred on the peak of the impedance change. The baseline was defined as the line between the mid-points of the linear regression of the first and last 3 min of the selected period. Where no impedance change was apparent, the analysis period was selected by alignment of the cup DC potential with records from the same experiment in which a clear impedance change was observed (*e.g.* Fig. 3.13, 3.14 and 3.16). Analysis of impedance and temperature records was performed on records corrected for baseline slope. The "area" (Table 3.5) was calculated as the sum of the area between the record and baseline between the two portions used to calculate the baseline. $\delta Z(\max)$ is the maximum absolute deviation of impedance from the baseline expressed as a proportion of the resting impedance.

Comparison of the means of two groups of data was performed by Student's unpaired t test. One way analysis of variance was performed on more than two groups. The variance of $\delta Z(\max)$ in different experiments was significantly larger than its variance in successive episodes of spreading depression in the same animal ($F = 14.1, 64.9$ for measurements on the cortex and scalp respectively, one way analysis of variance on data in Table 3.2). Replicated measurements within one experiment could therefore not be treated as independent. There was no significant linear correlation between impedance, or DC potential peak changes or FWHM (full width at half maximum), and the number of previous episodes of spreading depression, for measurements on the cortex (Table 2.3). The mean of the observations for a given variable within one experiment was therefore treated as a single observation (the standard error was calculated from these mean values with n as the number of experiments). Results are presented as mean \pm 1 standard

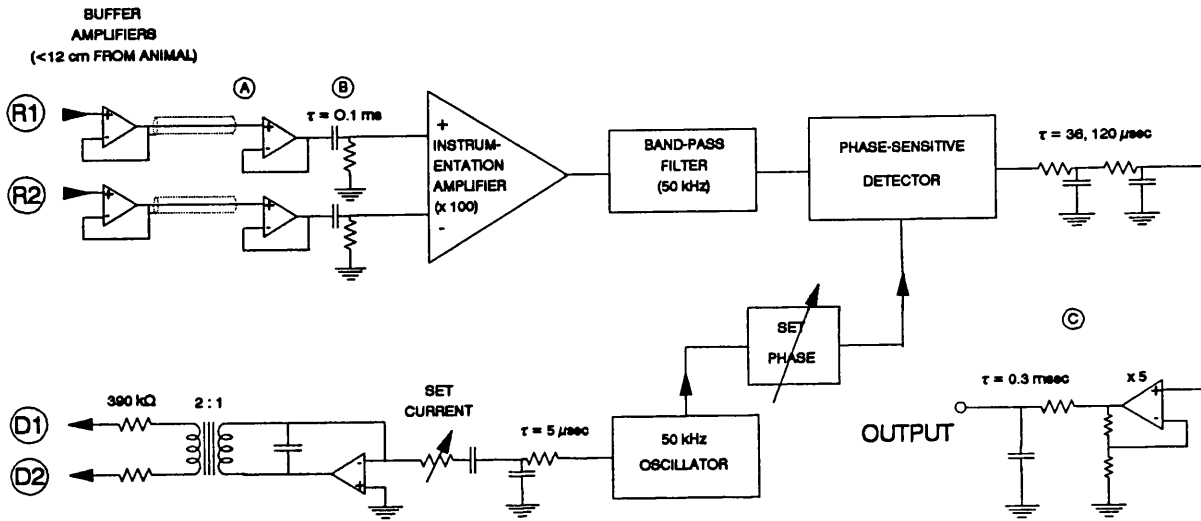


Figure 2.4. Diagram of the impedance measuring device. See text for details.

error (S.E.).

Variable	r	n	p
Impedance :			
$\delta Z(\text{max})$ (%)	0.13	15	NS
FWHM (min)	0.53	15	NS
DC potential :			
Peak (mV)	0.04	43	NS
FWHM (min)	0.07	43	NS

Table 2.3. Analysis for trends in measurements during successive episodes of spreading depression within one experiment. Data were collected with the araldite array on the cortex in up to 17 episodes of spreading depression in 4 rats, and were normalized by dividing each value by the equivalent value during the first episode of spreading depression. Impedance measurements were made with electrodes spaced 0.5 mm apart. r - linear regression correlation coefficient for the specified variable against number of previous episodes of spreading depression in the experiment.

2.3. MEASUREMENT OF SINGLE CHANNEL IMPEDANCE AT 50 kHz.

2.3.1. Principle and description of impedance measuring device.

Impedance was measured using four electrodes. A constant current at 50 kHz was applied to two "drive" electrodes (D1 and D2), and the impedance was taken to be proportional to the in-phase component of the potential difference between two other "recording" electrodes (R1 and R2). An overall diagram of the experimental arrangement for recording impedance on rat cortex is shown in Fig. 2.2. A more detailed diagram of the circuit is shown in Fig. 2.4. A 50 kHz master square wave signal was passed through a low pass filter ($\tau = 4.7 \mu\text{sec}$) to produce a sine wave. This passed to a step-up transformer, series resistances of 390 k Ω and then to drive electrodes D1 and D2. The transformer was balanced by adjustment of variable resistance and

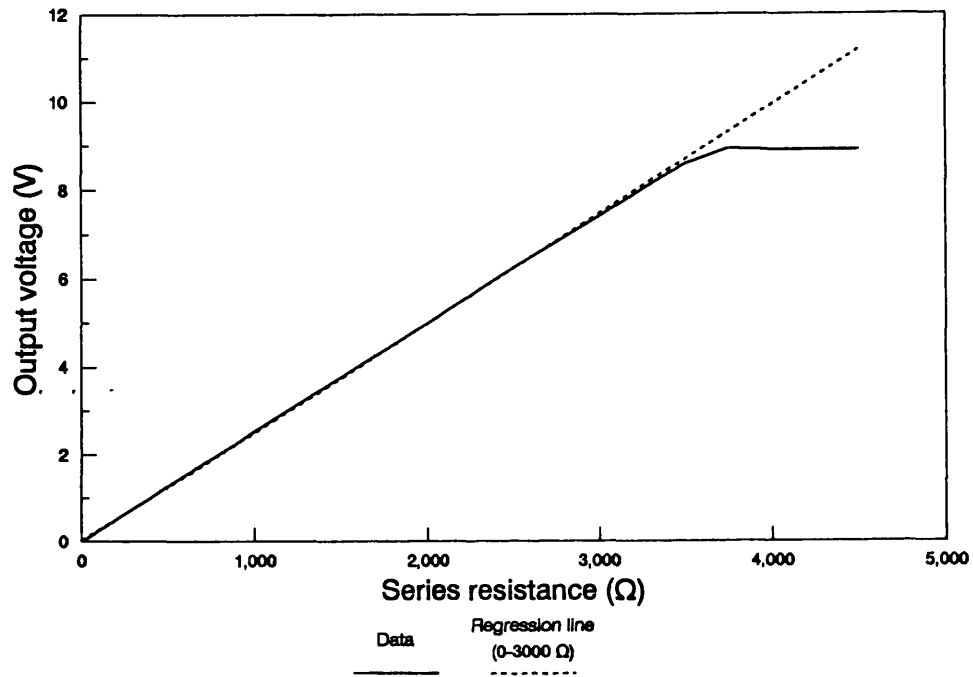


Figure 2.5. Calibration curve for impedance measuring device. R1 and R2 were connected to D1 and D2 respectively. The output voltage of the device is plotted against a varied series resistance inserted between R1/D1 and R2/D2. The relationship is linear up to about 3000 Ω.

capacitance placed on its input side, so that the two drive potentials were equidistant to earth. In practice, these could be adjusted so that the current to earth was less than 1% of the drive current. Currents applied were 22 - 56 μA (peak-to-peak). They were adjusted, if necessary, to avoid saturation of amplifiers on the recording side of the circuit.

The leads attached to the recording electrodes on the preparation were not screened. They were less than 12 cm long, and inserted into buffer amplifiers placed close to the preparation. The signal was passed from these along leads with driven screens, about 40 cm long, to the impedance measuring device. The two signals were A.C. coupled and passed to an instrumentation amplifier (AD 521, Analog Devices, Norwood, Massachusetts, USA) and a 50 kHz pass-band filter. A phase-sensitive detector was then used to transmit the full-wave rectified in-phase component of the signal. The phase was adjusted so that there was no detectable change in output when the electrode leads were connected to a variable resistance and capacitance in series and the capacitance was altered. The signal was then smoothed and amplified further to produce a D.C. output proportional to the tissue impedance. The frequency response of the system was therefore from D.C. up to a limit set principally by the final output filter, $f_c = 482$ Hz. With the exception of experiments intended to investigate faster changes (Fig. 3.12), small pulse and respiration related components were reduced by the addition of a single stage passive low-pass output filter, $\tau \approx 1$ sec.

2.3.2. Calibration of impedance measuring device.

A linear relationship between output voltage and test resistance was obtained for resistances up to 3 k Ω with a maximum drive current (Fig. 2.5).

2.3.3. Design and performance of impedance multiplexer.

A multiplexer was used in some experiments on cerebral ischaemia. It enabled the parallel acquisition of impedance from four different electrode

combinations. Switching was produced by four DG 526 (Siliconix, Santa Clara, California) analogue switch integrated circuit chips. The drive current or measured potential difference passed through only one switch each. The series resistance of each switch was 250 Ω . With a test arrangement of resistances with values estimated to be similar to those *in vivo*, the output of the impedance measuring device decreased by less than 1% when the multiplexer was added. The effect of signal attenuation due to stray capacitance in the multiplexer was therefore concluded to be negligible, and was ignored in data analysis.

The St. Thomas's oscilloscope program was modified so that four different combinations of electrodes could be selected in software and displayed on the computer screen. Generally, 12 electrodes were applied, and an automatic impedance testing routine was added. Switching between channels occurred about once every 4 sec.

2.3.4. Estimation of resting impedance values.

All impedance data are presented as a proportional change relative to the resting level so that results from different records are comparable. This was calculated by dividing the output of the impedance measuring device under the specified condition by its value under resting conditions. Absolute impedance values were estimated on the assumption that there was a linear relation between the potential difference between R1 and R2 and that between D1 and D2. Therefore the output of the impedance measuring device was multiplied by the ratio of the distance between D1 and D2 to that between R1 and R2. This value was then converted to impedance by the use of the calibration slope for the current selected data (*e.g.* Fig. 2.5).

2.4. IMPEDANCE IMAGING OF CEREBRAL ISCHAEMIA IN THE ANAESTHETIZED RAT.

2.4.1. Animal preparation.

2.4.1.1. Method of producing cerebral ischaemia.

Cerebral ischaemia was produced by the method described in section 2.1. All rats were paralysed with pancuronium bromide, artificially ventilated, and were anaesthetized with inspired halothane. The common carotid arteries were occluded for 15 min. More than one hour elapsed between successive episodes of ischaemia. Measurements were made with the rat in the prone position. Satisfactory carotid artery occlusion and reperfusion were inferred from inspection of the carotid arteries and observation of characteristic changes in the arterial blood pressure. Cortical DC potential was only measured in experiments which measured cortical impedance; the scalp and skull remained intact in experiments in which scalp impedance changes were measured.

Cortical or scalp temperature was measured using a thermocouple placed over the right parietal region. During cerebral ischaemia *in vivo*, cortical or scalp temperature was maintained as close as possible to the resting level by raising or lowering a table lamp placed over the rat's head. An Ag/AgCl earth electrode was placed in the animal's tail.

2.4.1.2. Electrode design and placement.

EIT images were obtained using an approximately elliptical array of sixteen Ag/AgCl electrodes placed either on the cortex or in the scalp. The cortical electrode array consisted of blocks of silver set into a ring of dental acrylic about 4 mm wide. It was made to correspond to the contours of the rat brain in the plane from the frontal to occipital lobes. The internal dimensions were 21mm in the sagittal and 13 mm in the coronal directions (termed "Y" and "X" axes respectively below). Each electrode surface was an area 3mm

high and 1mm wide on the inside of the array. These were placed at regular intervals symmetrically either side of the midline. They were connected to a flexible lead with a driven screen 12 cm in length by a solder joint which was sealed into the acrylic. The array was applied to the brain through an approximately elliptical craniotomy made by drilling with a dental burr 1mm in diameter. It was about 5 mm wide and stretched from the frontal lobes, about 18 mm anterior to the bregma, caudally to the occiput immediately above the foramen magnum. To prevent haemorrhage from the venous sinuses, this was performed in two stages : 1) Craniotomies were made and the dura was reflected over three separate areas which were about 5mm wide and in the occipito-frontal plane between the superior sagittal and both transverse venous sinuses. 2) The remaining segments of bone over the sinuses were then removed by drilling furrows which continued from the edges of the craniotomies already created. This left unsecured rectangles of bone, about 3 mm square, over each venous sinus. These could be removed without causing venous haemorrhage by gentle lateral leverage with watchmaker's forceps. The dura immediately over the venous sinuses was left intact. The electrode array was then lowered onto the exposed surface and secured by elastic bands at either end. Any exposed cortex was covered with PVC clingfilm.

Scalp electrodes were made of Ag wire, 0.5 mm in diameter. One end was soldered to a 12 cm length of multistranded copper wire, 1mm o.d. The solder joint was insulated with silicone rubber glue, and 4 mm of wire was left exposed. Flexible unscreened leads were used in order to minimize traction on the scalp. The electrodes were inserted at regular intervals in the fronto-occipital plane in a direction radial to the vertex. The dimensions of the approximate ellipse formed by the mid-points of the wires was about 25 and 18 mm in the Y and X axes respectively. The leads were attached to the scalp with cyanoacrylate glue. A layer of PVC clingfilm was placed over the leads and scalp and this was secured with a tubular elastic net (Netelast, size "B", Roussel medical).

The leads attached to the electrodes were connected to the front panel of the EIT device by screened leads which were 4 mm in outer diameter and

30 cm long. The leads were gathered into two bundles from either side of the head, and were not moved during recording.

2.4.1.3. *Post-mortem* measurements.

In one animal with cortical electrodes, and two with scalp electrodes, EIT images were collected from immediately after death for a period of 30 min. (The observed impedance changes were only due to post-mortem processes; no other manipulation was performed).

2.4.2. The electrical impedance tomography (EIT) system and application.

2.4.2.1. The EIT system.

Measurements were made with a Sheffield EIT data collection system (see Brown and Seagar, 1987). The impedance is measured by a four electrode system, similar to that described in section 2.3. A master clock runs at 820 kHz, and is used to generate a 51 kHz constant current sine wave which is applied to two drive electrodes. The potential difference between two recording electrodes is amplified and passed to a phase sensitive detector, adjusted to select only the in-phase component of the signal. This is sampled and stored in a microcomputer (Fig. 2.6).

A multiplexer is used to select a preset range of electrode combinations. The principle of measurement is that current is applied to a pair of adjacent electrodes and the potential difference is then recorded from different pairs of adjacent electrodes. As potential measurement from an electrode through which current is passing is unreliable, the potential difference is sampled from 13 available electrode pairs whilst any one drive electrode pair is selected. This is repeated for all possible 16 drive pairs, so that the final data set comprises 208 values. Each value is acquired in 380 μ sec, so that the entire set is collected in 79 msec. Because of the wide dynamic range of about 40,000:1 each signal is normalised between the phase sensitive detector and

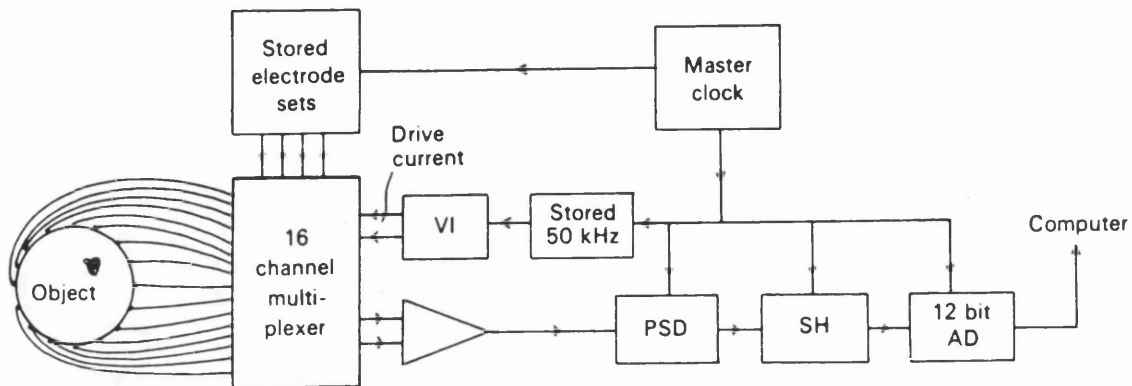


Figure 2.6. Block diagram of EIT data collection system. See text for explanation. VI - voltage to constant current converter; PSD - phase sensitive detector; SH - sample and hold circuit; AD - analogue to digital converter.



Figure 2.7. Physical dimensions of the Sheffield EIT system. The EIT hardware is housed in the box underneath the monitor. The other equipment is an IBM compatible computer and colour dot-matrix printer.

sample and hold stages("PSD" and "SH" in Fig. 2.6), by expressing it as a proportion of a stored value predicted theoretically for a homogeneous subject.

This data set is reconstructed by a single-pass weighted back projection algorithm (Barber and Seagar, 1987) on a Research Machines (Abingdon) microcomputer with an Intel 80186 microprocessor with an 80187 maths co-processor. Reconstruction of one image is performed in less than 5 sec. The algorithm used in these experiments assumes : 1) The electrode array is circular, and is surrounded by an area of infinite impedance, 2) Changes in impedance are small compared to the resting impedance, and 3) The object to be imaged has uniform initial impedance. Generation of images of the absolute impedance require precise knowledge of electrode spacing; therefore images generated with this technique were only of the difference in impedance with respect to a specified reference image.

A photograph of the Sheffield EIT system, to illustrate its small physical dimensions, is shown in Fig. 2.7.

In these experiments, 200 complete data sets were averaged to reduce noise, and one image was recorded each minute. The reference phase of the phase sensitive detector was set at the value which gave the least variability in the EIT image when saline in tanks containing the cortical or scalp array (see below) was varied from 0.118 - 0.354% g/l of NaCl. The maximum drive current possible was 5 mA peak-to-peak. This was adjusted to prevent saturation of the input amplifiers; the current used in records in the rat was about 2 mA peak-to-peak.

2.4.2.2. Experimental arrangements for calibration.

The different arrangements were :

1) "Large cylindrical tank". Sixteen brass bolts were placed halfway up and equally spaced around a plastic cylinder, 15.3 cm in diameter and 24 cm high. They were 3 mm in diameter and projected 15 mm into the tank.

2) "Cortical array tank". The cortical electrode array was set in a roughly cylindrical tank, constructed so that its internal cross-section was the

same as the inner dimensions of the electrode array. The walls were constructed of a rolled up flexible acrylic sheet, which was bonded to the electrode array and perspex base with silicone rubber glue. The electrode array was placed halfway up the tank, which was 5 cm high.

3) "Scalp array tank". The sixteen scalp electrodes were inserted at equal intervals through holes in an acrylic plate so as to form an ellipse 21 x 16 mm along its axes. A rolled flexible acrylic sheet was placed around the electrodes on the upper surface of the acrylic plate, forming an ellipsoidal tank which was filled with saline to a height of 3.5 cm. Bonding was performed with silicone rubber glue.

4) *Post-mortem* calibration. Some experiments were performed *post-mortem* in animals in which scalp electrodes had been placed. The animals were placed in a supine position on an acrylic mould which preserved the cervical lordosis and the position of the scalp electrodes. The mandible and palate were removed, and the ventral surface of the brain was exposed by removing the roof of the nasopharynx with bone clippers. Rods were inserted vertically into the brain, or else it was evacuated and replaced with saline solution or air. In this way the cranial contents could be altered without directly disturbing the scalp electrodes.

An Ag/AgCl earth electrode was placed at the top or bottom of the tank in 1-3) and in the tail in 4). Details of each calibration are presented with the results in section 3.3. The tanks were filled with saline, which consisted of 0.118 g/l (20 mMol/l) NaCl, unless otherwise stated; this had a resistivity similar to that of brain.

2.4.2.3. Data analysis.

Each reconstructed image generated by the Sheffield EIT system consists of an array of 32 x 32 pixels. Each dimension of the array corresponds to one axis in the plane of the electrode array (defined as the X or Y axis), so that non-circular electrode arrays are represented by a circular image. The value of the central 812 pixels of these, which form an approximately circular area,

represent a change in impedance (defined as the Z axis). The surrounding pixels were arbitrarily set to zero, and were not used in the data analysis described below. In the results section, these data have been displayed either as a three dimensional surface or as a contour map. In each case the orientation of the display is identified by a diagram of a corresponding slice through the rat's head. All images represent a change in impedance with respect to a specified reference frame.

A program was written (in Microsoft Quickbasic, version 4.5) which enabled manipulation and analysis of these images on an IBM compatible AT 286 microcomputer: Each pixel in *in vivo* or *post-mortem* images was corrected separately for baseline shift. The baseline was taken to be the extrapolation of the linear regression of the period of 10 min prior to carotid artery occlusion. Images from different ischaemic episodes were combined by taking the average for each pixel. The standard deviation in the XY plane was calculated by approximating a Gaussian curve in two dimensions to the impedance changes (for either the whole image or a specified peak) with respect to the XY plane. The standard deviation for either the X or Y axis was calculated in a similar way in one dimension. A peak in the image was defined as a point where up to three pixels of equal value were greater than all of the pixels in a surrounding grid of 5 x 5 pixels, and where this was separated from any peak with a greater magnitude by a trough whose value fell to $1/e$ times the average of the two peaks. Statistics regarding such a peak were calculated with respect to the area around the peak where the pixels had a value greater than the peak value / e . An estimate of the standard deviation for individual peaks was taken to be the radius of a circular area approximating to this area. The average pixel value was calculated as the mean pixel value over this area, and the volume under a peak was calculated as the sum of all the values of the pixels in it. The Full Width at Half Maximum (FWHM) was calculated as 1.665 times the standard deviation in the XY plane.

3. RESULTS.

3.1. IMPEDANCE CHANGES DURING CEREBRAL ISCHAEMIA IN THE ANAESTHETIZED RAT.

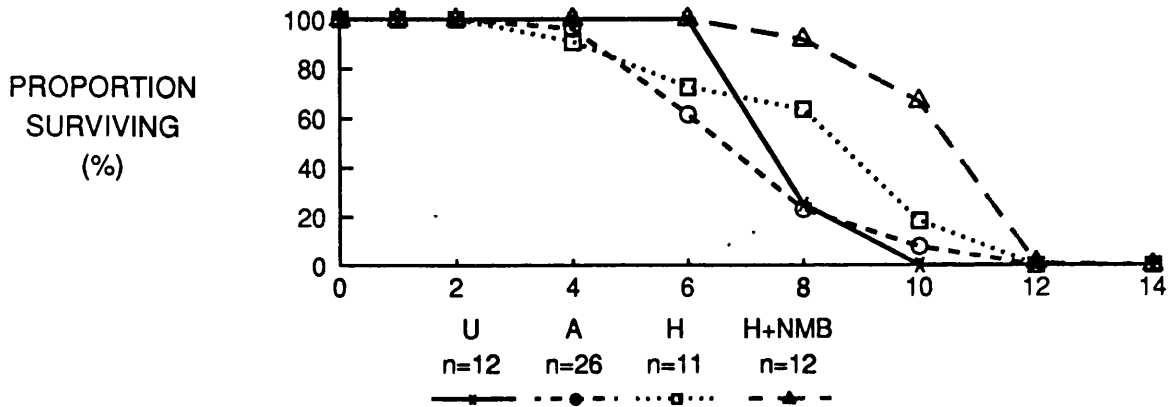
3.1.1. Technical issues.

3.1.1.1. Tolerance of the preparation to the procedures.

Up to eight 5 min, or three 15 min, or two 30 min episodes of carotid artery occlusion were performed in any one animal. In many experiments, less than this number were produced because cardiovascular deterioration led to death (Fig. 3.1). A characteristic pattern of deterioration was observed : The blood pressure tended to fall gradually over hours following diathermy of the vertebral arteries. Blood pressure rose by 49.6 ± 2.8 mm Hg from a resting level of 88.3 ± 2.4 mm Hg (mean \pm S.E., n=82) after occlusion of the carotid arteries, but on reperfusion, blood pressure returned variably either to its former level or fell to lower levels. The blood pressure often remained depressed, in spite of attempts to restore it.

Prolonged hypotension was usually accompanied by acidosis. In animals which respired spontaneously, the acidosis was usually accompanied by a fall in arterial pCO₂ to 25 - 35 mm Hg in spite of a normal arterial pO₂ of about 100mm Hg or more (Table 3.1). Carotid artery occlusion was accompanied by a moderate increase in respiratory rate which lasted several minutes. In 18 spontaneously respiring rats sampled from groups 1-3, the respiratory rate 30 min after induction (before vertebral artery diathermy) was 89 min⁻¹. Thereafter it did not consistently rise or fall throughout the experiment as blood pressure fell. Acidotic hypocapnic animals generally had an increased respiratory rate, but linear correlation between arterial pCO₂ or pH and respiratory rate was not significant (r= 0.30, 0.26, slope = -0.82 min⁻¹/mm Hg, -94 min⁻¹/pH unit respectively, p > 0.05; n=28 in animals in groups 1-3 following

A) Survival with respect to duration of experiment.



B) Blood pressure in survivors only.

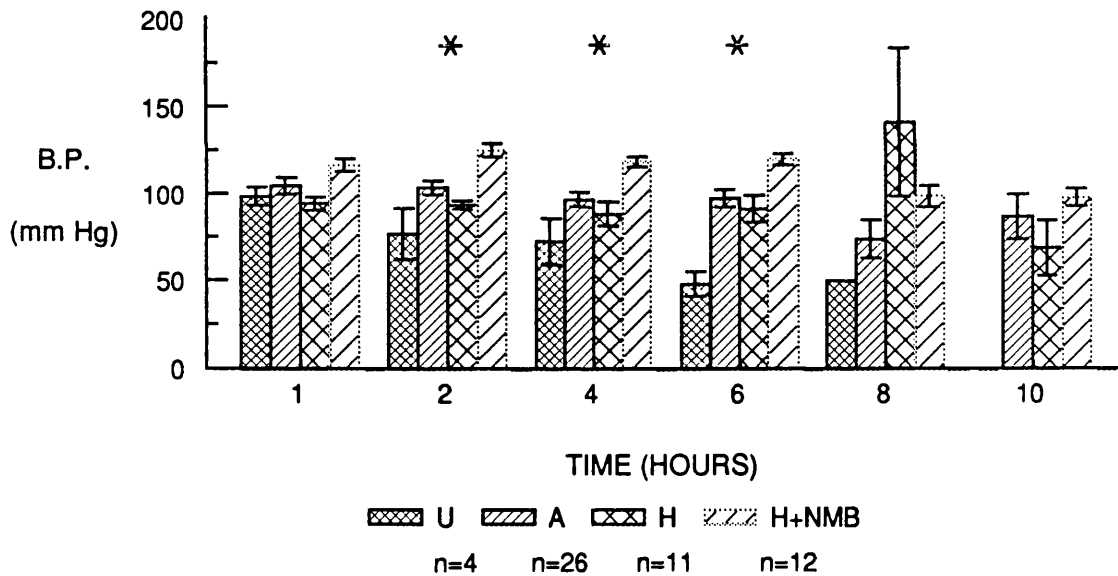


Figure 3.1. Rat survival and blood pressure with different anaesthetic regimens. U - urethane, A - Alphaxolone-alphadolone, H - halothane, H+NMB - halothane and neuromuscular blockade with pancuronium bromide. The number of animals in each group is shown underneath the graphs. The X axis in both graphs is time in hours after anaesthetic induction. Surgical procedures were carried out between 0 and about 3 hr. A) Proportion of animals surviving in relation to the duration of the experiment. The mean survival times were 7.7 ± 0.6 , 6.5 ± 0.4 , 7.6 ± 0.8 and 10.0 ± 0.5 hr ($p < 0.01$, one way analysis of variance for groups 1-4 respectively). B) Blood pressure of surviving animals only. Bars represent the mean and error bars ± 1 S.E. * - $p < 0.05$, one way analysis of variance.

diathermy when arterial $pO_2 > 95$ mm Hg, and respiratory rate and blood gases were measured simultaneously). The fall in blood pressure did not appear to be due to hypovolaemia : in two experiments the central venous pressure was 15 and 3 mm of water shortly before cardiovascular collapse when the arterial blood pressure had fallen to 37 and 49 mm Hg respectively.

3.1.1.2. Effect of anaesthetic regime on animal survival.

In the order of introduction, the anaesthetic regimes tried were : 1) Urethane, 2) Alphaxolone/alphadolone, 3) Halothane, all with spontaneous ventilation, and 4) Halothane with neuromuscular blockade and artificial ventilation. The best combination of survival and blood pressure was obtained with the last of these (Fig. 3.1). This did not appear to be due to a gradual improvement in experimental technique with time : There was no significant linear correlation ($p < 0.05$) between survival time and experimental order either within experiments using one anaesthetic regime ($r = -0.53, -0.37, 0.10, -0.12$; $n = 12, 26, 11, 12$ for the regimes above, respectively) or overall ($r = 0.22, n = 61$). The total period of carotid artery occlusion did not have a significant linear correlation with survival time overall ($r = 0.15, n = 61$), and was not significantly different between the four anaesthetic groups ($19.2 \pm 14.1, 19.8 \pm 16.6, 22.7 \pm 13.1, 19.6 \pm 9.6$ min in each group respectively; $p > 0.05$, one way analysis of variance). Within group 2, data was pooled with respect to the two induction techniques used, as there was no significant difference in mean survival times (Hypnorm : 7.0 ± 0.7 hr, $n = 14$; Ethyl chloride : 5.8 ± 0.3 hr, $n = 12$, $p > 0.05$). Similarly, data were pooled for group 3, as there was no significant difference between mean survival times for experiments performed with N_2O/O_2 mixtures of 70/30% or 50/50% (70/30% : 7.9 ± 1.1 hr, $n = 7$; 50/50% : 7.1 ± 1.3 hr, $n = 4$, $p > 0.05$).

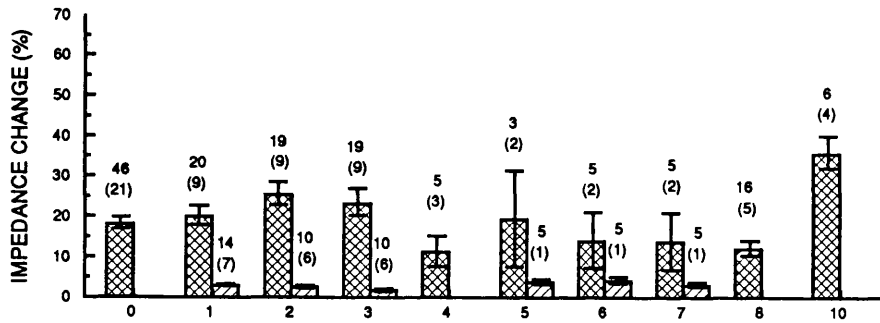
Artificial ventilation was occasionally used in groups 1-3 when apnoea occurred during an experiment when the animal was otherwise in a satisfactory condition (blood pressure above about 50 mm Hg), so that it seemed likely that recovery would occur. This usually occurred during a period

of cerebral ischaemia; artificial ventilation was sometimes only required for 5 - 15 min, as recovery occurred on cerebral reperfusion (in 3 episodes in 3 rats, 8 in 6 rats, or 4 in 3 rats in groups 1 - 3 respectively). In some animals, no spontaneous recovery occurred, and artificial ventilation continued until the end of the experiment. This occurred for 4.4 ± 1.9 hr (3 rats), 1.6 ± 1.5 hr (10 rats), and 0.5 hr (1 rat) in groups 1-3 respectively. There was no significant difference in survival time between these animals and others in each group (survival 8.4 ± 0.9 , 7.4 ± 0.7 (Group 1); 6.7 ± 1.0 , 6.4 ± 0.5 (Group 2); 8.5, 7.5 ± 0.9 (Group 3); time in hr for terminally ventilated group first, $p > 0.05$ in each group).

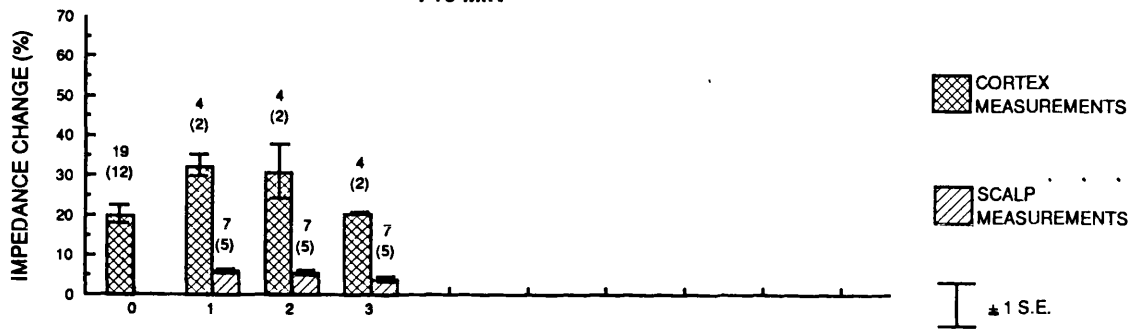
Anaesthetic :	Urethane	Alphaxolone/ alphadolone	Halothane	Halothane/ pancuronium
pO ₂ (0 - 10 hr)	114 ± 5.8 (13/5)	104.4 ± 4.5 (31/16)	121.6 ± 8.1 (17/7)	115.7 ± 4.4 (43/12)
pCO ₂ (4 - 10 hr)	26.8 ± 3.8 (7/3)	32.2 ± 1.6 (17/14)	34.8 ± 2.8 (13/7)	40.0 ± 1.6 (24/12)
pH (4 - 10 hr)	7.42 ± 0.03 (7/3)	7.32 ± 0.01 (17/14)	7.32 ± 0.01 (13/7)	7.30 ± 0.01 (24/12)

Table 3.1. Arterial blood gases in different anaesthetic regimes. These were measured variably and at differing times in different animals, and so are shown for illustrative purposes only. Figures in parentheses are total number of measurements/number of animals in which these were made. pO₂ measurements are pooled from 0 to 10 hr and pCO₂ and pH values are pooled from 4 to 10 hr, to illustrate pO₂ levels overall, and acid-base status after vertebral artery diathermy respectively. To limit the effects of frequent measurements in any one animal, only the first measurement within each two hour period (i.e. 0-2, 2-4, 4-6 hr ...) was used. The maximum number of measurements that could be contributed to the pool by any one animal is therefore 5 for pO₂, or 3 for pCO₂ or pH.

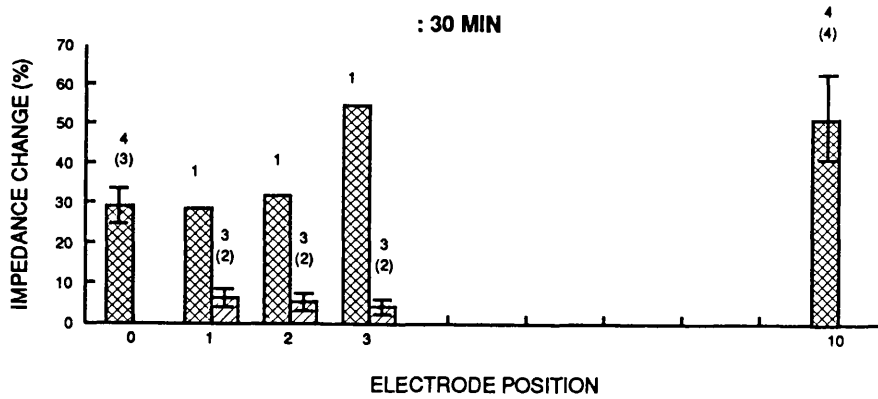
IMPEDANCE CHANGE AT : 5 MIN



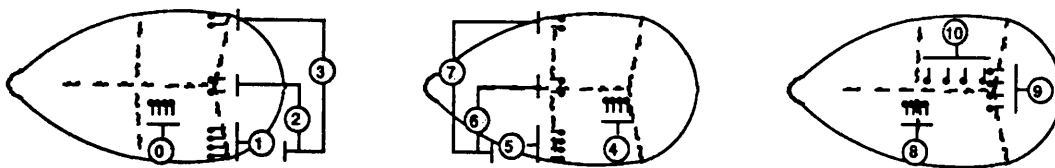
: 15 MIN



: 30 MIN



RAT HEAD VIEWED FROM ABOVE



● ELECTRODE
 --- POSITION OF SUTURES

○ CHANNEL NUMBER :
 0, 4 & 8 REFERENCE CHANNELS ON
 CORTEX ONLY. OTHERS EITHER
 ON THE CORTEX OR SUB-
 CUTANEOUSLY IN THE SCALP

3.1.1.3. Effect of intravenous adrenaline on scalp impedance.

No consistent scalp impedance changes were observed when adrenaline was given to increase systemic blood pressure. (In ischaemic episode 3, Fig. 3.7, scalp impedance increased after adrenaline administration but in other records fell or remained constant).

3.1.2. Scalp and cortical impedance changes during cerebral ischaemia measured at ambient temperatures.

3.1.2.1. Pooled data from all electrode positions.

A consistent increase was observed in both cortical and scalp impedance for all electrode positions and for each of the periods of carotid artery occlusions employed (Fig. 3.2).

3.1.2.2. Comparison of cortical and scalp impedance changes for data acquired simultaneously from electrode positions 0 - 3.

Impedance was recorded simultaneously from electrode positions 1 - 3 either on the cortex or in the scalp; position 0 acted as a reference on the cortex in both cases (Table 3.2, Fig. 3.3). Arterial pCO₂ and blood pressure prior to carotid artery occlusion differed between the two groups (B.P. was measured in all cases, but pCO₂ was not recorded in some of the cortex measurements at 5 min). However, there was no significant linear correlation in all experiments

◀ Figure 3.2. Summary of impedance changes during cerebral ischaemia measured in various electrode positions. Measurements were made 5, 15 or 30 min after carotid artery occlusion; all were at room temperature. The total number of measurements (with number of animals in parentheses) is shown above each vertical bar.

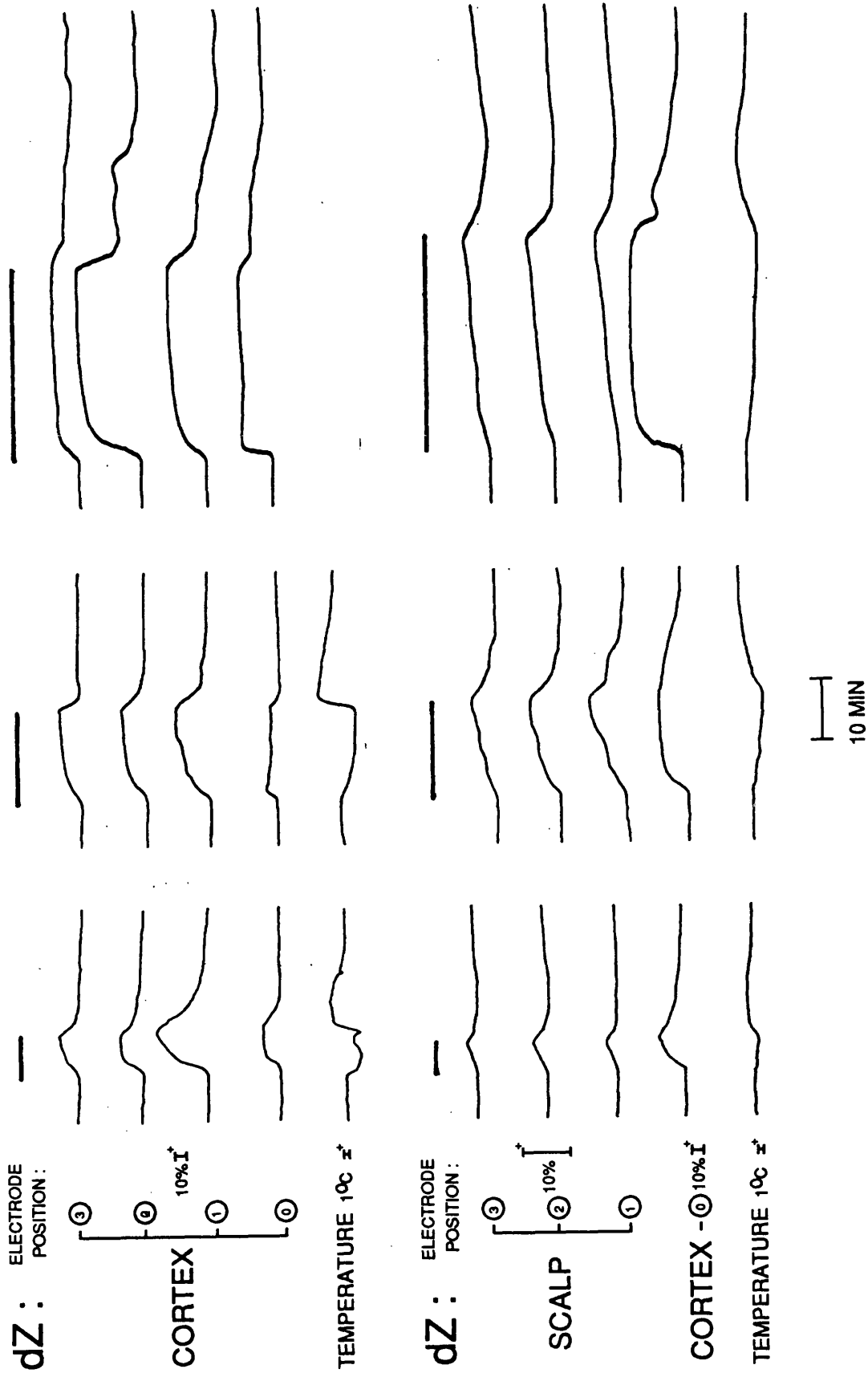


Figure 3.3. Examples of impedance and temperature changes measured on the cortex or in the scalp during episodes of carotid occlusion of varying duration. Impedance at electrode positions 1 - 3 and temperature were measured either on the cerebral cortex or in the scalp, whilst impedance at position 0 was measured on the cortex throughout to provide a reference. Temperature was not recorded during carotid artery occlusion of 30 min with measurement on the cortex. Measurements were made at room temperature. The horizontal bar represents the period of carotid artery occlusion.

between these variables and $\delta Z(5)$ or $\delta Z(15)$ measured on the cortex at electrode position 0, or $\delta Z(5)$ in the scalp at electrode position 1 (pCO_2 - $r=0.12$, 0.03 , 0.39 , $n=29$, 19 , 8 ; B.P. $r=0.11$, 0.11 , 0.30 , $n=46$, 19 , 24 respectively). δZ measured at electrode position 0 did not differ significantly between the two groups (Table 3.2).

Resting impedance measured from electrode positions 2 and 3 was higher than that from position 1 in each group for cortical but not scalp records. The impedance change did not differ consistently between electrode positions. δZ measured on the scalp was significantly greater than the baseline. $\delta Z(5)$ and $\delta Z(15)$ measured in the scalp were respectively about 10% and 15% of the value for cortical measurements.

a) IMPEDANCE MEASUREMENTS.

5 MIN ISCHAEMIA	CORTEX					SCALP				
	Z (k Ω)	$\delta Z(5/15)$ (%)	$T_w(u)$ (min)	$T_w(d)$ (min)	FWHM (min)	Z (k Ω)	$\delta Z(5/15)$ (%)	$T_w(u)$ (min)	$T_w(d)$ (min)	FWHM (min)
Channel 0 (Cortex only)	1.4 \pm 0.1 (15)	16.6 \pm 3.0 (15)	2.1 \pm 0.3 (15)	2.3 \pm 0.3 (10)	5.4 \pm 0.6 (10)	1.2 \pm 0.05 (8)	19.4 \pm 2.4 (8)	1.9 \pm 0.2 (8)	3.6 \pm 1.0 (2)	6.9 \pm 0.8 (2)
Channel 1	1.1 \pm 0.07 (15)	17.6 \pm 1.6 (15)	2.0 \pm 0.3 (15)	2.8 \pm 0.5 (10)	6.0 \pm 0.6 (10)	0.3 \pm 0.05* (8)	2.5 \pm 0.3* (8)	2.7 \pm 0.1 (8)	2.1 \pm 0.2 (2)	4.0 \pm 0.8 (2)
Channel 2	0.6 \pm 0.03 (15)	24.6 \pm 2.7 (15)	1.8 \pm 0.2 (15)	2.4 \pm 0.4 (10)	6.0 \pm 0.5 (10)	0.4 \pm 0.05* (8)	2.5 \pm 0.4* (8)	2.7 \pm 0.2 (8)	1.7 \pm 0.1 (2)	4.3 \pm 0.3 (2)
Channel 3	0.5 \pm 0.03 (15)	21.7 \pm 3.0 (15)	1.8 \pm 0.2 (15)	1.5 \pm 0.2 (10)	4.8 \pm 0.4 (10)	0.3 \pm 0.01* (8)	1.8 \pm 0.2* (8)	2.3 \pm 0.3 (8)	2.5 \pm 1.4 (2)	5.5 \pm 1.2 (2)
15 MIN ISCHAEMIA	2 rats					5 rats				
Channel 0 (Cortex only)	1.1 \pm 0.08 (4)	13.5 \pm 4.1 (4)	1.5 \pm 0.6 (3)	1.6 \pm 0.6 (3)	15.0 \pm 0.9 (3)	1.1 \pm 0.05 (7)	20.5 \pm 2.7 (7)	1.8 \pm 0.3 (7)	6.5 \pm 2.6 (4)	20.2 \pm 2.7 (4)
Channel 1	1.2 \pm 0.2 (4)	32.3 \pm 2.7 (4)	3.3 \pm 0.6 (4)	4.0 \pm 1.1 (3)	15.8 \pm 1.5 (3)	0.3 \pm 0.03* (7)	5.9 \pm 0.6* (7)	6.6 \pm 0.8* (7)	3.9 \pm 1.0 (4)	14.2 \pm 2.5 (4)
Channel 2	0.7 \pm 0.1 (4)	30.7 \pm 6.8 (4)	3.4 \pm 0.6 (4)	3.6 \pm 0.7 (3)	15.6 \pm 0.6 (3)	0.3 \pm 0.02* (7)	5.5 \pm 0.7* (7)	6.5 \pm 0.7* (7)	2.9 \pm 0.6 (4)	13.1 \pm 3.6 (4)
Channel 3	0.5 \pm 0.1 (4)	20.3 \pm 0.3 (4)	3.8 \pm 0.9 (4)	2.3 \pm 0.6 (3)	13.6 \pm 0.7 (3)	0.3 \pm 0.01* (7)	3.9 \pm 0.7* (7)	6.6 \pm 0.6* (7)	3.2 \pm 1.0 (4)	12.6 \pm 3.2 (4)

b) PHYSIOLOGICAL PARAMETERS.

PERIOD OF ISCHAEMIA	CORTEX						SCALP					
	$\delta T(5/15)$ ($^{\circ}C$)	pO_2 (mm Hg)	pH	pCO_2 (mm Hg)	B.P. (mm Hg)	Carotid occlusion (min)	$\delta T(5/15)$ ($^{\circ}C$)	pO_2 (mm Hg)	pH	pCO_2 (mm Hg)	B.P. (mm Hg)	Carotid occlusion (min)
5 min	-0.8 \pm 0.3 (8)	106 \pm 4.5 (6)	7.37 \pm 0.02 (6)	30.0 \pm 1.5 (7)	103 \pm 7 (15)	5.3 \pm 0.1 (15)	-0.8 \pm 0.2 (8)	101 \pm 5.1 (7)	7.39 \pm .05 (8)	40.9 \pm 2.9* (8)	104 \pm 6 (8)	5.1 \pm 0.1 (8)
15 min	-2.4 \pm 0.2 (3)	112 \pm 3.8 (4)	7.36 \pm 0.03 (4)	29.6 \pm 1.2 (4)	81 \pm 12 (4)	15.5 \pm 0.3 (4)	-1.9 \pm 0.3 (7)	99 \pm 5.5 (6)	7.38 \pm .05 (7)	42.0 \pm 2.7* (7)	111 \pm 6* (7)	14.8 \pm 0.4 (7)

Table 3.2. Changes in impedance during global cerebral ischaemia. Channels

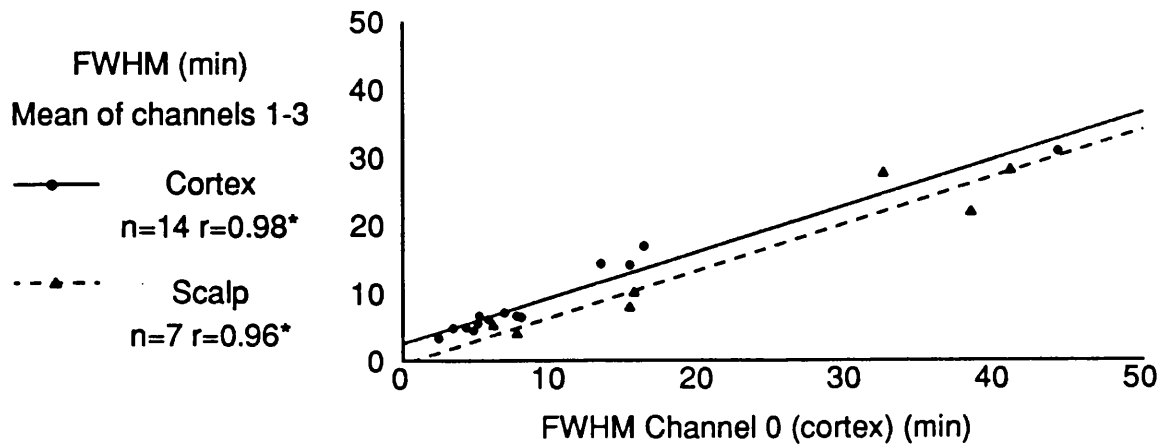


Figure 3.4. Comparison of the duration (FWHM) of impedance changes during cerebral ischaemia when measured either on the cortex or in the scalp. This includes measurements for δZ made at 5 min, 15 min (as in Table 3.2) and at 30 min. The mean of measurements from Channels 1-3 (measured on the cortex or in the scalp) are plotted against the measurements from Channel 0 (cortex only) measured simultaneously. The best fit linear regression is plotted as a continuous or broken line for cortex and scalp measurements respectively. * $p < 0.05$ for significance of linear regression.

(Table 3.2 (cont.)) 0-3 were recorded simultaneously either on the cerebral cortex or in the scalp in all animals; physiological parameters were not measured in all cases. Values are mean \pm S.E.; total number of episodes of ischaemia in different animals are in parentheses. FWHM and $T_{\%50}$ are omitted in some records either because values were taken from a longer period of carotid artery occlusion, or because impedance did not return to 50% of peak value. The precise durations of carotid artery occlusion are shown in b); values for "period of ischaemia" are for the grouping of data and are approximate. All animals were anaesthetized with alphaxolone/alphadolone. Measurements were at ambient temperature. * - $p < 0.05$, Student's unpaired t test for equivalent records measured in the scalp or on the cortex. \$ - $p < 0.05$ for difference between the specified variable measured at electrode positions 1-3, two way analysis of variance.

Impedance measured on the cortex and DC potential started to change within about 1 min of the onset of carotid artery occlusion (Fig. 3.3, 3.7). The impedance change consisted of an early steep increase which lasted about 3 min, followed by a gradual increase which usually continued until the end of the period of carotid artery occlusion. On cerebral reperfusion, impedance usually started to return to the baseline value over a period of about 10 min. In some experiments, the impedance increased for a further period before decreasing, or failed to decrease at all (Fig. 3.7).

Impedance changes measured in the scalp or on the cortex had a similar duration (Fig. 3.3). In records in which impedance returned to baseline (so that FWHM could be measured) the FWHM of scalp and cortical records corresponded closely (Fig. 3.4). There also appeared to be a qualitative correlation when impedance measured on the cortex failed to return to baseline on cerebral reperfusion (*e.g.* Fig. 3.7). However, the initial impedance increase measured in the scalp appeared to consist of a single gradual rise, unlike cortical changes which appeared to consist of a rapid followed by a slower rise (Fig. 3.3). This is reflected in the difference of $T_{\%50}$ for $\delta Z(15)$ (Table 3.2).

3.1.3. Assessment of the role of temperature changes during carotid artery occlusion.

Both cortical and scalp temperature fell spontaneously during cerebral ischaemia in experiments at ambient temperatures. The impedance changes

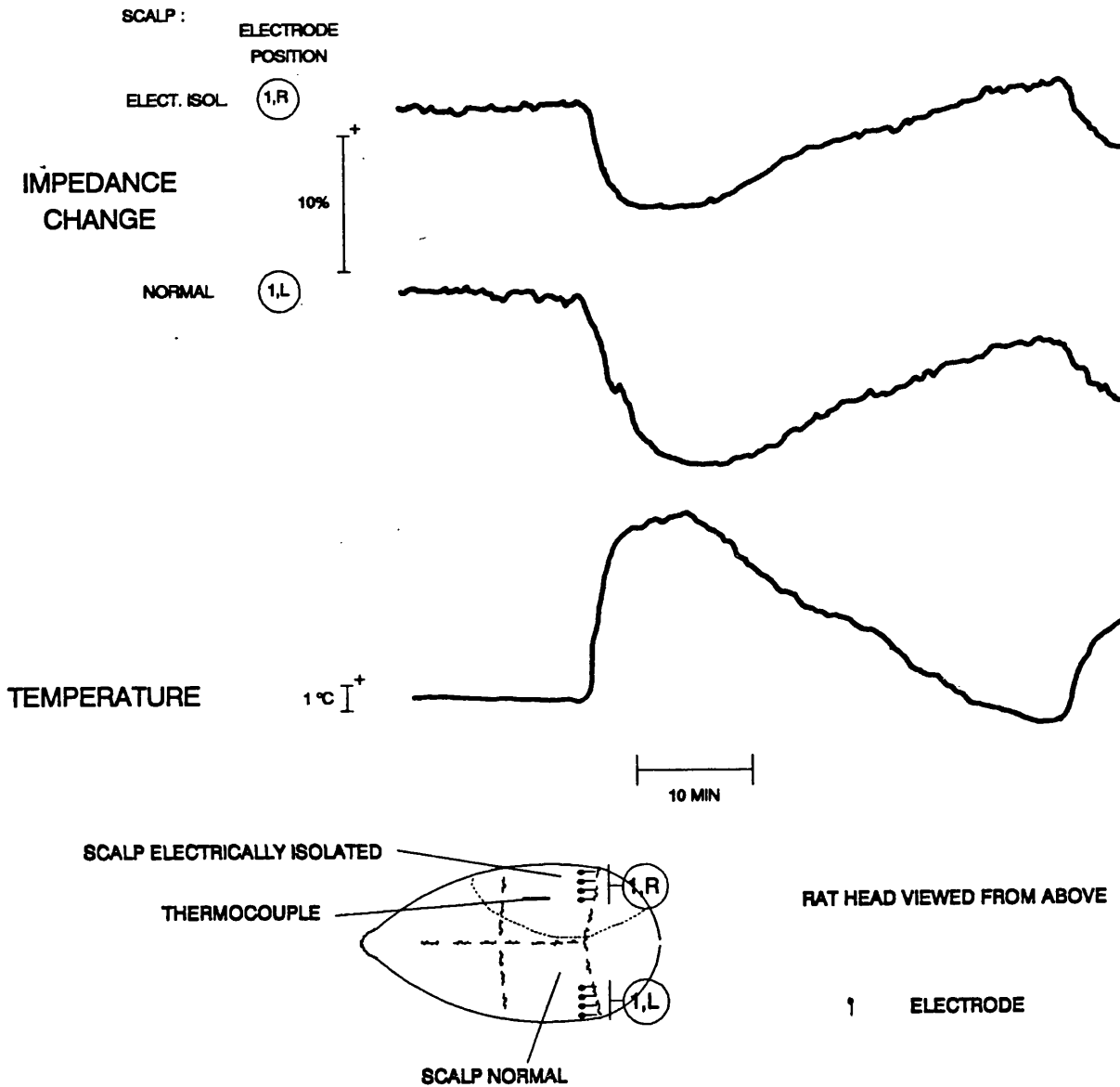


Figure 3.5. Example of the variation of scalp impedance with temperature under resting conditions. The temperature of the scalp was varied by altering the temperature of a water jacket placed on the scalp. The scalp was normal on one side and electrically isolated on the other. Linear regression data for the two sides respectively were : $r = -0.88^*$, -0.98^* , slope = -1.6, -1.2 %/°C, offset = -2.5, 0.9 % (* - $p < 0.05$). Scalp temperature varied from 31.8 to 36.3 °C.

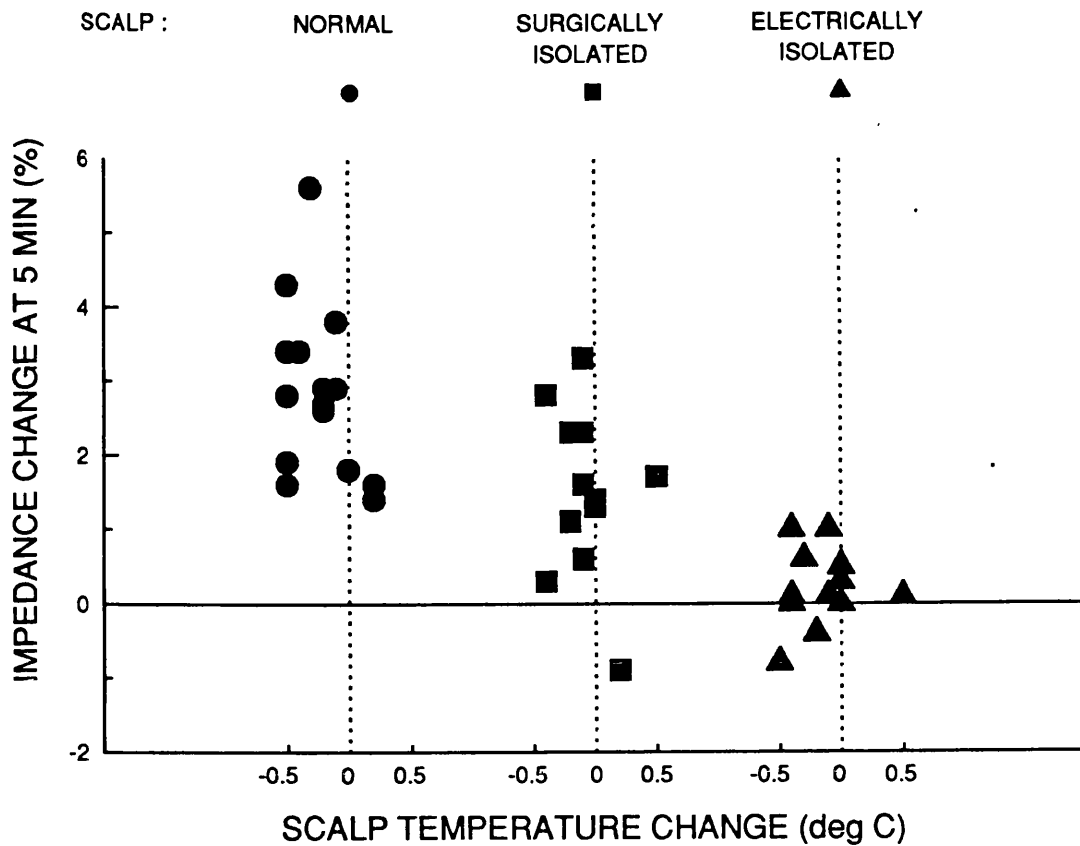


Figure 3.6. Impedance and temperature changes during cerebral ischaemia when scalp temperature was controlled artificially. The impedance and temperature change 5 min after carotid artery occlusion were measured from normal, surgically, or electrically isolated scalp in position 1. The scalp temperature was artificially controlled by warming with a water jacket or lamp. Only records with a temperature change of less than 0.5 °C have been selected. The changes were :

Change measured at 5 min :	Scalp:		
	Normal	Surgically isolated	Electrically isolated
Impedance	2.8±0.3*	1.5±0.3*\$	0.22±0.14\$
Temperature	-0.26±0.06*	-0.08±0.07	-0.15±0.07
n	16	12	13
animals	8	6	5

* - Different to zero; \$ - different to impedance change in normal scalp (p < 0.05, Student's unpaired t test).

during cerebral ischaemia appeared to vary inversely with such temperature changes (Table 3.2, Fig. 3.3). Under resting conditions, impedance measured in the scalp varied in a linear way with temperature (slope -1.2 to -1.6% per °C) when the scalp was warmed and cooled by a water jacket (Fig. 3.5). Impedance in the normal scalp measured 5 min after carotid artery occlusion increased by $2.8 \pm 0.3\%$ (n=16 in 8 rats) when temperature fluctuations were reduced to less than ± 0.5 °C by artificial warming. Under the same conditions, impedance changes in electrically isolated scalp were $0.2 \pm 0.1\%$ (Fig. 3.6 and 3.7).

3.1.4. Impedance changes in isolated scalp preparations.

At ambient temperatures, impedance measured in the scalp 5 min after carotid artery occlusion increased by $2.4 \pm 0.2\%$ (n=38 in 16 rats) or $2.7 \pm 0.4\%$ (n=25 in 8 rats) in normal and isolated scalp respectively. The temperature changed by -0.6 ± 0.1 °C in both cases. An example is shown in Fig. 3.8; whilst the scalp temperature fell and then rose by about equal amounts during and after cerebral ischaemia, the increase in scalp impedance during ischaemia was clearly greater than its subsequent decrease.

The impedance measured in isolated scalp 5 min after carotid artery occlusion increased by $1.5 \pm 0.3\%$ (n=12 in 6 rats) when temperature fluctuations were reduced to less than ± 0.5 °C by artificial warming (Fig. 3.6). In some experiments, the impedance change at 5 min after carotid artery occlusion measured on one side of the head in electrically isolated scalp was subtracted from a simultaneous measurement in surgically isolated scalp on the contralateral side. The difference was $1.1 \pm 0.3\%$ (n=13 in 6 rats) (see Fig. 3.9).

The most lateral electrode in electrode configuration 1 overlay the temporalis muscle in some animals, whilst all the electrodes in configuration 9 lay only over fascia and skull in the midline. There was no significant difference in $\delta Z(5)$ when measured simultaneously in these positions (δZ 4.3 ± 0.7 and 3.6 ± 0.8 respectively, n=6 in 1 rat, see Fig. 3.8).

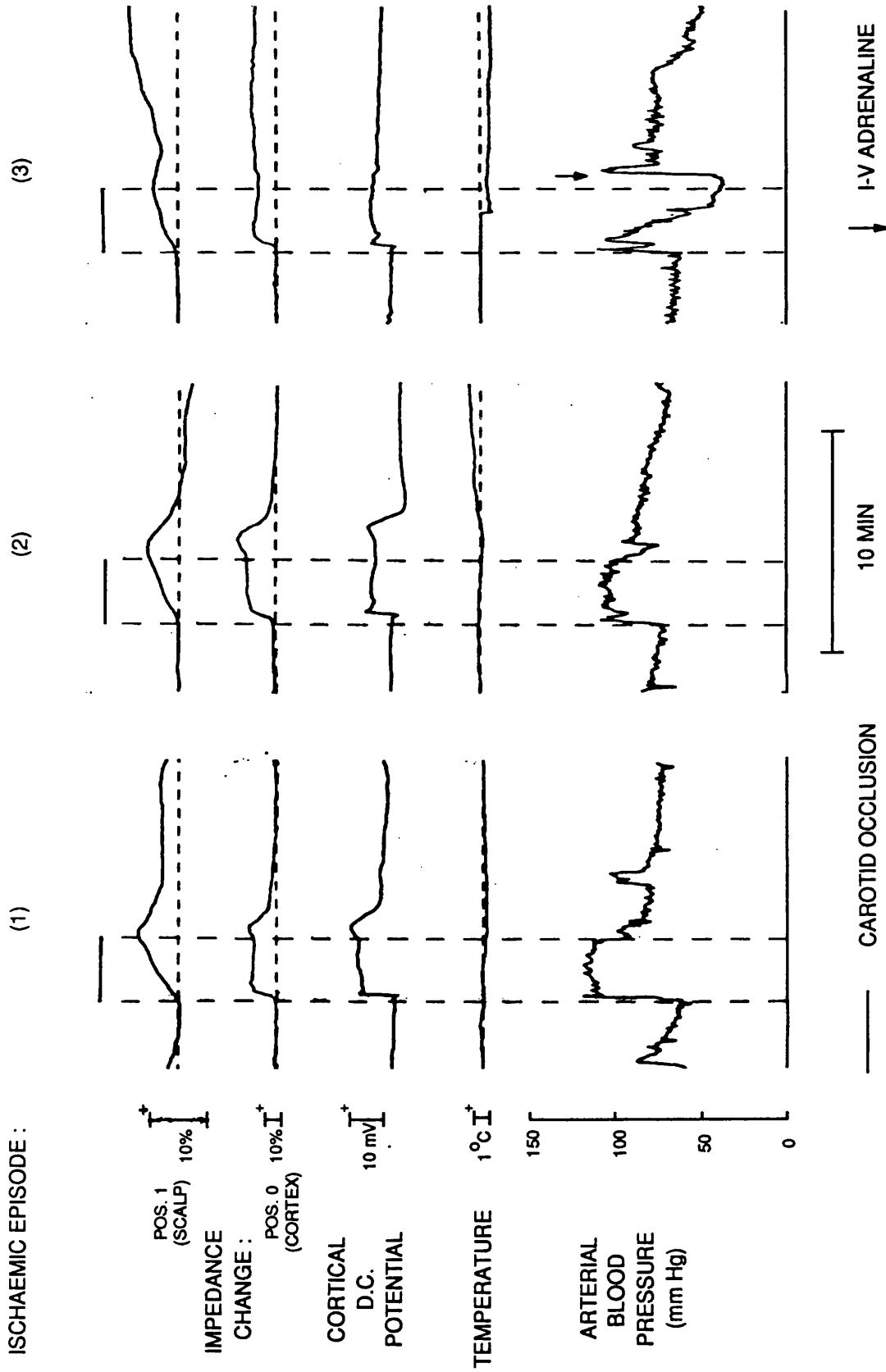


Figure 3.7. Illustration of the correspondence of the time course of scalp and cortical impedance changes. The records (1-3) were made during consecutive episodes of common carotid artery occlusion in one animal. Scalp temperature changes measured at 5 min after the onset of ischaemia were less than -0.5°C as a result of warming with a water jacket. It may be seen that the cortical impedance increase is prolonged in episode 2 compared to episode 1, and fails to return to baseline altogether in episode 3, in spite of maintenance of blood pressure. The time course of the scalp impedance change varies in a parallel fashion. In episode 3, adrenaline was given intravenously at the arrow to increase blood pressure. In other records, scalp impedance remained the same or decreased after adrenaline administration, so it is unlikely that the impedance increase could be due to this.

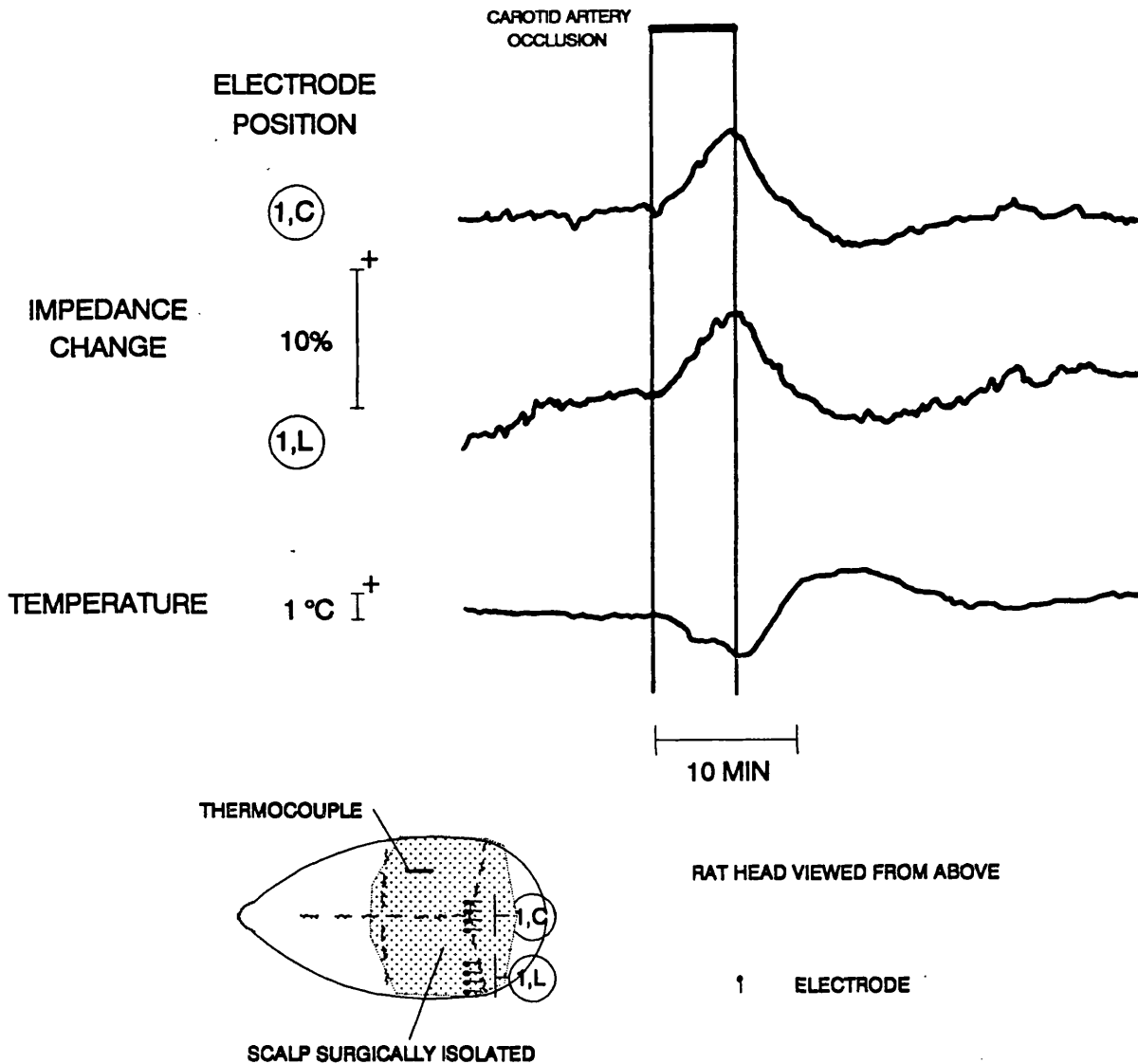


Figure 3.8. Example of impedance change in surgically isolated scalp during cerebral ischaemia at ambient temperature. Impedance was recorded from surgically isolated scalp from areas on the left and in the centre of the head. Impedance records are not corrected for baseline drift. Scalp temperature was not artificially controlled; it fell by -1.4°C at the end of common carotid artery occlusion and then rose by 1.7°C . Scalp impedance in the left and central areas respectively increased by 5.5 and 5.2%, and then fell to -2.9 and -3.0% of the original baseline on cerebral reperfusion.

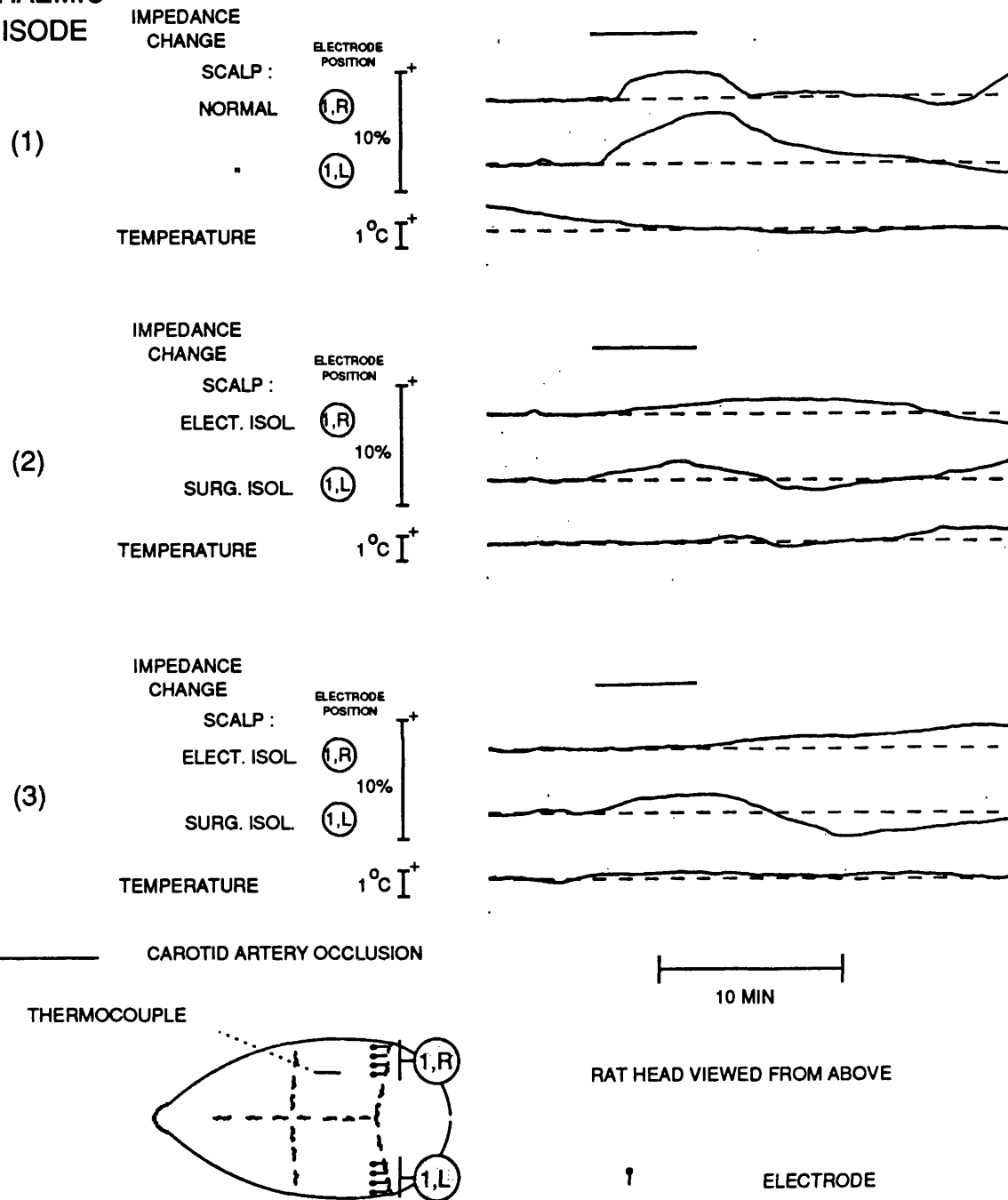
ISCHAEMIC
EPISODE

Figure 3.9. Examples of impedance changes during cerebral ischaemia in surgically and electrically isolated scalp. Scalp impedance in electrode position 1 bilaterally and temperature were recorded simultaneously during three consecutive episodes of carotid artery occlusion in one rat. Scalp temperature was controlled by the use of a water jacket. The impedance in normal scalp increased bilaterally during carotid artery occlusion in episode 1. Impedance changes from surgically isolated scalp on the left in episodes 2 and 3 resemble those in normal scalp, while those from electrically isolated scalp made simultaneously on the other side of the head do not. The variability of isolated scalp records was greater than that of normal scalp.

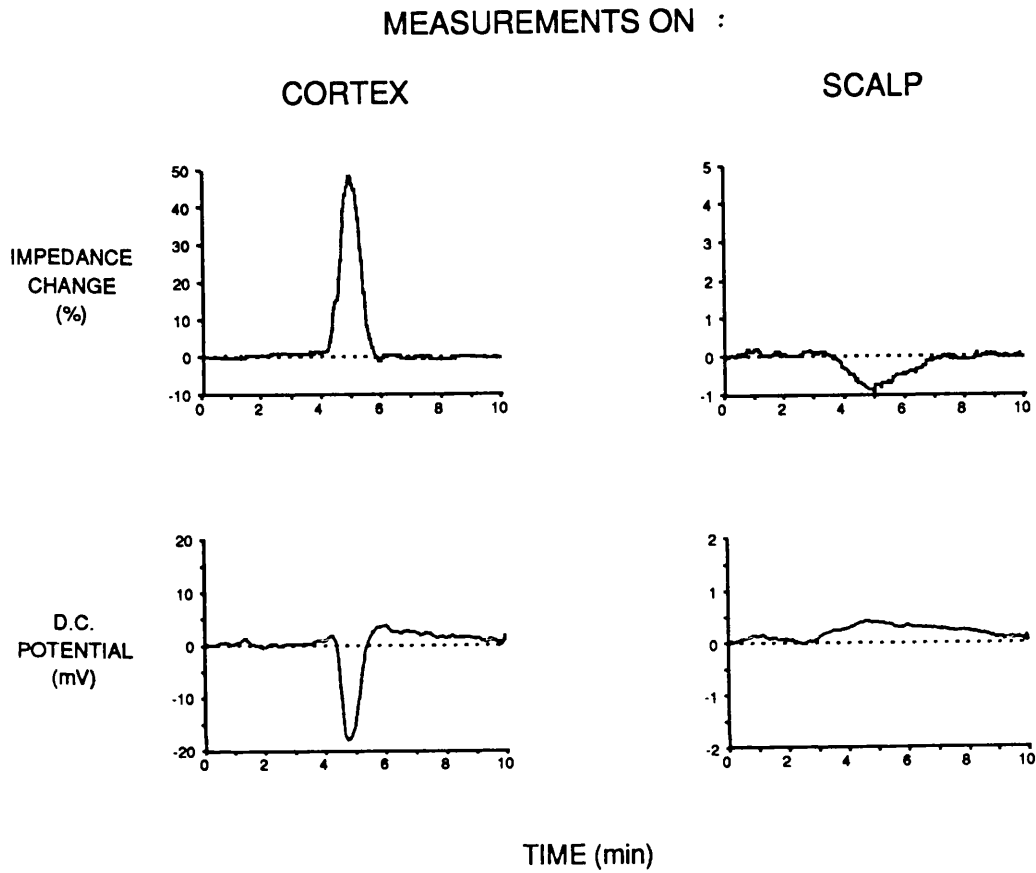


Figure 3.10. Typical examples of cortical impedance and D.C. potential changes during spreading depression. Measurements were made either on the cortex or the scalp with the araldite array at ambient temperatures. Electrodes were spaced 0.5 mm apart. D.C. potential was recorded from R1 in both cases.

3.2 IMPEDANCE CHANGES DURING SPREADING DEPRESSION IN THE ANAESTHETIZED RAT.

3.2.1. Impedance changes during spreading depression measured on the cortex and extracerebral layers.

Impedance measured on the cortex increased by about 40% during spreading depression. In contrast, a decrease of about 0.8% was measured on the scalp (Fig. 3.10, Table 3.3). The FWHM of the cortical changes was about 1 min while that of the scalp changes was about 2 min. The FWHM of the DC potential change measured on the cortex in cortical records was similar to that measured in the superfusing cup in scalp records.

Layer	δZ :		Z:		DC potential		n	rats
	Peak (%)	FWHM (min)	Peak (k Ω)	Peak (mV)	FWHM (min)	FWHM (min)		
Cortex	39.0 \pm 4.8	1.0 \pm 0.1	2.4 \pm 0.7	17.1 \pm 2.0	1.3 \pm 0.4		15	4
Scalp	-0.8 \pm 0.2	2.0 \pm 0.1	3.1 \pm 0.2	9.2 \pm 1.3	1.2 \pm 0.2		20	6
p	<0.05	<0.05	NS	-	NS			

Table 3.3. Impedance measurements during cortical spreading depression. Other measurements were made with the araldite array, pressed lightly onto the cortex but firmly onto the scalp. DC potential was measured from the perfusing cup for scalp recordings, and from R1 for cortical recordings. Electrodes were equally spaced 0.5mm apart.

Results obtained with other electrode configurations are shown in Table 3.4. Similar changes to those observed on the cortex with the araldite array with spacing of 0.5 mm were obtained with electrodes spaced equally 1mm apart. Similar changes to those observed on the scalp with the araldite array with spacing of 0.5 mm were obtained with the araldite probe with electrodes

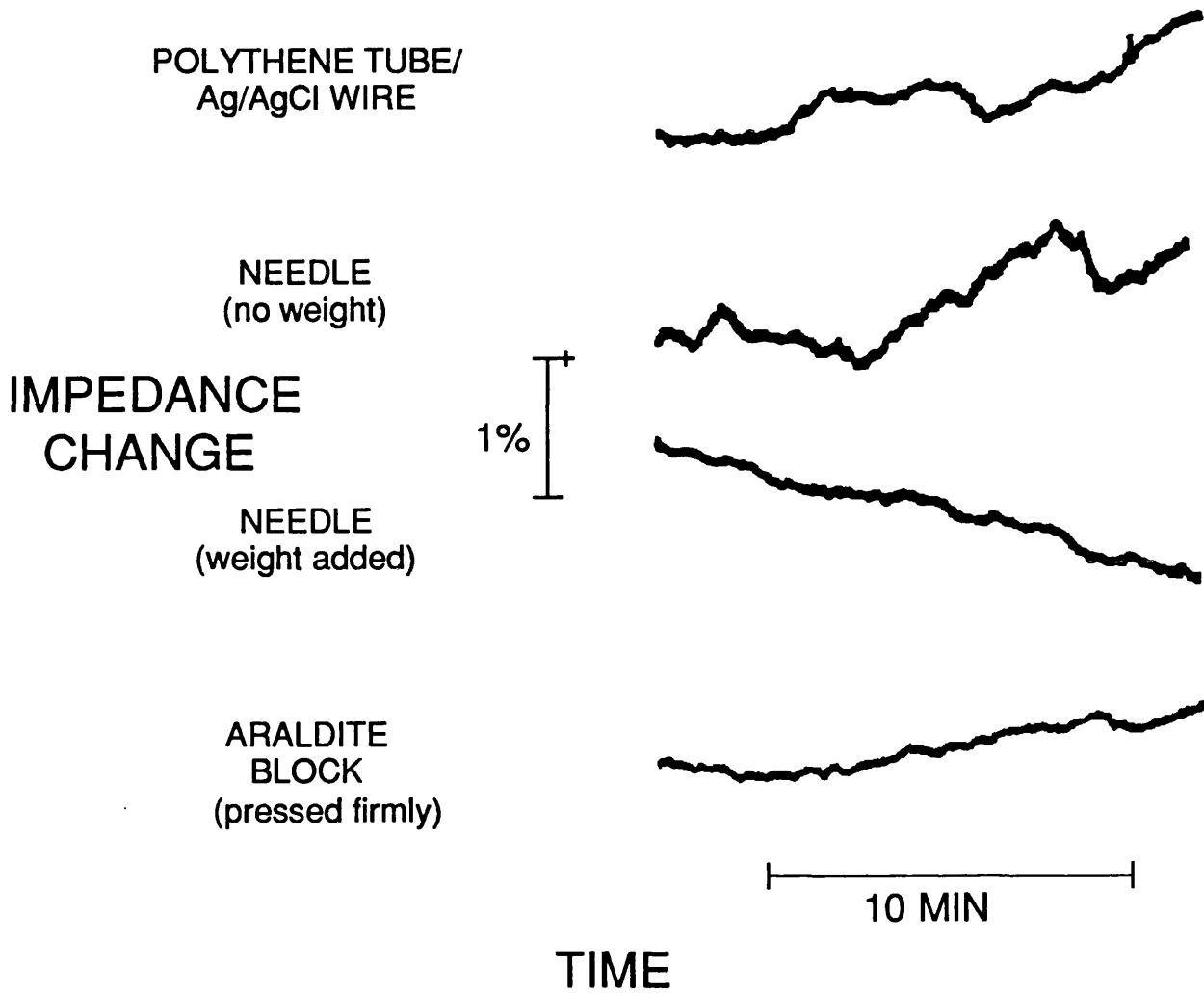


Figure 3.11. Baseline impedance changes observed under resting conditions with different electrode arrangements. Typical examples from individual traces to illustrate Table 3.5.

spaced equally 1mm apart and with wire electrodes pressed down by a weight. A significant but smaller impedance decrease of about 0.2% was observed with unweighted wire electrodes in the scalp; the baseline was more variable, and this is reflected in the relatively large standard error of the FWHM.

Layer	El.arr.	Spac. (mm)	δZ :		Z (k Ω)	Potential		n	rats
			Peak(%)	FWHM		Peak(mV)	FWHM		
Cortex	Araldite#	1	39.2	1.1	2.5	23.7	1.25	2	1
Scalp	Araldite#	1	-0.7 \pm 0.6	1.8 \pm 0.7	2.2 \pm 0.1	8.6 \pm 1.0	1.0 \pm 0.1	4	2
"	Wire+weight#	1	-0.6	1.7	1.4	10.6	0.9	2	1
"	Wire (no weight)\$	1.5	-0.2 \pm 0.04	3.8 \pm 1.4	0.4 \pm 0.07	5.6 \pm 0.9	1.4 \pm 0.1	27	5

Table 3.4. Measurements with further electrode arrangements during cortical spreading depression. # No significant difference in $\delta Z(\max)$ or DC potential to measurement on cortex or scalp respectively with araldite array and electrode spacing of 0.5 mm (data in Table 3.3). \$ $\delta Z(\max)$ significantly different to 0 and to measurements with araldite array on scalp (data in Table 3.3).

3.2.2. Improvement of scalp recording arrangement.

The effects of four different electrode arrangements on the baseline variability of scalp impedance were assessed (Fig. 3.11 and Table 3.5). The variability could be classified into three major components : 1) An approximately linear baseline drift, which took place over hours, 2) An irregular variation of up to 1% impedance change, which took place over minutes, and 3) A smaller largely regular variation of about 0.1% peak to peak impedance change at about 10 Hz. Peak to peak impedance variations of about 0.01% and 0.02% were observed by averaging with respect to the ECG and respiratory cycle respectively (Fig. 3.12).

The minute-to-minute variability was reduced to about one third when a weight was placed on the wire electrodes, or the araldite array was used with

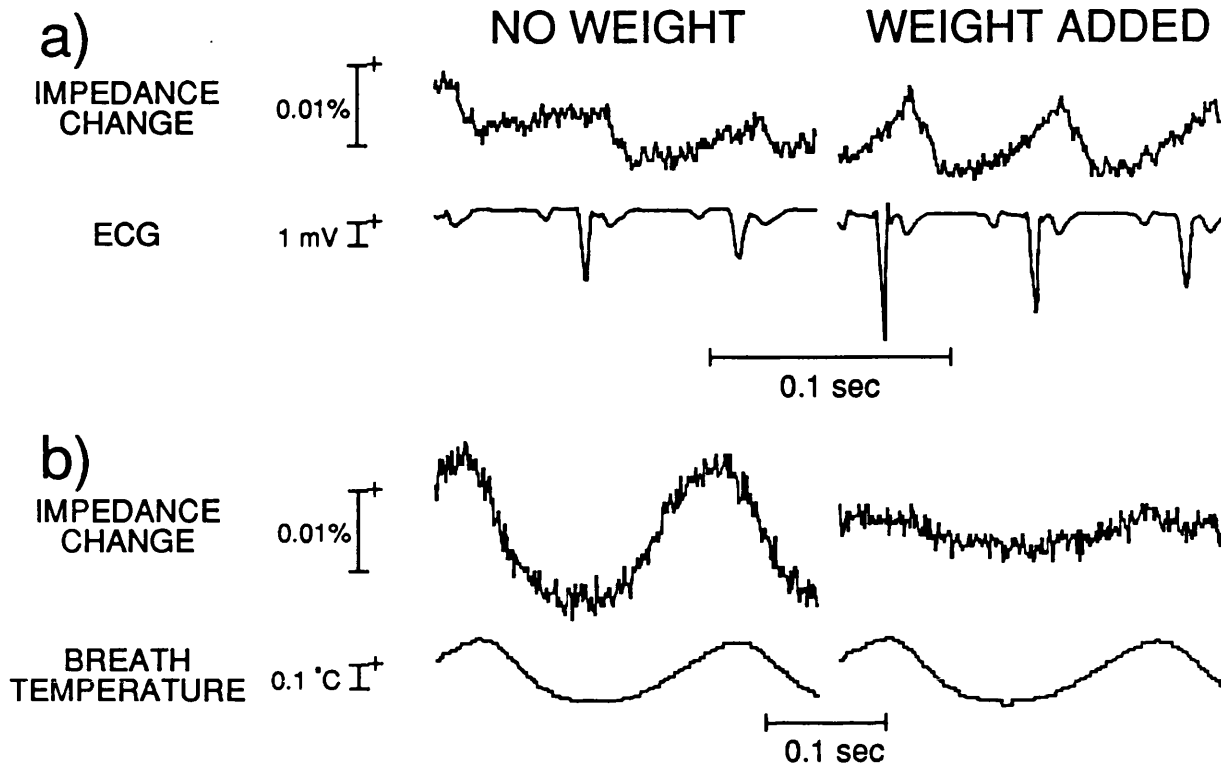


Figure 3.12. Impedance measured with scalp electrodes, averaged with respect to the ECG or respiratory cycle. Electrodes were spaced equally 1.5mm apart. $n = 1024$ for ECG and 512 for respiratory records. The output of the impedance measuring device was A.C. coupled with a bandwidth of 0.16 - 250 Hz.

firm pressure. This also reduced the respiration related impedance change, and slightly increased the pulse related component, but did not significantly affect the overall high frequency variation (Table 3.5 and Fig. 3.11 and 3.12). The least overall baseline variation occurred with the firmly applied araldite electrode, and this was used for further experiments.

Electrode arrangement	Z (k Ω)	Gradient (%/min)	Minute-to-minute variation (SD) (%)	c. 10 Hz variation (peak-to-peak) (%)	Expts.
Polythene tube/wire	0.47	-0.044	0.13	0.09	1
Wires (no weight)	0.35 \pm 0.07	-0.046 \pm 0.004	0.15 \pm 0.02	0.07 \pm 0.005	5
Wires + weight	0.48 \pm 0.15	0.075 \pm 0.05	0.047 \pm 0.01	0.06 \pm 0.003	3
Araldite	2.3 \pm 0.28	0.009 \pm 0.01	0.063 \pm 0.01	0.06 \pm 0.003	5
p*	-	<0.05	<0.05	NS	

Table 3.5. Baseline scalp impedance variations under resting conditions.

* - one way analysis of variance (minute-to-minute variation (standard deviation) data were transformed by taking log values).

3.2.3. Further characterization of the decrease in scalp impedance.

No significant impedance change was observed when spreading depression was initiated on the contralateral side of the head (Fig. 3.13, Table 3.6), or 10 min *post-mortem* (Fig. 3.14).

Cup/el.array positions	Area (%.min)	DC potential Peak (mV)	FWHM (min)	n	rats
Ipsilateral	-2.6 \pm 0.06	11.0 \pm 1.6	1.0 \pm 0.05	9	2
Contralateral	-0.01 \pm 0.1	13.4 \pm 3.0	1.6 \pm 0.8	5	2
p	<0.05	NS	NS		

Table 3.6. Scalp impedance changes with superfusing cup ipsi- or contralateral to the araldite recording array. DC potential was measured in the superfusing cup.

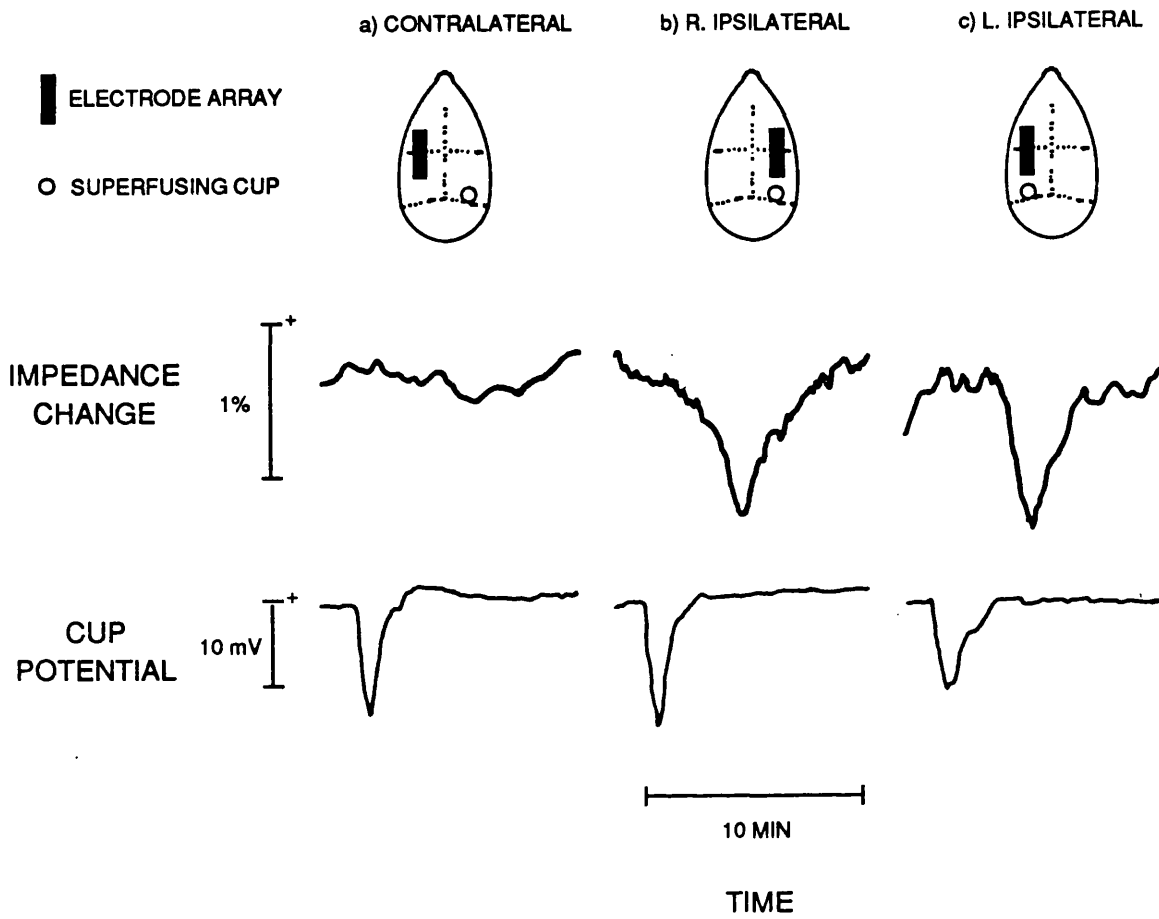


Figure 3.13. Scalp impedance changes during spreading depression initiated on the ipsilateral or contralateral side of the head. The records shown were made consecutively in one animal.

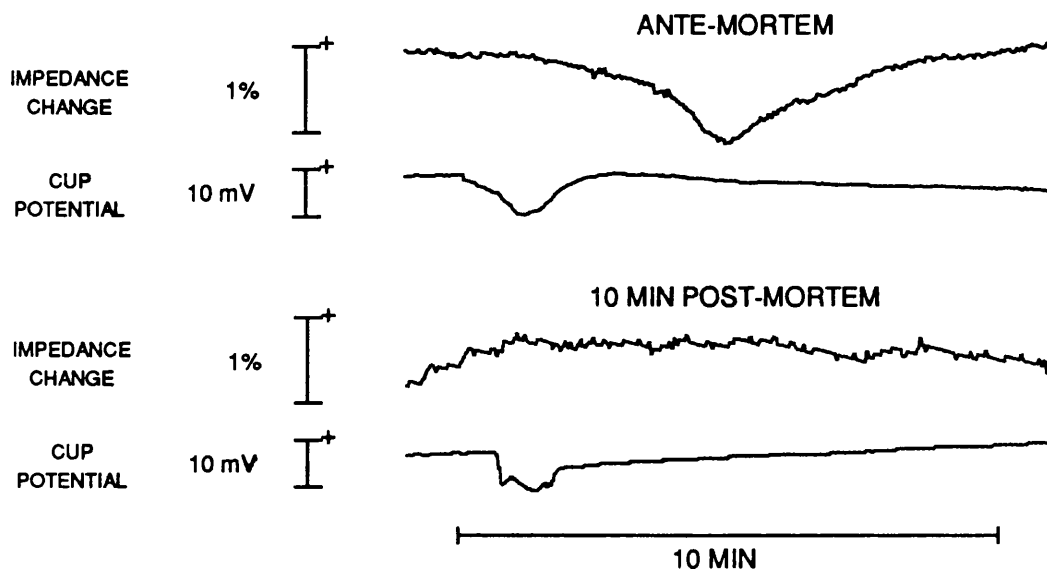


Figure 3.14. Comparison of scalp impedance changes *ante-* and 10 min *post-mortem*. Impedance from adjacent electrodes from the araldite array and DC potential in the superfusing cup were measured simultaneously after the application of 150 mMolar KCl solution to parietal cortex. Although there was a brief depolarization in the cup *post-mortem*, no impedance change was observed.

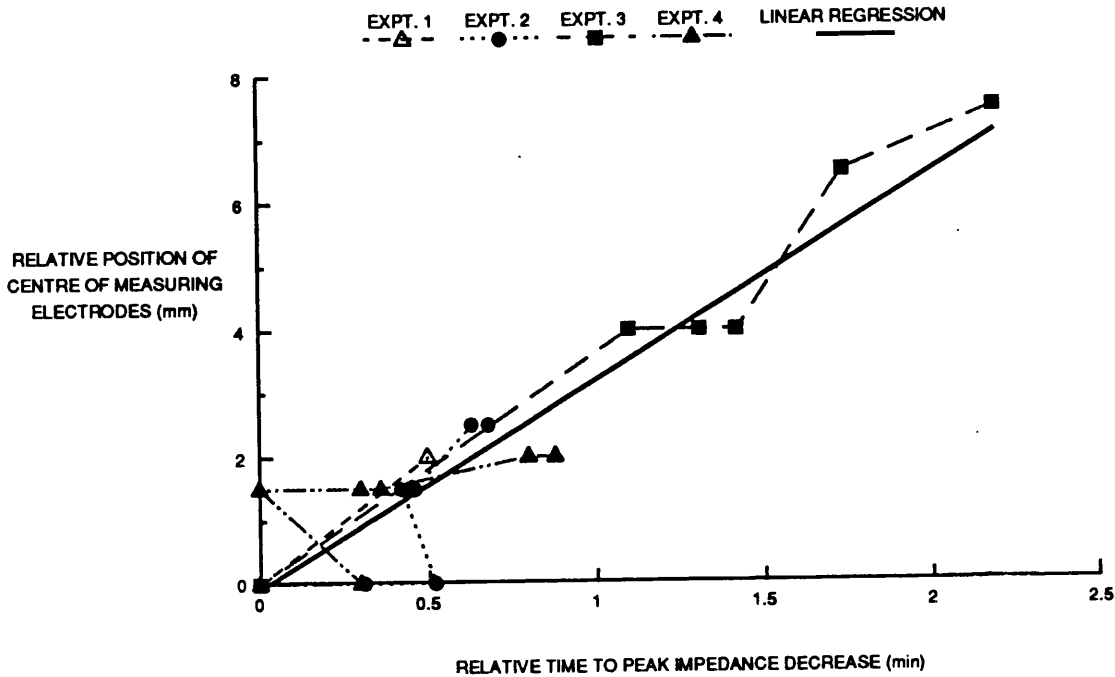


Figure 3.15. Propagation of the scalp impedance change during spreading depression. The site of measurement of scalp impedance was varied by selecting different sets of four adjacent electrodes from the araldite array. In one experiment (3) a greater range was produced by moving the araldite array between recordings. To facilitate comparison in different animals, the data were normalized by subtracting the measurements for the electrode position most proximal to the cup from each of the other measurements in the same animal. There was a significant linear correlation between the interval from the peak potential increase measured in the cup to the greatest impedance decrease measured on the scalp and the distance of the electrode set employed from the cup ($r = 0.94$, gradient 3.3 mm/min , $n = 23$ in 4 rats).

There was a significant linear correlation between the time to trough of the impedance decrease and the distance of the electrodes from the superfusing cup (Fig. 3.15). The slope of the linear regression corresponded to a propagation speed of 3.3 mm/min, compared to 3.2 ± 0.4 mm/min for similar measurements on the cortex (n=19 in 3 rats).

3.2.4. Effect of temperature changes during spreading depression.

Under resting conditions, scalp impedance decreased by about 0.4% for each °C due to external warming (Table 3.7).

Thermocouple position	r	Slope %/°C	Measurement range °C	p
Epidural	0.98	-0.44	34.7-37.1	<0.05
Scalp	0.97	-0.38	35.5-38.2	<0.05

Table 3.7. Scalp impedance variation during warming of the scalp by a lamp. Impedance was measured with the araldite array, with electrodes spaced 0.5 mm apart. Warming took place over 12 min.

An increase in epidural and scalp temperature occurred spontaneously during spreading depression in experiments performed at room temperature. When this increase was minimized by external warming of the scalp, no significant change in scalp impedance was observed (Fig. 3.16, Table 3.8).

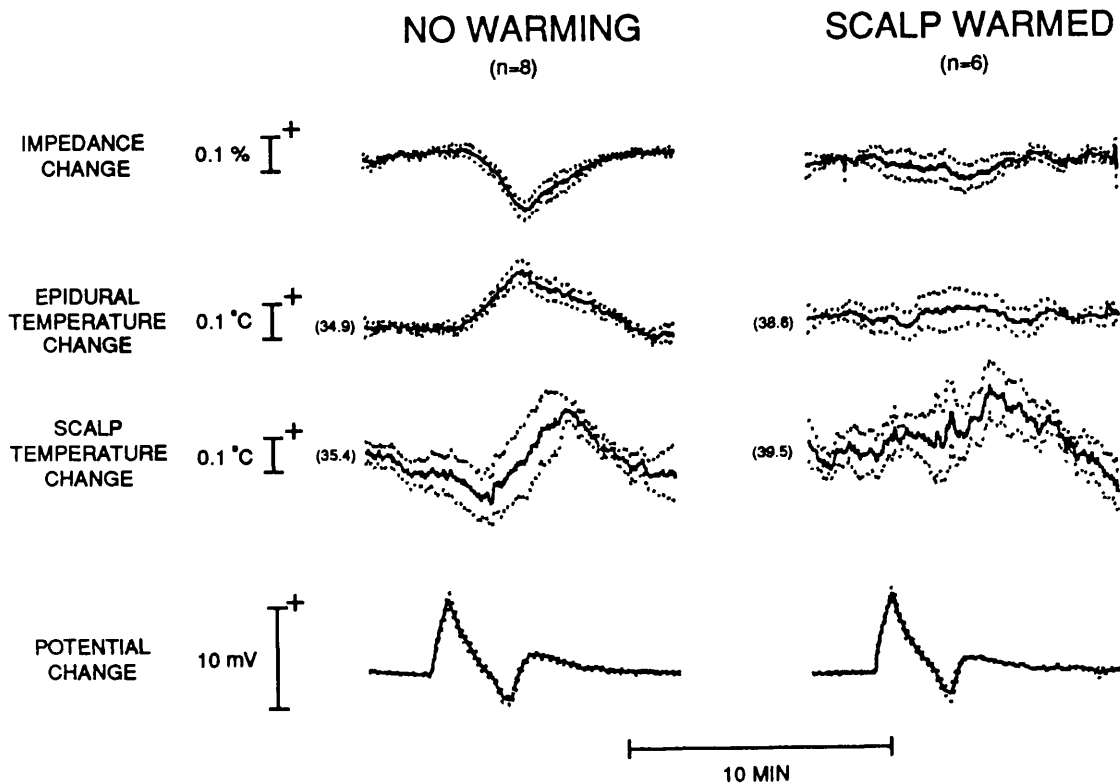


Figure 3.16. Effect of external warming on changes in scalp impedance. Averaged measurements made in one rat are shown. The skull and scalp were intact except for a craniotomy for the superfusing cup. Scalp impedance was measured with the araldite array with electrodes spaced 0.5 mm apart. DC potential was measured from an electrode in the cup (polarity reversed) and an epidural electrode under the araldite array in series. Scalp and epidural temperature were measured simultaneously. Records were obtained either at room temperature (records on left) or during equilibrium conditions after warming of the scalp by a lamp placed about 12 cm away (records on right). The results were subsequently averaged into groups with and without warming by aligning to the initial deflection of cup potential. The heavy and dotted lines respectively represent the mean and limits of one standard error. Figures in parentheses next to temperature records are the initial temperatures. Both scalp impedance and temperature records were corrected for baseline shift (see methods section for details). See Table 3.8 for quantitative analysis.

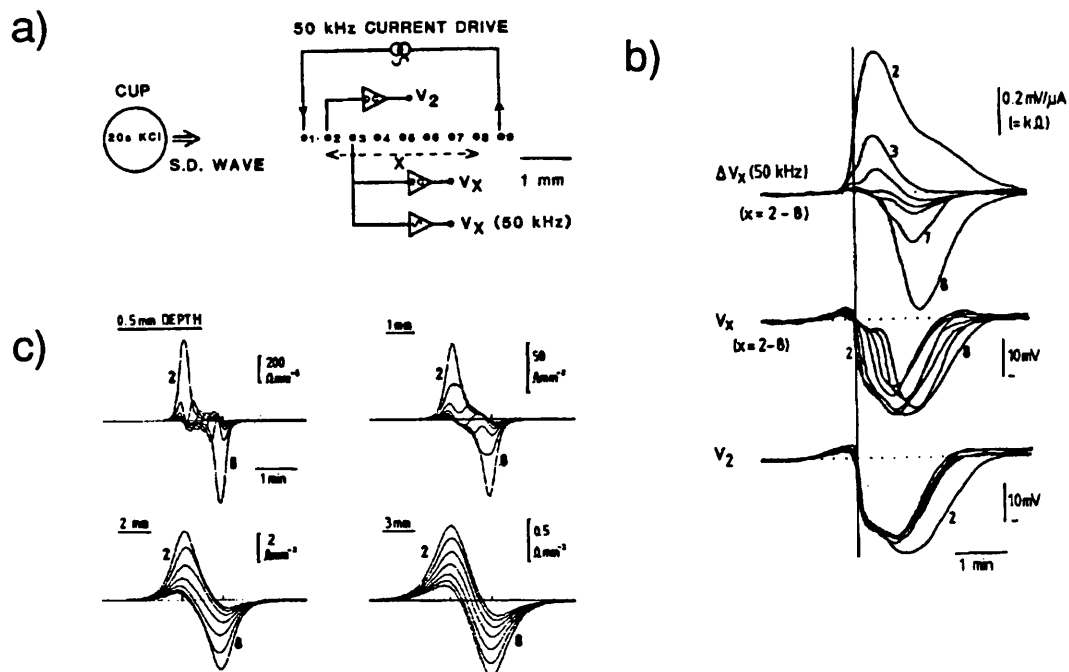


Figure 3.17. Impedance measurements during spreading depression with R2 earthed to provide data for modelling of the impedance change. a) Experimental arrangement. The araldite array was placed on the cortex and remained in the same position. Electrode positions (numbered 1-9) refer to the electrodes selected within the array. Position 1 is nearest to the site of initiation of spreading depression. b) Recordings made during successive episodes of spreading depression with R1 moved in turn from electrode position 2 to 8. Drive current was applied to electrodes at positions 1 and 9 throughout. R2 was earthed. Upper records (V_x) correspond to the voltage at R1 expressed relative to current passed between the drive electrodes. The middle and lower records are the DC potential measured at the specified position of R1 and position 2 respectively. Records were subsequently aligned and superimposed. c) Predictions from a computer model of a point impedance increase which propagates at varying distances below the surface of the cortex. The Y axis scale indicates the change in the impedance signal predicted per cubic millimetre of tissue in which the impedance is zero. Propagation at a depth of 1 mm corresponds closely to the observed data. See section 4.2 for further details.

Variable	Peak change		p
	No warming	Scalp warmed	
Scalp $\delta Z(\text{max})$ (%)	-0.16 \pm 0.03	-0.05 \pm 0.04	<0.05
Epidural temp.(°C)	0.16 \pm 0.03	0.02 \pm 0.05	<0.05
Scalp temp.(°C)	0.02 \pm 0.11	0.05 \pm 0.07	NS
Dural DC potential :			
Peak (mV)	-4.3 \pm 0.2	-4.4 \pm 0.3	NS
FWHM (min)	0.48 \pm 0.03	0.42 \pm 0.02	NS

Table 3.8. Effect of external warming on scalp impedance changes. Data for records illustrated in Fig. 3.16. "Dural DC potential" refers to the negative changes in potential records. All values except for dural potential were measured at the time of the peak change in $\delta Z(\text{max})$ in records at room temperature. Scalp $\delta Z(\text{max})$ correlated with epidural temperature - $r=0.77$, slope=-0.63%/°C, $p<0.05$, but not scalp temperature - $r=0.33$, NS.

3.2.5. Characterization of 50 kHz measurements on the cortex during spreading depression.

The spatial characteristics of the change in cortical impedance during spreading depression were analyzed in detail in one animal. Drive current was passed through the two outermost electrodes of the araldite array, and measurements from a single recording electrode in each of the seven intervening positions were made during successive episodes of spreading depression (Fig. 3.17). The change in the 50 kHz potential was symmetrical around the middle recording position, and the largest changes occur nearest to the drive electrodes. DC potential changes were all similar.

3.3. IMPEDANCE IMAGING DURING CEREBRAL ISCHAEMIA IN THE ANAESTHETIZED RAT.

3.3.1. Baseline drift.

Baseline impedance drift was measured over a period of 10 min during resting conditions (Table 3.9). The standard deviation of measurements *in vivo* were about ten times greater than those made in tanks. The correlation coefficients for impedance change against time for both linear and logarithmic regression were 0.76 ± 0.19 (n=5 in 2 rats, $p < 0.05$ in 4 out of 5 records) and 0.83 ± 0.06 (n=9 in 4 rats, $p < 0.05$ in all records), for cortical and scalp records respectively.

Experimental arrangement	Electrode arrangement	Difference in δZ and 10 min (%) Mean	measured at 0 over whole image S.D.*	n
Large cylindrical tank + saline	Brass bolts	-0.12 ± 0.10	0.35 ± 0.03	3
Tank + saline	Rat cortical array (Ag/AgCl)	0.03 ± 0.02	0.29 ± 0.07	3
Tank + saline	Rat scalp model (Ag/AgCl)	0.30 ± 0.24	0.22 ± 0.06	3
<i>In vivo</i>	Rat cortical array (Ag/AgCl)	-0.41 ± 0.24	2.78 ± 0.39	5 (2 rats)
<i>In vivo</i>	Scalp electrodes (Ag/AgCl)	-0.42 ± 0.45	2.17 ± 0.43	9 (4 rats)

Table 3.9. Changes in impedance under resting conditions in different experimental situations. The average and population standard deviation (*) refer to the impedance change of all pixels in the images collected 10 min after a reference image.

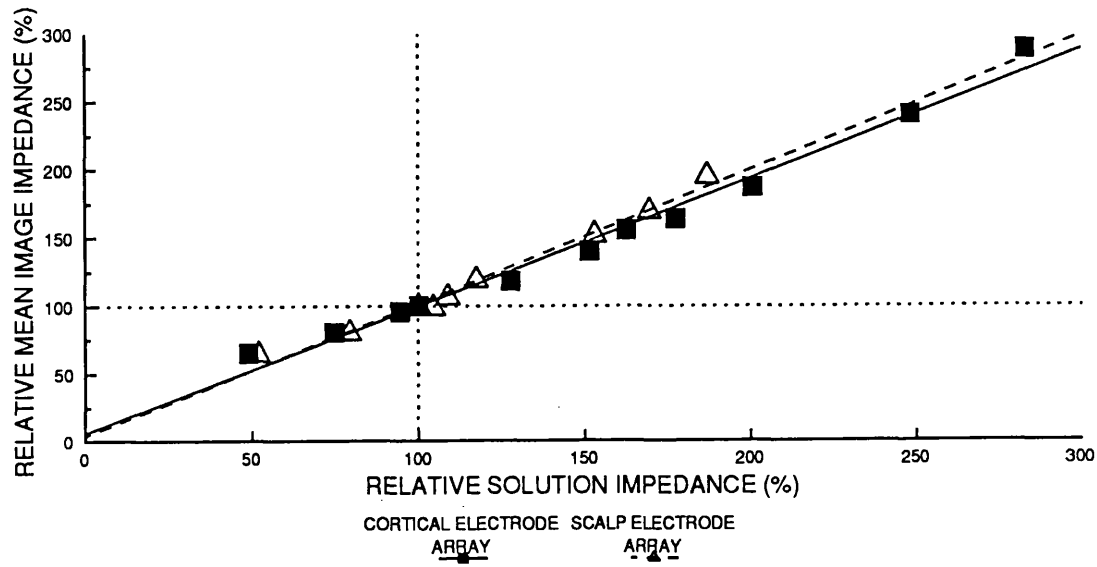


Figure 3.18. Calibration curve for EIT system. The mean image impedance was measured when saline solutions of varying concentrations (100% = 0.118g/l NaCl) were introduced into the cortical or scalp electrode array tanks. All standard errors were less than 0.3%.

3.3.2. Calibration.

3.3.2.1. Relationship between EIT image and variation of the resistivity of the saline in tanks.

EIT images were acquired as cortical and scalp electrode tanks were filled with saline solutions of varying concentrations. The resistivity of the saline was measured with the single channel impedance measuring device described in section 2.3 using four Ag/AgCl wire electrodes set 3 mm apart in a block of araldite. Linear regression data were : $r = 0.98, 0.98$ ($p < 0.05$) and slope = 0.94 and 0.98 for the cortical and scalp arrays respectively (Fig. 3.18).

3.3.2.2. Discrimination by EIT of the cranial contents and scalp with measurement with scalp electrodes.

Post-mortem, a change in the contents of the cranial cavity from saline to air produced an approximately gaussian central increase in impedance (Figure 3.19). The FWHM of the increase was 27.5% of the image diameter. In reality, the cranial cavity occupied about 80% of the length of the scalp electrode array along both the X and Y axes.

Impedance decreased reversibly by about 5% around the circumference of the EIT image when the scalp *in vivo* was selectively warmed by placing an electric light above the scalp (Fig. 3.20). This decrease reversed to an extent on return of the scalp temperature to its resting value.

3.3.2.3. Localization of polythene rods.

The correspondence of the peak impedance change and physical position of a polythene rod suspended vertically in either the large cylindrical or cortical array tanks is shown in Figure 3.21. The difference (expressed in % of the axis dimensions of the tank) between the position of the peak impedance change in the image and the centre of the rod was $3.9 \pm 0.17\%$ ($n=9$, as the rod was

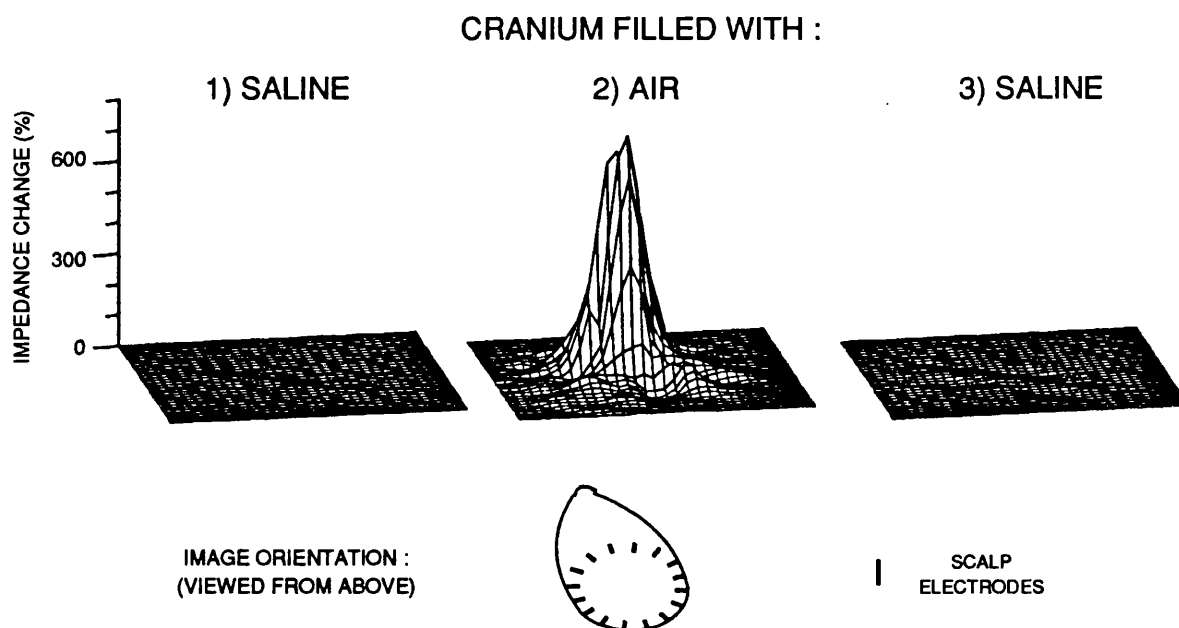


Figure 3.19. Sensitivity of EIT measured with scalp electrodes to replacement of cranial contents by air. Measurements were made with scalp electrodes about one hour *post-mortem*. The brain was evacuated but the meninges were left intact. A reference image was made with the cranial cavity filled with saline. The images shown were made 3, 12 and 13 min later, when the cranial cavity was filled successively with saline, air and saline. Quantitative measurements were :

Cranial contents	FWHM (%)	Mean δZ under peak (%)*	Peak position (X,Y), (%)#
Saline	62.6	2.6	52, 41
Air	27.5	472.2	46, 55
Saline	52.0	4.4	43, 42

* - average of pixels with a value greater than $1/e$ x peak value.

- origin is left, occipital.

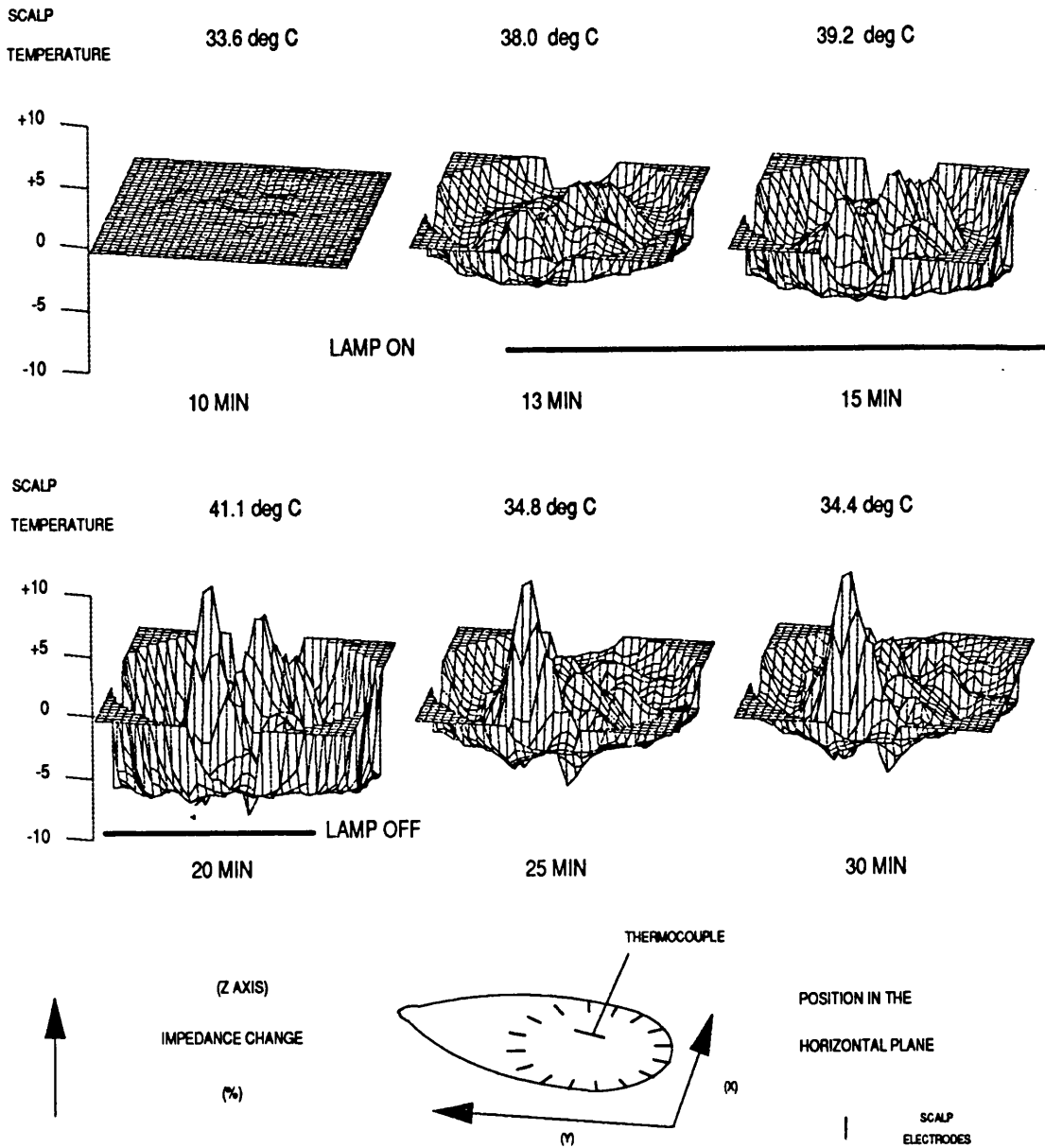
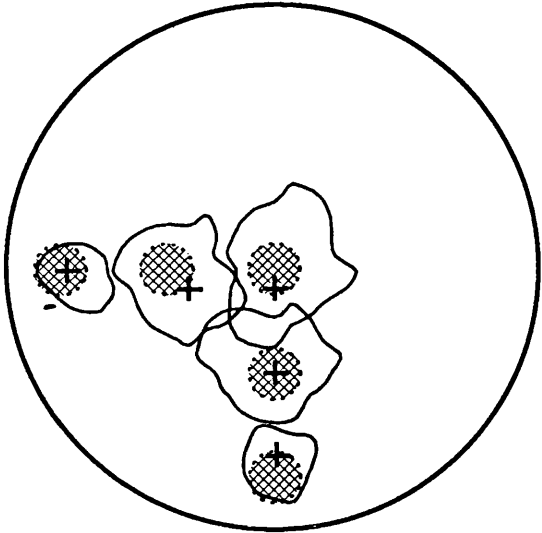


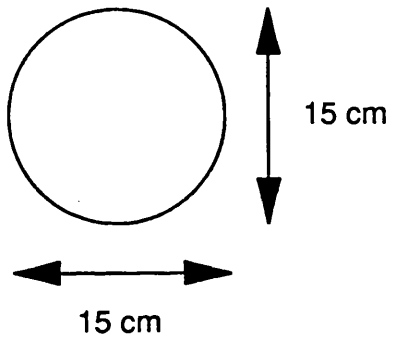
Figure 3.20. EIT images taken during changes in scalp temperature *in vivo*. Images were collected using scalp electrodes over a period of 30 min. A 60 W light bulb was placed about 10 cm above the rat's head from 10 to 20 min. The time and scalp temperature measured by a subcutaneous thermocouple are shown by each image. Images were corrected for baseline shift over the first 10 min.

APT IMAGE
(IMAGES FOR 5 SEPARATE ROD POSITIONS SUPERIMPOSED)

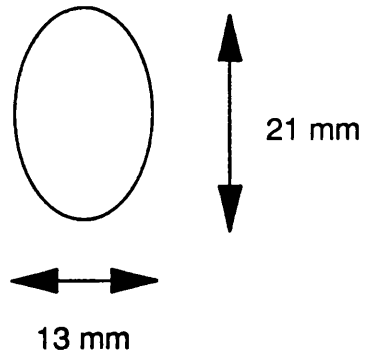
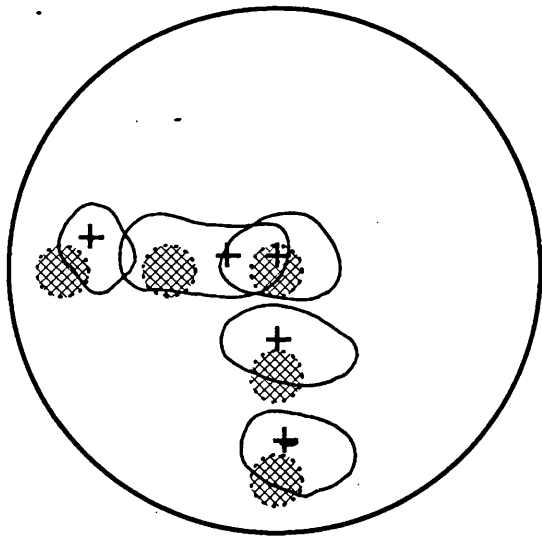


ELECTRODE ARRANGEMENT

CYLINDRICAL TANK



RAT CORTICAL ARRAY



- +** POSITION OF PEAK IMPEDANCE CHANGE
-  CONTOUR LINE AT 50% OF PEAK IMPEDANCE CHANGE
-  CROSS-SECTION OF POLYTHENE ROD

◀ Figure 3.21. Localization of a polythene rod in the large cylindrical or cortical electrode array tanks. A polythene rod was suspended vertically in various positions in saline in either tank. The diameters of the polythene rods were 15 mm and 1.5 mm for the large cylindrical and cortical array tanks respectively. Each rod extended vertically more than twice the tank diameter in both directions. The peaks and boundaries of the FWHM of the image impedance change and the positions of the rods have been superimposed for several rod positions. The positions of the rod relative to the elliptical cortical electrode array are represented as a proportion of axis lengths so as to be comparable in the circular EIT image.

moved in increments of 10% from X, Y coordinates of 50%, 10% to 50%, 50% to 10%, 50%) in the large cylindrical tank, and $7.4 \pm 0.35\%$ (n=9, increments of 20% from 50%, 90% to 50%, 10%, and 90%, 50% to 10%, 50%) in the cortical array tank. The ratio of the FWHM along the Y compared to the X axis was 0.99 ± 0.03 and 1.3 ± 0.03 for the large cylindrical and cortical array tanks respectively.

Under the same conditions, extrapolation from a series of images suggested that a rod placed centrally could be discriminated from a second rod when their centres were 32% or 26% apart for the large and cortical array tanks respectively (Fig. 3.22). The respective gaps between the rods at these points would be 22% and 18%.

An increase in impedance in the EIT image measured with scalp electrodes *post-mortem* occurred when a single polythene rod was inserted into the brain 12% of the array diameter lateral to the midline. When a second rod was added in the same position but on the opposing side of the midline, the impedance increased further, but it is not possible to distinguish two peaks separated by a trough of 1/e of their average value (Fig. 3.23).

3.3.2.4. Sensitivity to localized small changes in impedance.

There was a significant linear correlation between both the peak impedance change and the average change over the area above the peak value

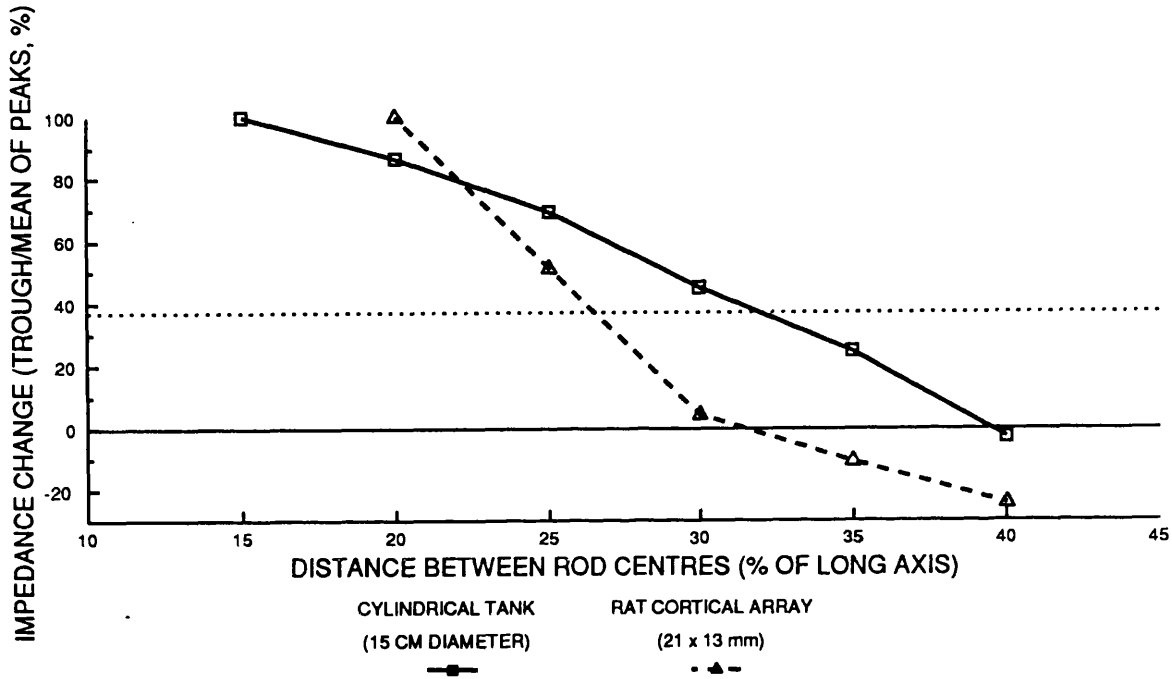


Figure 3.22. Discrimination of two polythene rods by EIT. One polythene rod was suspended in the centre of either the cylindrical tank or cortical array tank. Recording conditions were as in Figure 3.21. Images were collected as a second identical rod was approximated to the first, along the long axis in the case of the cortical array. The lowest impedance change measured along a line between two peaks corresponding to each rod, expressed as a percentage of the mean of the two peaks, has been plotted against the distance separating the centres of the two rods. The trough value falls to $1/e$ of the mean peak value when the rods are separated by 32% and 26% of the tank diameter in the large cylindrical and cortical array tanks respectively.

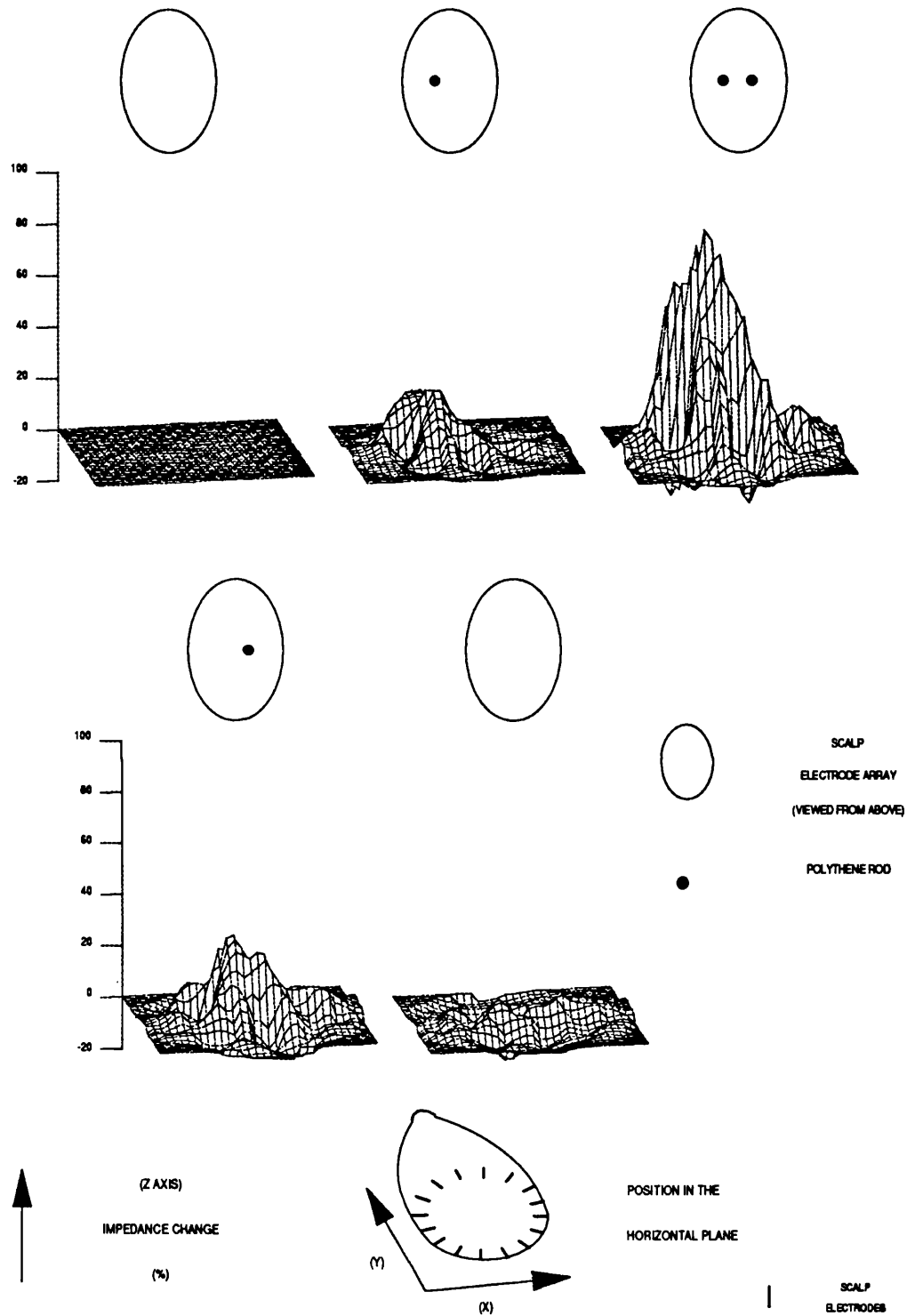


Figure 3.23. Imaging of intracranial polythene rods by EIT with scalp electrodes. Images were taken about 45 min *post-mortem*. The rat was supine, and the ventral surface of the brain was exposed. Polythene rods, 2.4 mm in diameter, were inserted vertically into the brain with their centres 3mm to either side of the midline in the positions shown above each image. When the left rod was removed (lower left image), the hole was filled with 0.9% saline.

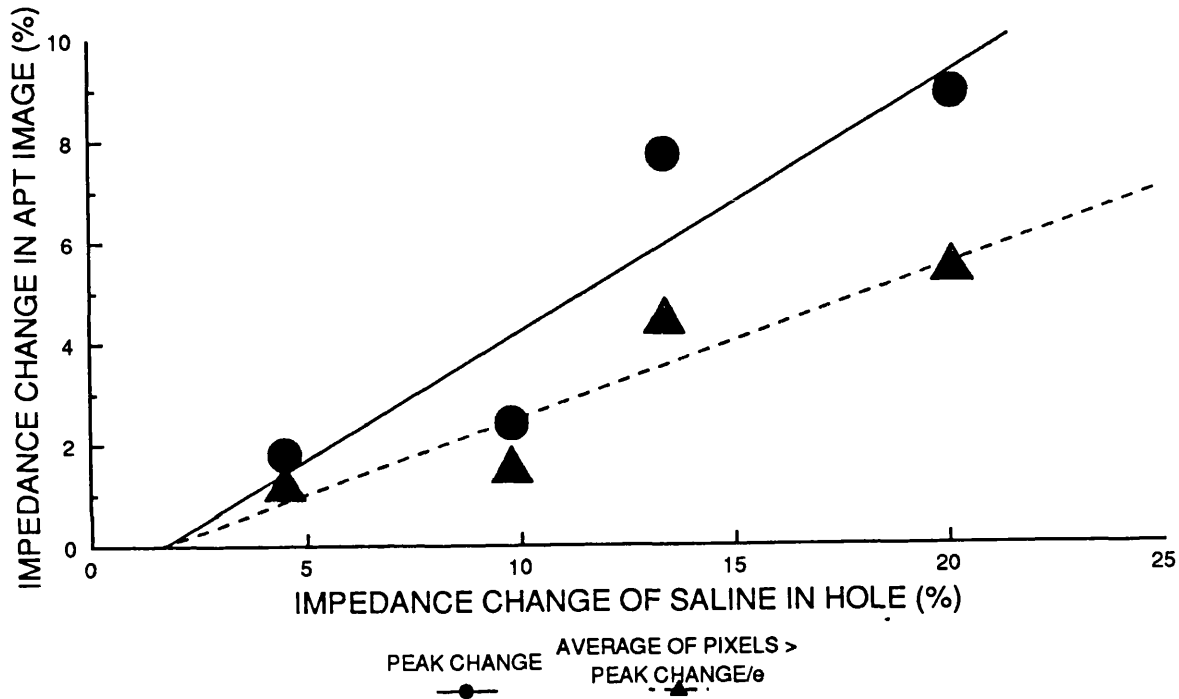


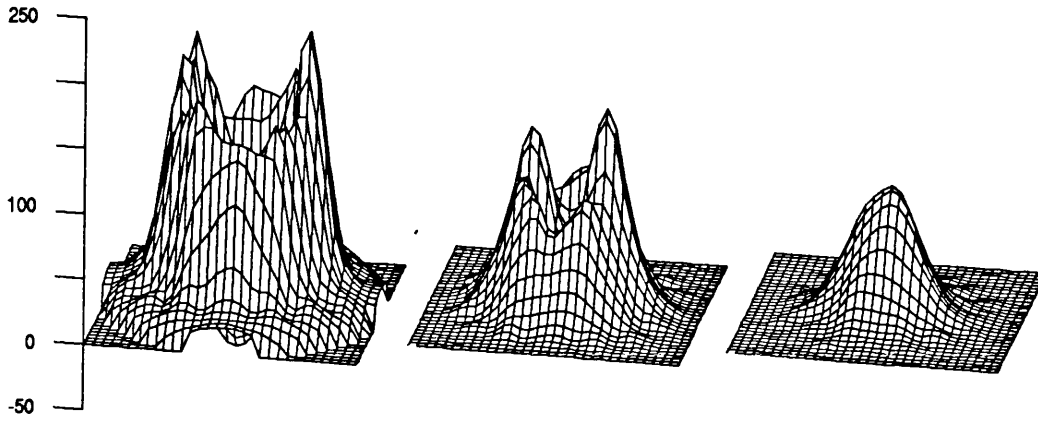
Figure 3.24. Detection of small localised impedance changes by EIT. The rat cortical tank was filled with agar made from 3% agar and 0.118% saline. A vertical central hole, 2.25 mm in diameter, was made in the agar. The measurements presented were obtained from the differences between paired images obtained with 0.118% saline and test solutions in the central hole. Linear regression data (shown as lines) are : $r = 0.84, 0.86$, slope = 0.51, 0.30 for the peak impedance change and average change of pixels greater than the peak value / e respectively. The FWHM was 20.9 ± 1.3 and 12.8 ± 0.8 % (expressed as % of the axis length) for the X and Y axes respectively.

HEIGHT OF SALINE
ABOVE ELECTRODE RING :

2 cm

4 cm

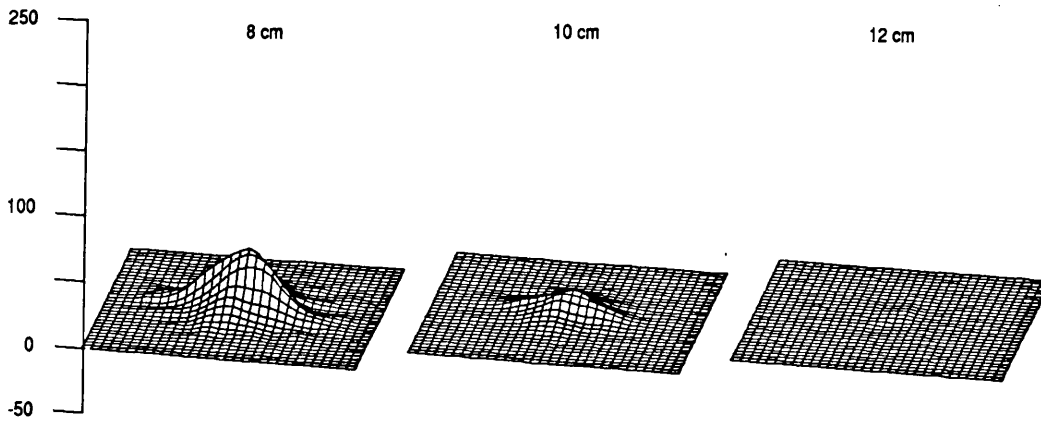
6 cm



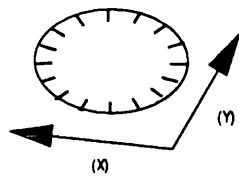
8 cm

10 cm

12 cm



(Z)
↑
IMPEDANCE CHANGE
(%)



POSITION IN THE
HORIZONTAL PLANE

ELECTRODES

◀ Figure 3.25. Effects of impedance changes out of the plane of the electrode ring on the EIT image. Images were collected with saline at levels from 2 to 12 cm above the electrode ring in the large cylindrical tank. Images represent the change in impedance with respect to the image obtained with the saline level 12 cm above the electrode ring. The standard deviations (S.D.*) of the equivalent gaussian volume, and the average values of pixels greater than the peak value/e were :

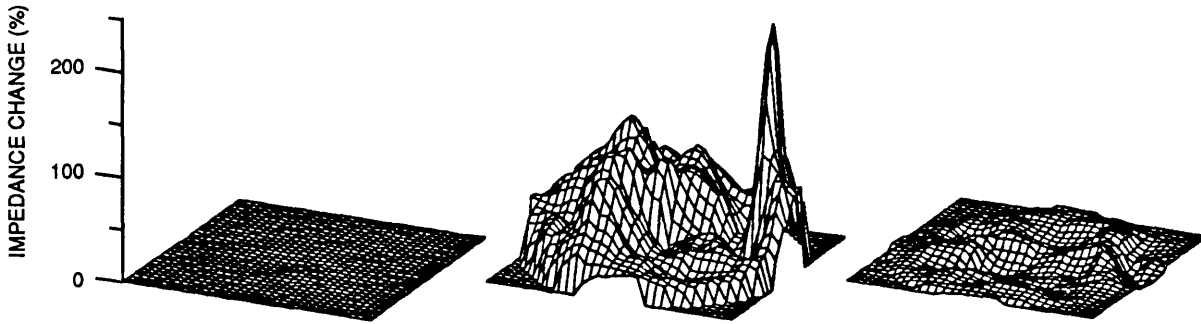
Height of saline above electrode ring (cm)	Average value of pixels > peak value /e (%)	S.D.* in XY plane (% of tank diameter)
12	0.4	10.9
10	10.3	9.7
8	28.0	18.1
6	61.0	20.3
4	85.9	25.6
2	136.1	21.3

divided by e and the resistivities of test solutions placed in a hole in agar filling the cortical electrode array. The resistivities of the test solutions were up to 20% more than that of the agar (Fig. 3.24). The FWHM of the increases were 20.9 ± 1.3 and 12.8 ± 0.8 % (expressed as % of the axis length) for the X and Y axes respectively. The physical dimensions of the hole were 17.3 and 10.7% along the X and Y axes respectively.

3.3.2.5. Effects of impedance changes out of the plane of the electrodes.

The height of saline in the large cylindrical tank was varied from the reference height of 12 cm above the electrode array to 2 cm above it. Changes in the images ranged from a toroidal increase with the largest change, and a central approximately gaussian shape for the smaller changes (Fig. 3.25).

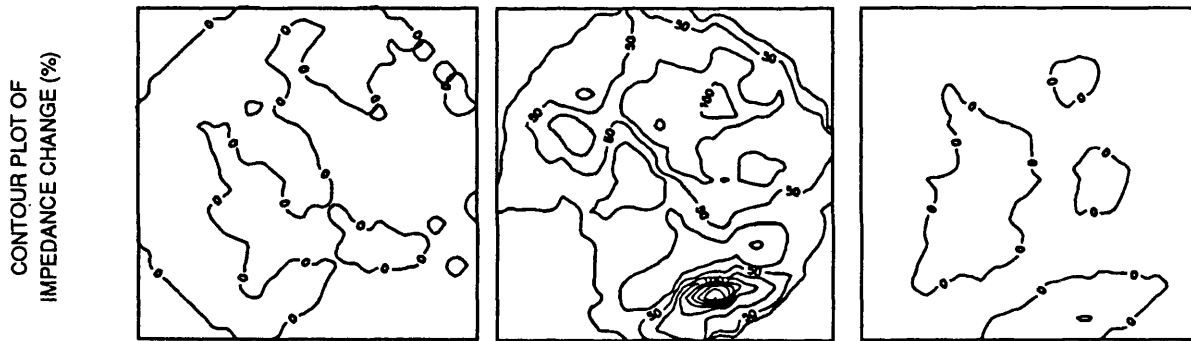
TIME : 10 MIN 25 MIN 50 MIN
 CAROTID ARTERY OCCLUSION



CORTICAL TEMPERATURE CHANGE
 RELATIVE TO t=10 MIN (deg C)

+0.4±0.1

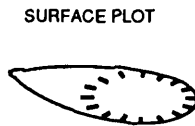
+1.0±0.4



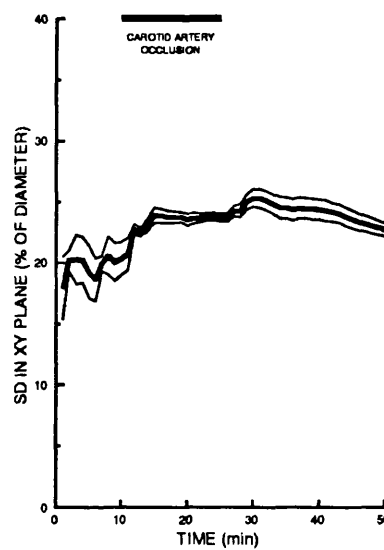
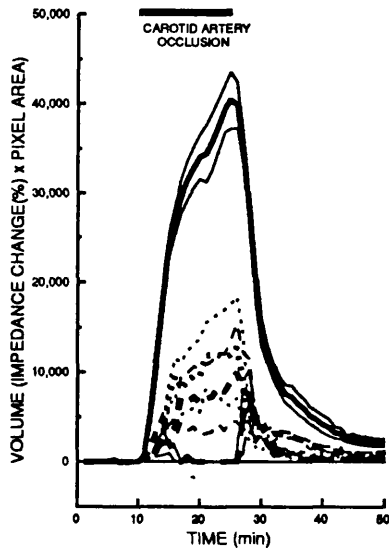
SURFACE PLOT

CONTOUR MAP

IMAGE ORIENTATION :
 (VIEWED FROM ABOVE)



CORTICAL
 ELECTRODE



TOTAL IMAGE

PEAK 1

PEAK 2

PEAK 3

Figure 3.26 (a). EIT images measured on the cortex during cerebral ischaemia.

3.3.3. EIT images collected during cerebral ischaemia *in vivo* and *post-mortem*.

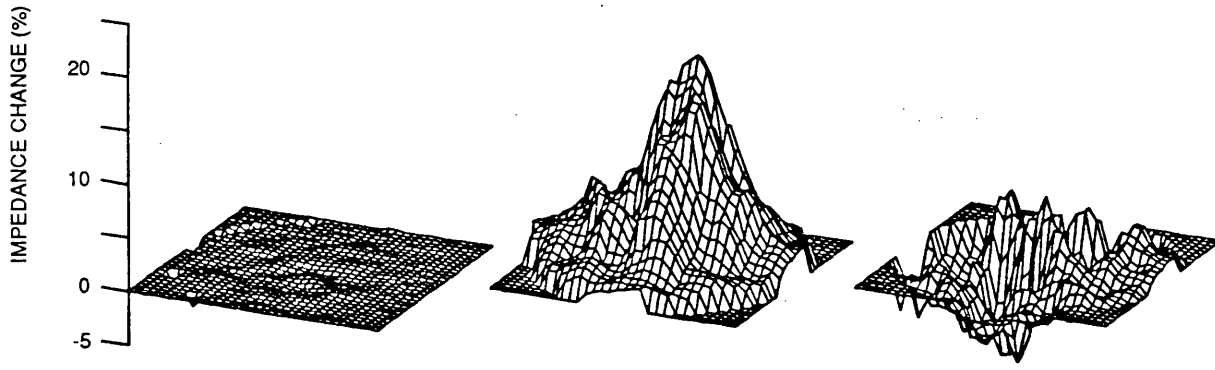
3.3.3.1. Measurements with cortical electrodes.

In another series of experiments, EIT images were collected with the cortical electrode array *in vivo*. During cerebral ischaemia, an impedance increase was observed, which reversed on reperfusion (Fig. 3.26a). Two major peaks occurred which corresponded in position to the occipital and frontoparietal regions, slightly to one side of the midline. Both were present in each of the four images in two rats which were averaged to produce the displayed surface plot. Their peak amplitudes were 228 ± 89 and 141 ± 10 % (n=4 in 2 rats) respectively. Impedance changes with respect to time are illustrated in the lower left graph in Fig. 3.26(a). The volume (the sum of the impedance changes in all pixels) of the whole image increased rapidly for about 4 min, then increased until the end of carotid artery occlusion at a lesser rate. A guide to the time courses of the individual peaks is also shown in the same graph. This was obtained by an automatic software routine; peak 1 refers to the highest peak, peak 2 to the next highest, and peak 3 to the third highest. The volume displayed for each peak is that of an area around the peak whose values are equal to or greater than $1/e$ of the peak height. Only the three highest peaks were chosen for analysis. Therefore the totals of the peak volumes do not add up to the total for the whole image. It may be seen that two major peaks (which correspond to the peaks mentioned above) are present for the majority of the period of carotid artery occlusion. Their time course has

Figure 3.26. ((a) left, (b-d) on following three pages). Averaged EIT measurements in the rat made with either cortical or scalp electrodes during cerebral ischaemia (a & b, n=4 in 2 rats in each case) or post-mortem (c & d, n=1 & 2 respectively). EIT images were collected every minute either during cerebral ischaemia produced by occlusion of the carotid arteries for 15 min, or from the time of death for a period of 30 min. The upper and middle images are surface and contour plots of the same data. Lower left : The volume of the whole image and largest three peaks with respect to time are shown. Heavy and light lines represent the mean and limits of ± 1 S.E. respectively. Lower right : The standard deviation in the XY plane of the whole image is shown. This is calculated by taking the standard deviation of gaussian volume approximated to the image (see section 2.4.2.3).

TIME : 10 MIN 25 MIN 50 MIN

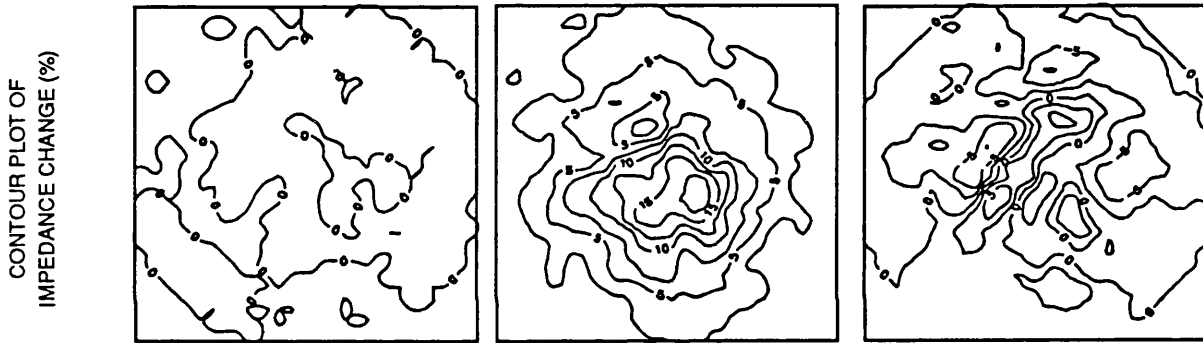
CAROTID ARTERY OCCLUSION



SCALP TEMPERATURE CHANGE
RELATIVE TO t=10 MIN (deg C)

-0.1±0.1

+0.1±0.2



SURFACE PLOT

CONTOUR MAP

IMAGE ORIENTATION :
(VIEWED FROM ABOVE)



SCALP
ELECTRODE

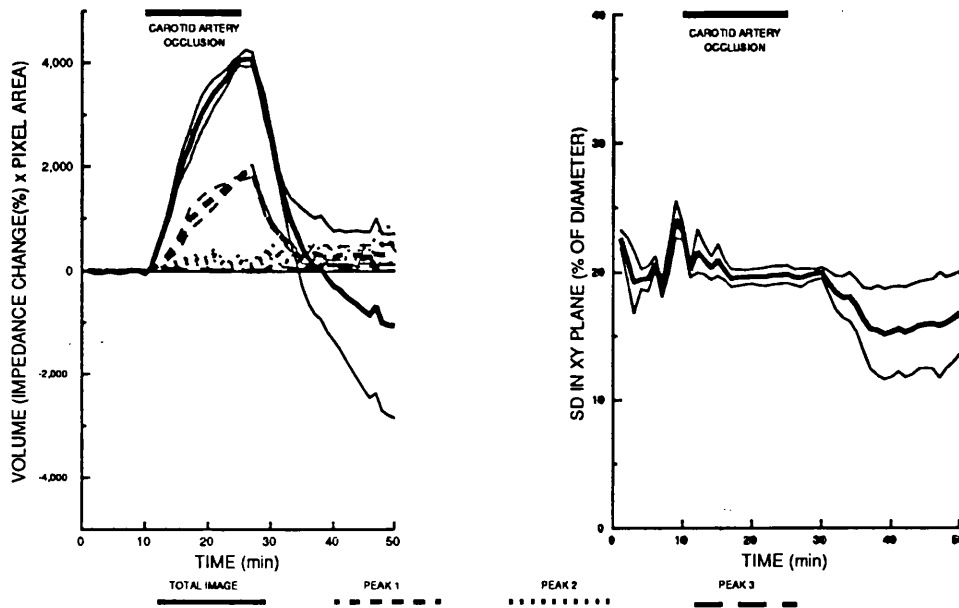


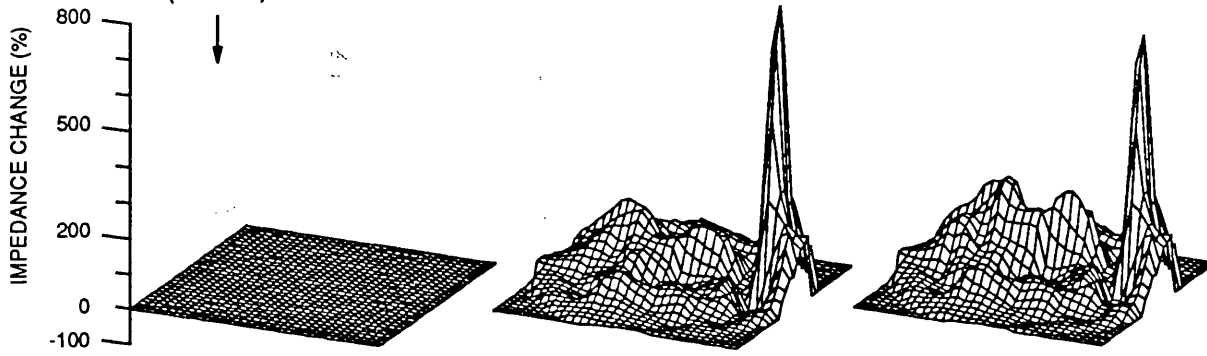
Figure 3.26 (b). EIT images measured with scalp electrodes during cerebral ischaemia.

TIME : 1 MIN

15 MIN

30 MIN

DEATH
(0 MIN)



CORTICAL TEMPERATURE CHANGE
RELATIVE TO $t = 0$ MIN (deg C)

-1.3

-2.2



SURFACE PLOT

CONTOUR MAP

IMAGE ORIENTATION :
(VIEWED FROM ABOVE)



CORTICAL
ELECTRODE

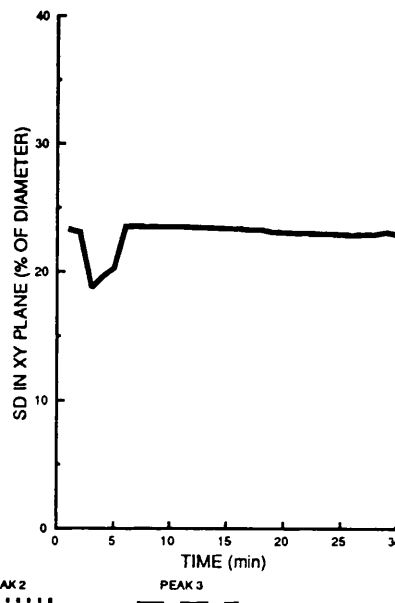
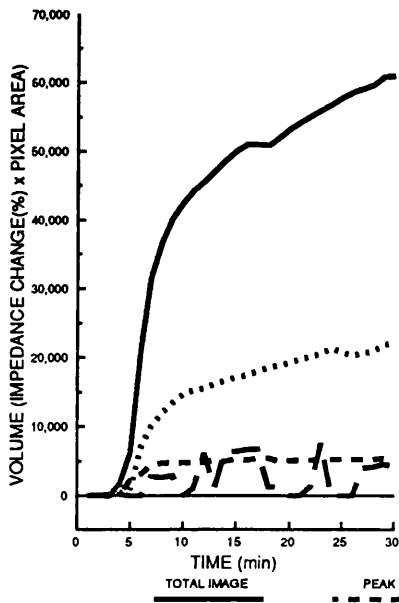


Figure 3.26 (c). EIT images measured on the cortex *post-mortem*.

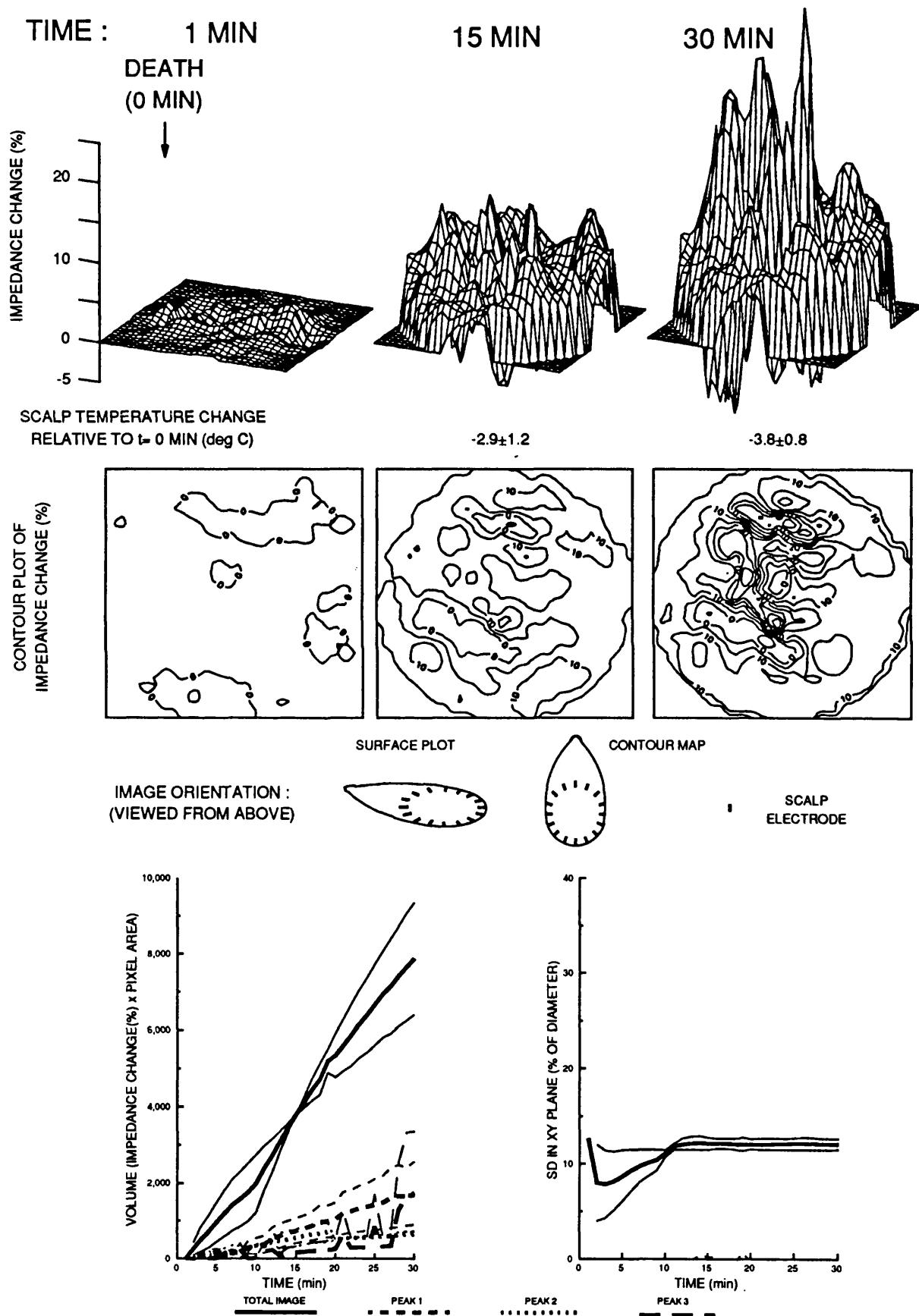


Figure 3.26 (d). EIT images measured with scalp electrodes *post-mortem*.

a similar bipartite character to that of the volume of the whole image. Peak 1 is the occipital peak; because it is narrow, its volume is less than that of peak 2, the frontoparietal peak. The lower right hand graph displays the estimated standard deviation of the whole image with respect to time (see section 2.4.2.3), calculated on the assumption that the image is gaussian. In this case, the image is not gaussian, as it has two main peaks, but the value gives an approximate guide to the area of the whole image over which an impedance increase was present. For most of the period of carotid artery occlusion, the S.D. calculated in this way was about 24%.

Images were also collected for a period of 30 min, commencing immediately *post-mortem*. Impedance increased in a similar distribution to records *in vivo*, but the volume increase in the first 15 min was greater than that *in vivo* by about 25%. The impedance of the occipital peak increased by 798% at 15 min (1 rat). The impedance changes continued for the duration of the period of recording (Figure 3.26c).

3.3.3.2. Measurements with scalp electrodes.

During cerebral ischaemia *in vivo* measured with scalp electrodes, the images showed a predominantly central impedance increase (Fig. 3.26(b)). The volume change reached a maximum of about 10% of the increase when measured with cortical electrodes, and the peak impedance increases were $22.4 \pm 2.8 \%$ (n=4 in 2 rats). The impedance returned to the baseline on reperfusion, but with greater variability than in the cortical records. The time course of the major central peak is illustrated in Fig. 3.26(b), lower left. Only one substantial peak is present throughout the period of carotid artery occlusion; peaks 2 and 3 were calculated automatically but may be seen to be much smaller and represent small fluctuations towards the periphery of the image. The impedance of the major peak may be seen to increase more rapidly over the first 5 min or so of cerebral ischaemia. The FWHM of the total image at maximum impedance change was 20%, compared to 24% for the cortical image at the same point. In addition, a peripheral impedance increase of several per cent is present, which extends to the edge of the image.

Post-mortem, the impedance increase was more widespread and irregular, and continued to increase until the end of the period of measurement (Fig. 3.26d). The peak increase was $24.5 \pm 2.3 \%$ (n=2) after 15 min.

4. DISCUSSION (1) : SIMPLE MATHEMATICAL MODELS OF SOME OF THE EXPERIMENTAL SITUATIONS DESCRIBED ABOVE.

4.1. INTRODUCTION.

Some simple mathematical models of some of the preceding experiments have been constructed. The model parameters were measured directly or inferred from experimental measurements where possible; others were derived from the literature. In view of this, and the use of various simplifying assumptions, the projections are approximate.

A model intended to confirm the depth of the disturbance in cortical impedance during spreading depression is presented in section 4.2. Models of impedance changes measured in the scalp during stroke or spreading depression are presented in section 4.3. They are restricted to representation of data measured with a single impedance channel with the electrodes closely and equally spaced. In this way analysis was simplified to a two dimensional problem by simulating the various layers as planes. Projection of the way in which such changes would be attenuated when measured at different positions around the head, as in some of the scalp single channel or EIT records, is largely an engineering problem and has not been addressed in this study.

4.2. MODEL TO ESTIMATE THE DEPTH OF THE CORTICAL IMPEDANCE CHANGE DURING SPREADING DEPRESSION.

Slow potential changes (Monakhov et al, 1962) and impedance increases (Hoffman et al, 1973) during spreading depression have been recorded in all layers of the cerebral cortex in the rat. Using a four electrode method in the cat, Freygang and Landau (1955) measured a resistivity decrease of 13% across the full thickness of the cortex during spreading depression. A larger decrease of 23% was measured in the superficial 0.8 mm. There do not appear to be any

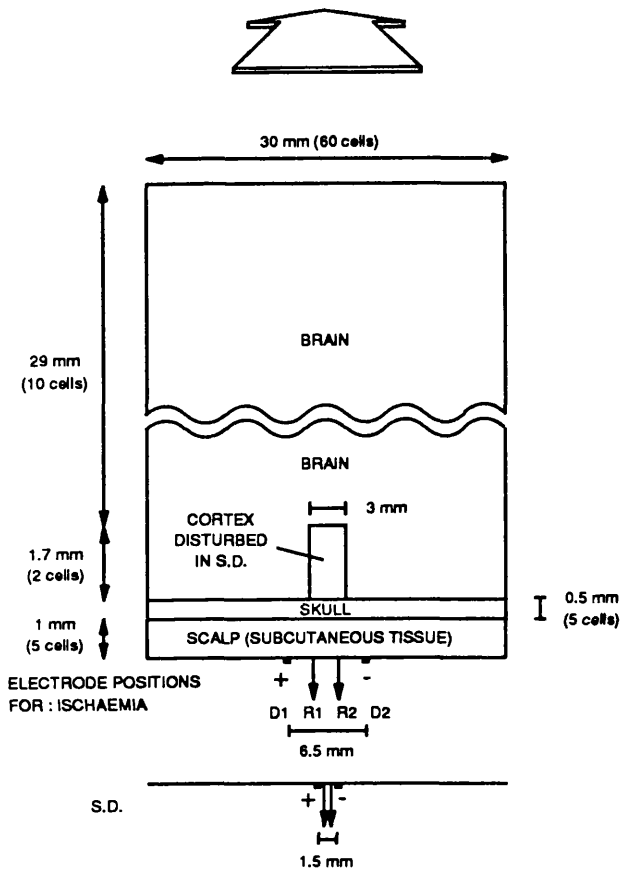
other published investigations into the depth profile of the impedance disturbance in spreading depression.

In order to model the impedance change during spreading depression (section 4.3), it was desirable to confirm whether the impedance change in rat cortex occurred across the full thickness of the cortex, which is about 1.7 mm in the parietal region (Paxinos and Watson, 1982). The experiment described in section 3.2.5 (Fig. 3.17) was performed to yield data for this analysis. The in-phase component of the potential at one recording electrode (V_x) in various positions whilst the drive electrodes were fixed was measured with respect to time during successive waves of spreading depression. The shape of the relation of V_x with time (and therefore the position of the wave of spreading depression) was related to the depth of the disturbance; this could be modelled to suggest the depth of the impedance change.

A mathematical model was constructed in which a specified small volume of infinite resistivity (Vol_{SD}) moved at 4 mm/min at depths of 0.5 - 3mm below the surface of a semi-infinite medium of constant resistivity (420 Ω .cm). It can be shown that the impedance change due to this can be represented by a dipole at the centre of Vol_{SD} . The magnitude of the dipole is proportional to the current flowing across the surface of Vol_{SD} and to its volume. V_x can then be calculated according to the field produced by the dipole. It is assumed that the volume of Vol_{SD} is sufficiently small that the current entering it from the surrounding medium is not significantly perturbed, and that the field produced by a current entering it is the same as the field due to a dipole in its centre. This should be the case if each dimension of Vol_{SD} is less than the distance between the drive electrodes.

The shape of the calculated change in V_x with time depends on the depth of Vol_{SD} ; this corresponds most closely with the experimentally observed results when the centre of Vol_{SD} moves 1 mm below the surface (Fig. 3.17c). A more sophisticated model would be needed to infer the local resistivity change within Vol_{SD} and its dimensions. However, it seems reasonable to infer that the impedance disturbance extends approximately equally in a vertical direction from its centre at 1mm and so occupies the full depth of the cortex.

a) TRANSLATIONAL SYMMETRY



b) ROTATIONAL SYMMETRY

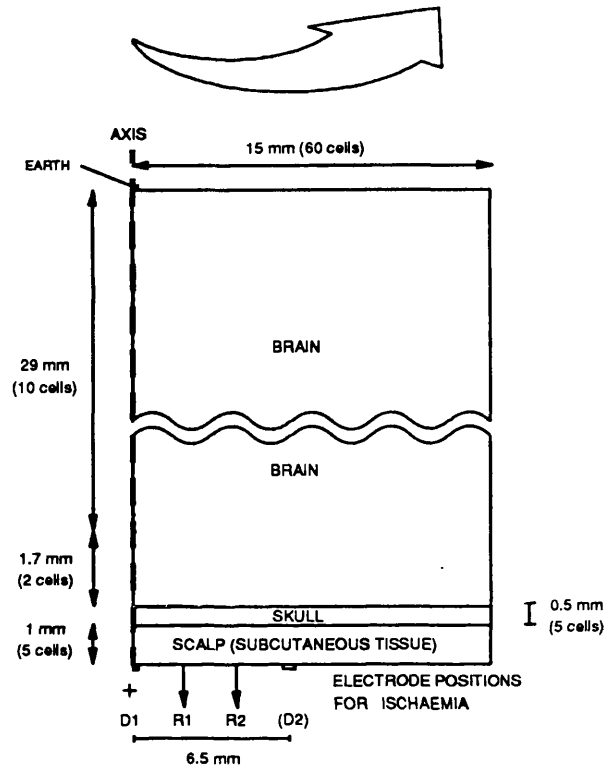


Figure 4.1. Matrices used in finite element models of impedance measurement. The matrices shown are for models of brain, skull and scalp. The models of measurement with cortical electrodes are identical, except that the skull and scalp layers were absent, and the electrodes were sited on the cortex. The direction of projection is shown by the arrow above each matrix.

This should also satisfy the assumption made in the model that the dimensions of the disturbed area were less than the drive electrode separation of 4mm used experimentally.

4.3. FINITE ELEMENT MODEL OF IMPEDANCE CHANGES MEASURED IN THE SCALP DURING CEREBRAL ISCHAEMIA OR SPREADING DEPRESSION.

4.3.1. Description of the model.

The extent to which impedance changes measured on the brain are attenuated when measured on the scalp was modelled by a program (Laplace version 2.3 (Hagelstein and Associates, Livermore, California, USA)) which was run on an IBM compatible AT 286 microcomputer. It solved Laplace equations in two dimensions through numerical finite element analysis. Experiments during cerebral ischaemia, measured with needle electrodes equally spaced 2mm apart, or during spreading depression, measured with the araldite electrode array, were simulated. The potential distribution due to applied current was calculated by analogy to an electrostatic field problem. Applied current and conductivity were equated with charge density and the dielectric constant respectively. All external boundaries (except earth, which was set at zero potential) were represented by a "reflective" condition, in which the electric field was tangential along the boundary. A matrix was constructed in which a cross-section of the brain, an area of cortex within the brain whose impedance varied during spreading depression, the skull and the scalp were represented by a number of rectangular cells (Fig. 4.1). The impedance of dura is substantially less than that of the adjacent skull (see section 1.3.4), so the two were lumped together. In the skin, the largest impedance consists of the stratum corneum (Yamamoto and Yamamoto, 1976). In the experiments simulated, however, needle electrodes were inserted subcutaneously in the scalp in experiments on cerebral ischaemia, or the araldite electrode array was placed on abraded depilated scalp in experiments on spreading depression. The

scalp was therefore modelled as a single layer of subcutaneous tissue. Each layer was assumed to be homogeneous and planar.

Arbitrary units were used, as the purpose was to calculate a change in impedance. The apparent impedance was taken to be proportional to the potential difference between the two simulated recording electrodes, which were placed at two points equally spaced between the centres of the drive electrodes. This value was obtained first with the resistivity of brain set at a resting value, and then after it had been set to an appropriate value for cerebral ischaemia or spreading depression. The impedance change was calculated as the percentage change in impedance measured in the disturbed as opposed to the resting state. The output of the program was in the form of plots of lines of isopotential (*e.g.* Fig. 4.2 and 4.3). By enlarging the lines of isopotential, an accuracy of about $\pm 0.2\%$ was obtained.

The model approximated to three dimensions by projection of the two dimensional matrix in specified directions. In translational projection, the matrix was extrapolated in a direction perpendicular to both existing axes (*i.e.* into the page, see Fig. 4.1a). This produced an accurate model of planar layers, but the electrodes were represented as infinite cables. Point electrodes could be approximated by using rotational projection around one long axis (Fig. 4.1b). A single point electrode was simulated by a point electrode at the origin. An earth boundary condition was specified at the other end of the axis of rotation (Fig. 4.1b) in order to provide a current sink and simulate the model with translational symmetry. Providing the model was symmetrical about each drive electrode, the potential difference measured between R1 and R2 was half of the value that would have been measured in an identical 3-D model with both drive electrodes acting as a dipole, by the principle of superposition. In the case of the model of cerebral ischaemia, there would only have been a minimal asymmetry between the models for each drive electrode on this basis, and any effects due to this were assumed to be negligible. The impedance change was calculated as the percentage change in the potential difference between R1 and R2 with the brain in resting or disturbed states. Rotational projection was not used in the case of spreading depression as it would not

have been possible to preserve symmetry of the discrete volume of disturbed cortex. This was unfortunate, as point electrodes were used experimentally. However, the prediction of the model with translational symmetry could be taken to be an upper bound for the prediction of a model with point electrodes, as infinitely long electrodes would tend to train current through the region of disturbed cortex and overestimate the impedance change.

4.3.2. Selection of model parameters.

The drive electrodes were represented by cells 0.5mm wide and 0.1mm deep. Their centres were made 6.5mm apart to simulate recording with wire electrodes on the cortex or in the scalp during cerebral ischaemia (section 2.1.3 and Fig. 2.3), or 1.5 mm apart to simulate recording with the araldite electrode array with adjacent electrodes selected during spreading depression (section 2.3.2). The area representing brain was made to be 31 mm deep and 30 mm wide, so that current density at the boundaries away from the drive electrodes would be negligible. A region which represented the area of cortex disturbed at the time of the peak impedance change during spreading depression was placed symmetrically about the drive electrodes. As the FWHM of the cortical impedance change in SD was 1 min (Table 3.3) and it propagated at 3mm/min (section 3.2.3), this area was made 3mm wide. A narrower disturbance could have given a similar FWHM as it passed between the drive electrodes. However, a similar peak impedance increase was observed when electrodes were equally spaced 1mm apart (Table 3.4), which suggests that the impedance disturbance occupied a substantial fraction of the distance of 3mm between the drive electrodes. The region was set to be 1.7mm deep (see section 4.2 above). The skull and scalp were represented by layers 0.5 and 1 mm thick respectively.

The in-phase component of the impedance of rat skull was measured experimentally, using the device described in section 2.3. Ag/AgCl wire electrodes, 0.5mm in diameter and 4mm long, were used. One drive and one recording electrode were set into the end of a plastic tube 8cm long and 1cm

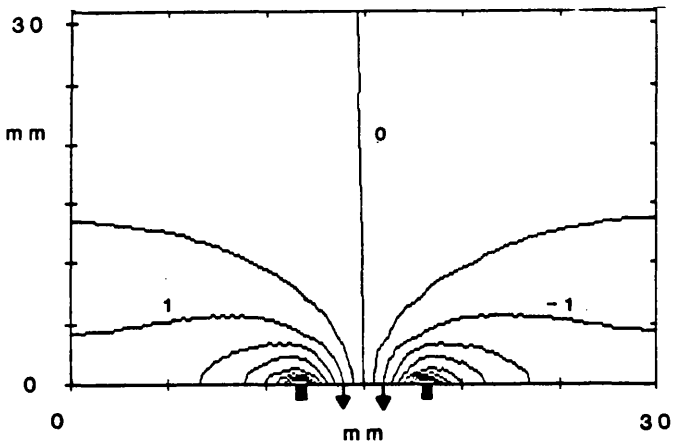
in diameter. A rubber bung with a central orifice 4 or 8mm in diameter was inserted in the other end. Two such horizontal tubes were opposed to each other at the rubber bung. A piece of parietal skull from a recently killed rat was inserted between the rubber bung and a watertight seal was produced by gentle lateral pressure on both tubes. Each was then filled with 0.9% saline, and an impedance measurement was taken. This was corrected for the resistivity of the saline, which was measured by repeating the process after the bone had been removed. The skull was measured with a micrometer and was 0.4 - 0.5 mm thick. The resistivity in specimens from two rats varied between 9,000 and 13,000 Ω .cm. This varied by less than 4% when measured repeatedly over 10 min. As the first measurement was made within 5 min of insertion of the sample into the saline, it seemed unlikely that the measured impedance was significantly altered by diffusion of saline into the bone.

The impedance of each tissue was taken to be the same as its resistivity. The resistivity of various regions of rabbit cerebrum or cortex measured at 1-5 kHz has been variously reported as 208 - 746 Ω .cm (see Geddes and Baker, 1967). The resistivity of fresh cortical bone of the rat femur measured at 50 kHz was about 14,000 Ω .cm (Kosterich et al, 1983), which is in reasonable agreement with the experimentally measured figure above. As there do not appear to be reports of the specific resistivity of the dermis, subcutaneous scalp was taken to have a similar resistivity to mammalian skeletal muscle. This has been reported to be between 435 and 1130 Ω .cm measured at 10 - 100 kHz in several species (see Geddes and Baker, 1967).

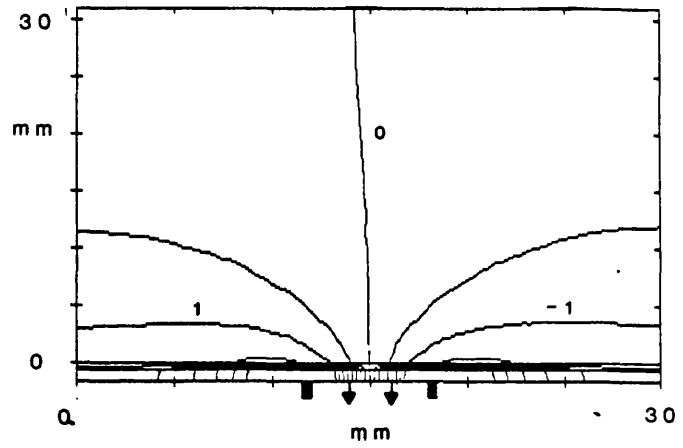
There is clearly substantial variability in the above figures. As a rough approximation, the conductivity of the resting brain and subcutaneous scalp tissue was set as 1.0 (in arbitrary units), and that of skull as 0.05. The conductivity of the disturbed brain was set at a value that gave approximately the impedance change measured experimentally when calculated for a model with electrodes resting on the brain surface (and no skull or scalp layers). This was 0.83 for cerebral ischaemia and 0.7 for spreading depression (Table 4.1).

a) MODEL OF CEREBRAL ISCHAEMIA (RESTING)

BRAIN ONLY

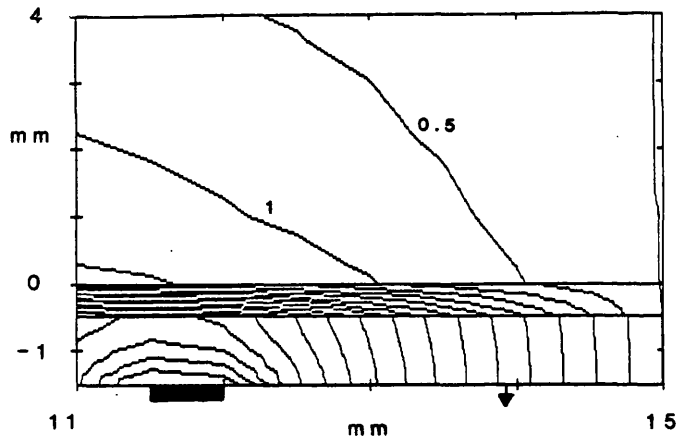


3 LAYERS

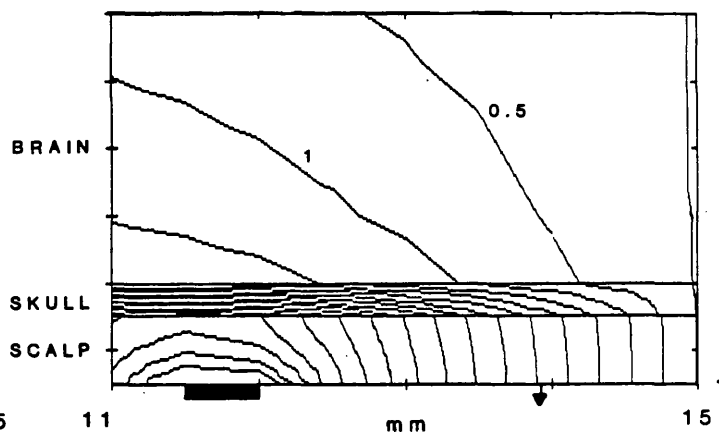


b) 3 LAYER MODEL OF CEREBRAL ISCHAEMIA (ENLARGED)

RESTING

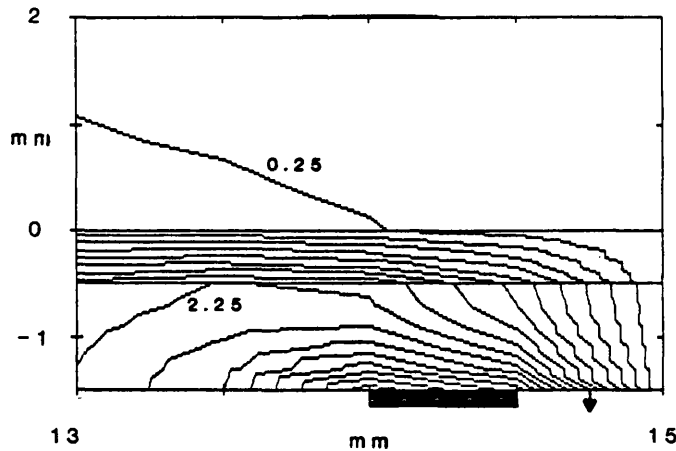


DURING ISCHAEMIA

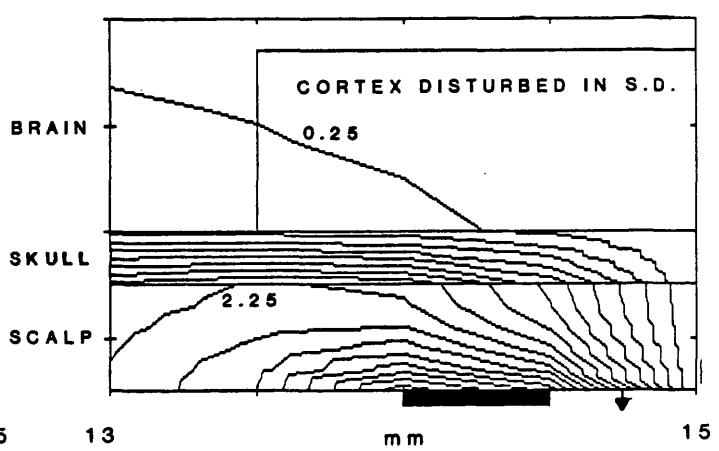


c) 3 LAYER MODEL OF S.D. (ENLARGED)

RESTING



DURING S.D.



ELECTRODES : ■ DRIVE

↓ RECORDING

◀ Figure 4.2. Results of models of impedance measurement during cerebral ischaemia or SD with translational projection. The left and right drive electrodes were set to be positive and negative respectively. Lines of isopotential in the plane of the model matrix are shown. For clarity, closely spaced isopotentials around the drive electrodes have been omitted; the intervals between displayed lines are equal. For comparison between plots, some lines are labelled (in arbitrary units). The lower four plots are enlargements of the areas around the positive drive electrode. It may be seen that during both cerebral ischaemia and spreading depression, the potential gradient in the brain changes appreciably, but the effect on the potential measured at the recording electrode is negligible in the case of spreading depression.

4.3.3. Results.

Results are shown in Table 4.1, Fig. 4.2 and Fig. 4.3. With translational projection, the model predicted an impedance increase of 2.1% during cerebral ischaemia measured with scalp electrodes; the change during spreading depression was unmeasurable (<0.2%). With rotational projection, the impedance increase during cerebral ischaemia was reduced to 1.0%; the change during spreading depression could not be directly calculated, but could be expected also to be less than 0.2%.

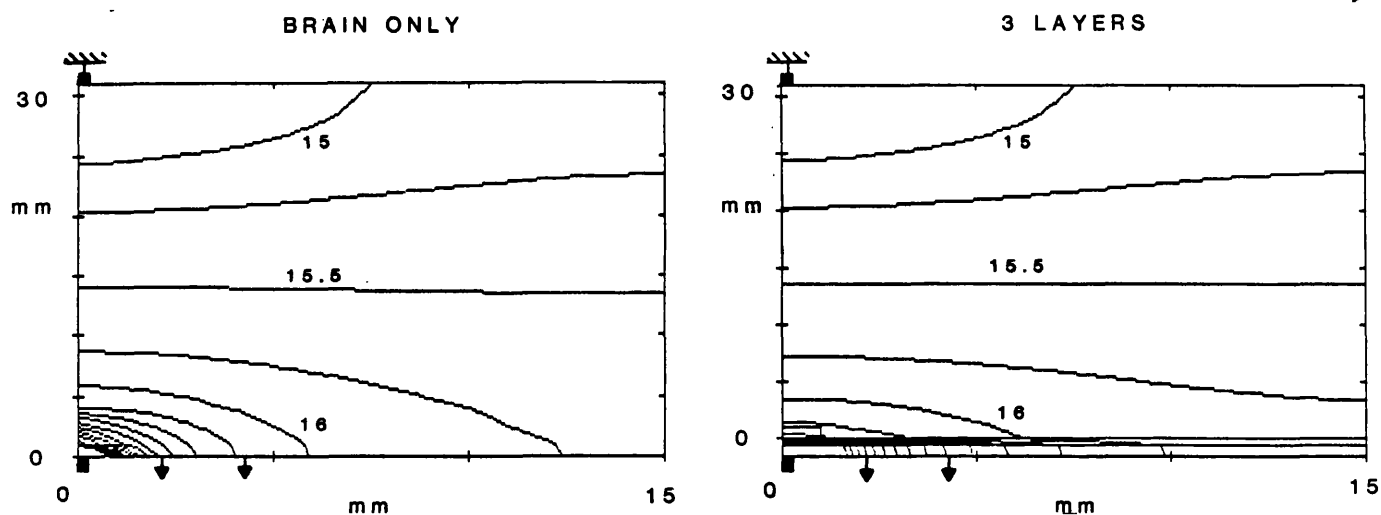
<u>Condition</u>	<u>Projection</u>	<u>Model</u>	<u>Impedance change (%)</u>
Cerebral ischaemia	Translational	Brain only	20.6
"	"	3 layers	2.1
"	Rotational	Brain only	21.9
"	"	3 layers	1.0
Spreading depression	Translational	Brain only	38.7
"	"	3 layers	<0.2

Table 4.1. Results of finite element model.

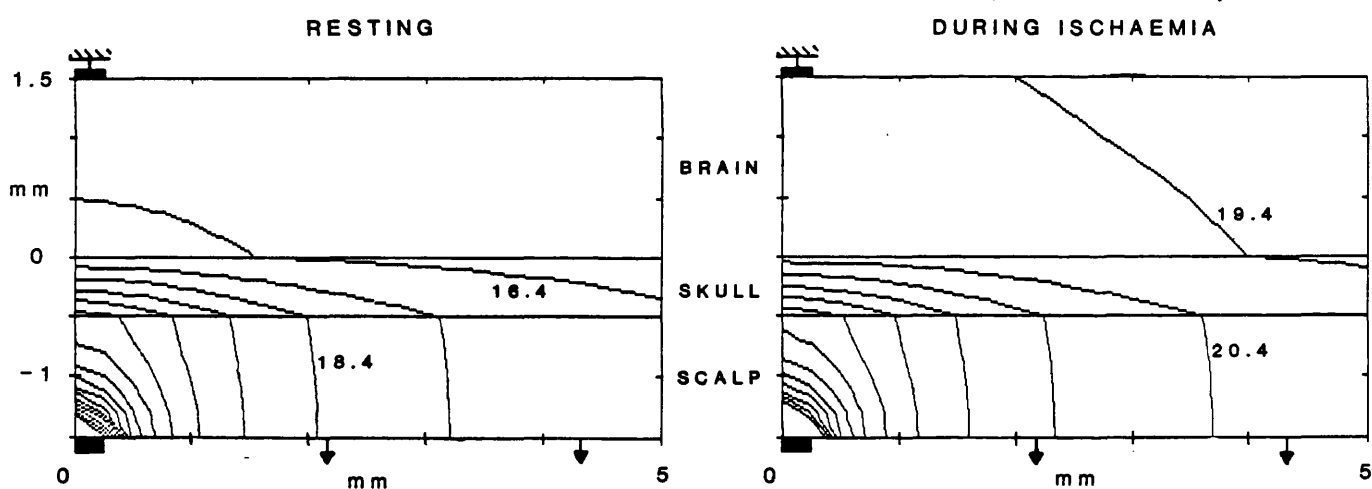
4.3.4. Discussion.

The model appears to be a reasonable approximation to the experimental situation. Inspection of Fig. 4.2 indicates that the great majority of the current passes within a few millimetres of the drive electrodes, where the curvature of the skull in the parietal region is slight. The treatment of the

a) MODEL OF CEREBRAL ISCHAEMIA (RESTING)



b) 3 LAYER MODEL OF CEREBRAL ISCHAEMIA (ENLARGED)



ELECTRODES : ■ DRIVE ↓ RECORDING

Figure 4.3. Results of a model of impedance measurement during cerebral ischaemia with rotational projection around the left hand vertical axis. The single drive electrode was made positive and current passed to earth. Isopotentials are displayed as in Fig. 4.2. The lower two plots are enlargements of the area around the drive electrode.

layers as planes should therefore be fairly accurate. The impedance of the resting brain is unlikely to be homogeneous. White matter lies immediately underneath the cortex, and had a specific resistivity 50% greater than grey matter in the cat (Freygang and Landau, 1955). It also has been reported as being markedly isotropic (Nicholson, 1965). However, the increase in impedance measured experimentally with cortical electrodes during cerebral ischaemia did not differ significantly when measured with drive electrodes 6, 13 or 26 mm apart (Table 3.2). Since the different spacings would have led to current paths that included different amounts of white matter, it seems justifiable to treat the brain (and its specific impedance increase during cerebral ischaemia) as homogeneous within the limits of accuracy of the model. The impedance of subcortical white matter in the cat measured with square wave pulses 0.3 - 0.7 msec in duration decreased during spreading depression (Freygang and Landau, 1955). This possibility was not included in the model. However, this decrease was about 40% of the magnitude of the increase measured in the overlying cortex. As most of the current passing into the brain in the model passes into the cortex, it is unlikely that this effect would have altered the prediction that the impedance change was undetectable.

The scalp was modelled as a layer 1mm thick, on which were placed square electrodes. Experimentally, cerebral ischaemia was measured with subcutaneous electrodes, and spreading depression was measured with surface electrodes firmly applied, which would have compressed the scalp. However, these inaccuracies are unlikely to have altered substantially the magnitude of the low resistance current path between the drive electrodes presented by the scalp when considered in relation to the high resistance presented by the skull.

4.3.5. Predictions of the finite element model for impedance changes during SD with different electrode spacings.

Scalp impedance measurements during CSD were made mainly with electrodes spaced 0.5 mm apart. This arrangement was chosen *a priori*, as likely to detect impedance changes in the cortex due to anoxic depolarization.

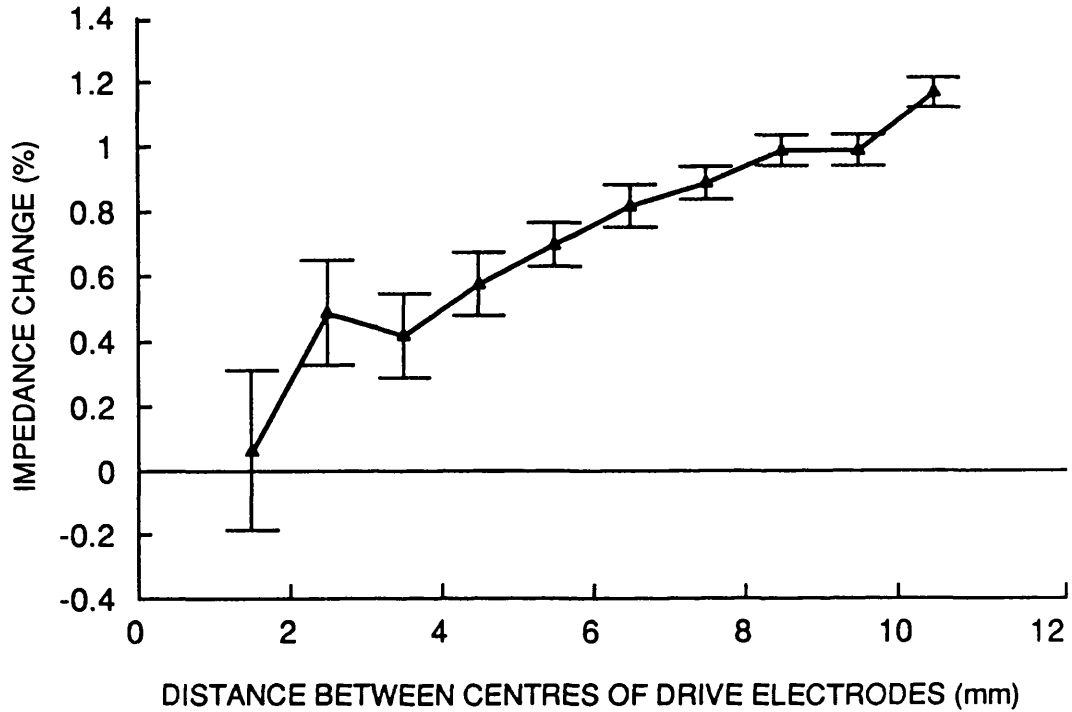


Figure 4.4. Predicted impedance changes for different spacings of electrodes on the scalp during cortical spreading depression. Projection was translational. Error bars refer to the estimated error in measurement from the plots of isopotential.

As it appeared that this was not the case, the possibility that wider electrode spacings could yield larger impedance changes during CSD was examined, using the above model.

The matrix for CSD in Fig. 4.1 was used. Parameters were chosen and varied to simulate CSD as in section 4.3.2. The four electrodes were equally spaced on the scalp in the model matrix; the drive electrodes were placed from 1.5 to 10.5 mm apart.

The model predicted that the impedance increase measured with scalp electrodes during CSD should become larger as the electrodes are more widely spaced (Figure 4.4). There was a small inaccuracy in the predicted impedance changes, because they were calculated by measurements made on printer plots of isopotential. These errors were estimated, and included in the figure as error bars. When electrodes were 10.5 mm apart, the model predicted an impedance increase of 1.2%. Simulations with more widely spaced electrodes were not performed, as the representation of the various layers as planes would have been unjustified (the diameter of a rat's head is about 20 mm).

4.3.6. Conclusions.

The models are likely to be a reasonable approximation to the experimental situation, to an accuracy of less than an order of magnitude. The geometry of the electrodes could not be modelled precisely, but approximate bounds could be determined by the choice of translational or rotational projection of the two dimensional model. The predicted impedance change would only be that due directly to anoxic depolarization in the cortex. In practice, any such impedance increases would be offset by impedance changes due to other causes.

The peak impedance change predicted during cerebral ischaemia, measured with scalp electrodes, was between 1 and 2 %, and that during CSD was less than the resolution of the model of 0.2%. In contrast, an impedance increase of 1% is predicted during CSD if scalp electrodes are spaced 3 mm apart. The impedance decrease attributed to a scalp temperature increase

during CSD measured with scalp electrodes was about 0.8% (Table 3.3). This suggests that it may be possible to detect an impedance decrease with more widely spaced scalp electrodes during CSD at ambient temperatures, and it should be possible if scalp temperature was controlled so that it remained constant.

5. DISCUSSION (2) : INTERPRETATION OF RESULTS.

5.1. IMPEDANCE CHANGES DURING CEREBRAL ISCHAEMIA.

5.1.1. Anaesthetic problems associated with the animal model.

The observations regarding anaesthetic regime were secondary to the main aims of the project. These results therefore have the limitations of a retrospective analysis : certain relevant variables were not measured systematically, and the anaesthetic groups could have been subject to conditions which differed in respects other than anaesthetic regime. Possible such differences are now considered : 1) The difference in survival between groups did not appear to be due to other factors such as an improvement in surgical technique with time as there was no trend against time within any of the anaesthetic groups, or overall. 2) All animals were probably comparable as they were kept under similar conditions and were of the same strain. 3) All animals were well oxygenated, so it did not appear that the improvement with group 4 (halothane and neuromuscular blockade) was simply due to improved ventilation. 4) There was no significant difference within the groups related to the method of induction or gas mixture used. 5) Artificial ventilation was employed in groups 1-3 (urethane, alphadolone/alphaxolone, halothane with spontaneous respiration) when essential. It was only used for a small proportion of the total experimental time, and the survival time of animals in which it was employed did not differ significantly from the other animals in their group. 6) The groups did not differ significantly with respect to the total duration of cerebral ischaemia. In the four vessel occlusion model of cerebral ischaemia in rats, the area of brain section in which moderate-to-severe neuronal damage was present varied approximately linearly with the duration of carotid occlusion for 10 - 30 min (Pulsinelli and Brierly, 1979). There are no published data comparing the histological effects of multiple ischaemic episodes in the same animal in this model, but, on the basis of this evidence, it seems reasonable to assume that the degree of cerebral damage

was roughly proportional to the total duration of cerebral ischaemia.

It therefore seems reasonable to consider that the four anaesthetic groups were comparable, and that it was very likely that the improved results in group 4 were due to the anaesthetic regime. However, other explanations cannot certainly be ruled out, and a prospective study is needed to confirm these results. A similar improvement with halothane and neuromuscular blockade compared to halothane alone has been observed (N. Todd, personal communication) which was the reason for selection of the former regime in Todd et al. (1986).

The cause of the observed cardiovascular deterioration did not appear to be a non-specific anaesthetic effect. Intraperitoneal urethane has been reported to give stable blood pressure over two or three hours in rats not subjected to surgical procedures (Carruba et al, 1987, Buelke-Sam et al, 1978). However, when given by the intraperitoneal route, it caused a rise in haematocrit due to exudation of plasma into the peritoneum, which could be offset by intravenous infusion of about 3 ml of plasma (Van der Meer et al, 1975). Hypovolaemia did not appear to be the cause of the deterioration in this work, however, as the central venous pressure was normal during pre-terminal hypotension in several rats studied. Equally, continuous intravenous alphaxolone/alphadolone gave surgical anaesthesia without significant deterioration in cardiopulmonary function over up to 8 hours in rats (Green et al, 1978). Neither did the cardiovascular deterioration appear to be a direct result of the carotid artery ligation, as vital signs were well maintained during single episodes of cerebral ischaemia in the original four vessel occlusion model in which no anaesthetic was used at the time of carotid artery ligation (Capdeville et al., 1986; Pulsinelli and Brierly, 1979).

The main cause of the cardiovascular deterioration was probably neurogenic shock produced by several episodes of global cerebral ischaemia. This may have been worsened by persistent brain stem ischaemia which followed vertebral artery diathermy. In studies in the original four vessel model of cerebral ischaemia in the rat, blood flow measured by dye perfusion (Pulsinelli and Brierly, 1979), or ^{14}C -iodoantipyrine autoradiography (Furlow,

1982, Jorgensen and Diemer, 1982) decreased markedly in frontoparietal areas, but was generally preserved or slightly diminished in the cerebellum and brainstem. These experiments were performed in rats which had a recovery period of 24 hr between vertebral and carotid artery occlusion, unlike this study, in which all procedures were performed at one operation. The preservation of posterior territory blood flow may have been related to this. Regional cerebral blood flow has also been measured by hydrogen clearance using platinum electrodes in rats in which vertebral and carotid artery occlusion were performed at the same operation (Todd et al, 1986). The blood flow after 15-60 min of cerebral ischaemia decreased to 5-7% of the resting value in frontal, parietal and occipital areas. The EIT images collected in the present study (Fig. 3.26) revealed a large impedance increase in the occipital region, which could have indicated posterior territory ischaemia. However, these images are preliminary and further investigation of other artefactual possibilities, such as movement at the brain/ electrode interface, would be needed before these could be taken definitely to indicate brain-stem ischaemia.

The advantage of halothane in maintaining blood pressure appeared to be its short duration of action of 1-3 min (Flecknell, 1987). In comparison, the half life of alphaxolone/alphadolone is 6-8 min (Vickers et al, 1983), while the effects of urethane last for 8-10 hours (Flecknell, 1987). All three can cause cardiovascular depression (Altura and Weinberg, 1979, Child et al, 1971, Prys-Roberts et al, 1972) so it appeared likely that they inhibited the cardiovascular response to neurogenic shock in a dose-dependent way. Improved results were obtained by titrating halothane or alphaxolone/alphadolone against blood pressure during and after cerebral ischaemia. Recovery of the blood pressure was presumably due to the removal of their cardiovascular depressant effects coupled to other manoeuvres. Previous maintenance levels of anaesthetic were restored when blood pressure was normalized. As animals were rendered unresponsive by the cerebral ischaemia, the level of anaesthetic could be lightened in this way without any recovery of responsiveness by the animal.

The cause of the additional improvement when neuromuscular blockade and artificial ventilation were introduced is not clear. It does not appear to

have been due to the elimination of hypoventilation, as arterial pO_2 was well maintained in all groups. Acidosis was accompanied by hypocapnia, so it appeared that a compensatory hyperventilation occurred, which would have helped to maintain normoxia. In unanaesthetized goats with a similar model of cerebral ischaemia, reduction of cerebral blood flow to about 40 - 85% of normal caused hyperventilation (Chapman et al, 1979), so brain stem ischaemia might actually have assisted in the respiratory compensation for acidosis. The role of the carotid bodies is unlikely to have been large. In rats anaesthetized with sodium pentobarbital, the "hypoxic drive" (the proportion of ventilation in air attributable to an oxygen need) diminished from 30% to 11% when the sinus nerves were sectioned (Hayashi et al, 1983). During the periods of common carotid artery occlusion it is likely that local ischaemia would have increased respiratory drive, but at all other times and in animals which had internal carotid artery occlusion, carotid artery blood would have been normoxic. It therefore appears that moderate brain stem ischaemia improves ventilation and causes a respiratory alkalosis. As a partially compensated metabolic acidosis was observed in this study, it is unlikely that correction of ventilation by artificial ventilation was the essential factor in improving animal survival.

Artificial ventilation may have improved animal survival by reducing metabolic acidosis due to respiratory effort in animals breathing spontaneously. Acidosis was corrected by the administration of sodium bicarbonate, but the frequency of measurement of blood pH was limited by the need to remove as little blood as possible. Acidosis therefore tended to recur between infusions of sodium bicarbonate.

In future studies, it would be of interest to compare each anaesthetic with or without artificial ventilation, and to investigate if brain stem function is directly compromised by the procedure by measuring baroreceptor or ventilatory function, brain stem evoked responses, blood flow by C-13 iodoantipyrine autoradiography or performing post-mortem histology. In their original description, Pulsinelli and Brierly (1979) do not describe why they chose a recovery period of 24 hr between vertebral artery diathermy and

carotid artery occlusion. It may be that better results can be obtained because brain stem blood flow recovers. From a practical point of view, it would be preferable to perform all surgery at one operation. Todd et al (1986) and the results in group 4 in this study indicate that it is possible to obtain satisfactory cardiovascular conditions with all surgery performed in one operation, although any effects of cerebral ischaemia might be influenced by the presence of the anaesthetic. It would be of practical use to other investigators employing this animal model to establish if a recovery period is desirable, and to confirm if the anaesthetic regime suggested by this study would give the most satisfactory experimental conditions.

5.1.2. Comparison of impedance changes measured on the cortex and in the scalp at ambient temperatures.

Impedance increases recorded during cerebral ischaemia with cortical electrodes were consistent with previous reports, both in terms of amplitude and time course.

An impedance increase of 27% in parietal cortex was recorded with 1 kHz applied current in monkeys after 30 min of systemic hypotension (Gamache et al, 1975). A larger impedance increase of 114% in parietal cortex was recorded after 30 min of cerebral ischaemia in the cat. Ischaemia was produced by clamping the innominate, left common carotid and internal mammary arteries and applied current consisted of square wave pulses 3 ms in duration (Hossman, 1971). Impedance increases have been observed in the fronto-parietal cortex of rats during common carotid artery occlusion. The extracellular space was calculated to decrease from 18% to 10% of the brain volume after 15 min of ischaemia (Von Hanwehr et al, 1986). (The impedance measurements were not presented directly). In each of the above studies, impedance was measured with four electrodes whose tips were spaced 4mm or less apart, and were inserted into the cortex.

In these published studies, cortical impedance increased rapidly over the initial 5-10 min, and then increased at a lesser rate. It returned to the

baseline on reperfusion over about 5-15 min. Similar temporal characteristics were observed in the present study. Cortical impedance rose rapidly over the first 2-3 min, and then continued to increase until the end of the period of ischaemia, but at a lesser rate. On release of carotid artery occlusion, it usually decreased with a $t_{1/2}$ of about 3 min, but sometimes did not return to baseline, or failed to decrease at all. This latter event generally occurred after several episodes of ischaemia and so is not directly comparable with other published studies, in which a single episode of ischaemia was produced.

In this study, it was of interest that large and similar impedance increases were recorded with electrode pairs spaced from 1 to 26 mm apart (Fig. 3.2) on the cortex. There do not appear to be any previous reports which have analyzed the relevant issue of how the impedance increases might vary according to the regions of brain which the measuring currents traverse. The published studies mentioned above all had impedance measuring electrodes placed close together so as to measure cortical impedance. In experiments which investigated impedance changes at 1 kHz in the rabbit post-mortem, two electrodes were placed 8 mm apart over occipito-parietal cortex. Impedance increased by about 85% after 5 min; most of this occurred rapidly after about 3 min and was probably due to anoxic depolarization (Van Harreveld and Ochs, 1956). In this case, some of the current would have passed sub-cortically, and this suggests that large impedance changes can still be recorded with more widely spaced electrodes. In the present study, there was no significant difference in $\delta Z(5)$ or $\delta Z(15)$ recorded with cortical electrodes between channels 1-3 when analyzed quantitatively (Table 3.2). This was performed in relatively small numbers of episodes of cerebral ischaemia; a larger study might indicate differences. The explanation for this is unclear. Anoxic depolarization has not been recorded in white matter; when investigated, the impedance decreased during anoxic depolarization in adjacent grey matter (Freygang and Landau, 1955, section 1.3.3). It might therefore have been expected that a lesser, or even no, impedance change might have been expected with widely spaced electrodes, when more current would have traversed white matter. It is likely that deep grey matter contributed to the impedance increases; anoxic

depolarization has been recorded in hippocampus, basal ganglia and thalamus (see Bures et al, 1974). In addition, the impedance of grey matter is generally less than white matter, especially if the current passage is transverse to the orientation of fibres in white matter (see section 4.3). The large impedance increases observed with widely spaced cortical electrodes may therefore have occurred because sub-cortical current traversed grey matter preferentially to white matter.

With measurement with scalp electrodes, the direction of the impedance change was the same as that measured with cortical electrodes : both increased. The scalp increases were all attenuated compared to those measured with cortical electrodes (Fig. 3.2). Qualitatively, the time courses of cortical and scalp records was similar. Scalp impedance increased at the onset of cerebral ischaemia and decreases after reperfusion matched closely to the cortical impedance changes (Fig. 3.3 and Fig. 3.4). This correspondence was also present in some cases when cortical impedance did not recover (e.g. Fig. 3.7).

However, there was a difference in the quantitative nature of the scalp and cortical impedance changes. This is illustrated in Fig. 3.3. At the onset of cerebral ischaemia, cortical impedance increased in the manner described above : a rapid increase over 2-3 min was followed by a gentler increase which lasted until reperfusion. In contrast, the scalp impedance increases appeared only to consist of a more or less linear increase until the time of reperfusion. The decrease in impedance on reperfusion was similar in both scalp and cortical records.

These observations were made consistently in all records made, which encompassed a variety of electrode positions, durations of ischaemia, and anaesthetic regimes. In order to quantify the changes, a sub-group was chosen, in which all records were collected under uniform conditions (Table 3.2). In these records, all animals were anaesthetized with alphaxolone/alphadolone, and four impedance channels were collected concurrently. Measurements presented were for periods of carotid artery occlusion of 5 or 15 min. (30 min records were excluded, because the number of measurements was small.

Examples with this duration of ischaemia are included in Fig. 3.3 to illustrate the time courses of impedance changes.) In any one experiment, channels 1-3 were recorded all on the cortex or all in the scalp throughout; channel 0 was always in the same position on the cortex. Ideally, it would have been desirable to record impedance from the cortex and the scalp in an overlying position during the same experiment; this did not seem possible technically, as conditions for scalp recording would have been disturbed by insertion of cortical electrodes. Therefore a comparison cortex and scalp records from channels 1-3 can only be made between groups of animals, and it is therefore necessary to support the assumption that the two groups were comparable. For this purpose, physiological variables, such as blood gases, pH, blood pressure and the temperature change are presented (Table 3.2b). These variables were unfortunately not measured systematically in all animals. This was because they were not recorded in initial experiments when the outcome of impedance measurements was unclear, and the anaesthetic problems were not anticipated. Their measurement was introduced for the purpose of assessing and reversing possible causes of animal deterioration during the experiments. They are therefore presented for illustrative purposes. The arterial $p\text{CO}_2$ was significantly higher in the groups with scalp recording, and blood pressure (at the onset of the ischaemic episode) was significantly lower in the group with cortical recording and ischaemia for 15 min. Physiological variables, including temperature change, did not differ significantly in other respects. It is conceivable that these differences might have caused a different impedance increase in the group with cortical electrodes, as a low $p\text{CO}_2$ causes cerebral vasoconstriction (see Van Harreveld and Ochs, 1957). The reason for the differences is not clear. With the exception of one episode of ischaemia of 30 min (which contributed one value to each of the groups with ischaemia of 5 or 15 min), all experiments with solely cortical electrodes were performed before those with scalp electrodes. However, there was no formal change in technique as time progressed; in particular, all animals respired spontaneously.

However, the essential issue is whether cortical impedance was comparable in the groups with cortical or scalp recording. This was specifically

addressed by recording impedance on channel 0 with cortical electrodes in all experiments. This did not differ significantly between equivalent groups with cortical or scalp recording, so it seems reasonable to conclude that the effects of any differences in arterial pCO₂ or B.P. were not significant.

Assuming that the two groups were comparable, it is possible to make some quantitative comparisons, which will be discussed further in following sections. The impedance increase in channel 3 (electrode pairs placed bitemporally 26 mm apart) was generally less than that in channels 1 and 2, but this only reached significance for episodes of ischaemia for 15 min with scalp recording (Table 3.2a). The peak scalp impedance increases were 8.3 - 14.2% and 17.9 - 19.2% of the cortical changes, for episodes of cerebral ischaemia which lasted 5 or 15 min respectively. The time courses were quantified by measuring the time taken for the impedance to change to half of its peak value at the onset ($t_{1/2(u)}$) or at the end ($t_{1/2(d)}$) of carotid artery occlusion. The bipartite initial impedance increase in cortical records would be reflected in a shorter $t_{1/2(u)}$ than in scalp records where the increase was linear. As expected, $t_{1/2(u)}$ was less in cortical than scalp records, but the difference was only significant for periods of ischaemia of 15 min. $t_{1/2(d)}$ and the FWHM did not differ significantly between cortical and scalp recorded groups. This indicates that the impedance decrease on reperfusion was similar in both groups, as was the total duration of impedance increase.

5.1.3. Role of spontaneous temperature changes in causing scalp impedance changes.

Cortical temperature might be expected to decrease during cerebral ischaemia, due both to a decrease in blood flow and a fall in metabolic activity. In this study, cortical temperature fell by 0.8 and 2.4 °C at the end of 5 or 15 min of cerebral ischaemia, respectively (Table 3.2).

During cerebral ischaemia, scalp temperature would be expected to fall as a result of cerebral cooling. In addition, the four vessel model used in this study might be expected to cause cooling of the scalp itself because occlusion

of the carotid artery would diminish blood flow to the scalp, which would then equilibrate with room temperature. There do not appear to be published studies of the anatomical origins of scalp blood flow in the rat. In humans, the forehead and anterior part of the scalp and anterior meninges receive their blood supply from the ophthalmic branch of the *internal* carotid artery. The remainder of the scalp and meninges are supplied by branches of the *external* carotid artery (Romanes, 1972). In the rat, the anatomy differs slightly: the ophthalmic artery is a branch of the pterygopalatine artery, which arises from the cervical portion of the internal carotid artery (Greene, 1963). Occlusion of the common carotid artery below its bifurcation in the neck seemed likely to reduce almost all scalp and meningeal, as well as cerebral, blood flow. If scalp blood supply in the rat is similar to that in man, occlusion of the internal carotid artery (near the bifurcation and so below the pterygopalatine artery) might be expected to spare most scalp and meningeal blood flow. It might also decrease the reduction of cerebral blood flow, compared to that during occlusion of the common carotid arteries, because blood flow might occur through intra-/extra-cranial anastomoses such as the supra-orbital and middle meningeal arteries (Romanes, 1972). In some experiments, therefore, the internal, instead of the common, carotid artery was occluded. In the event, however, there was no significant difference in $\delta Z(5)$ measured in position 1 in the scalp (Table 2.2b). Internal carotid artery occlusion was less desirable for practical reasons, as the carotid snare tended to twist and occlude the artery inadvertently. Experiments therefore had to be performed with the animal supine so that the carotid arteries could be directly visualized. It was preferable to have the rat in a prone position, as the numerous and fragile electrode connections could be inspected and adjusted if necessary. Occlusion of the common carotid artery was therefore adopted, and results obtained with common or internal carotid artery occlusion were pooled. This does not exclude the possibility that a difference in effect on scalp temperature (and therefore impedance) existed if internal, as opposed to carotid, artery occlusion was employed, but it appears that variability due to other factors obscured any effects which might have been present. A larger controlled study would be necessary to elucidate this

point.

Ionic mobility and therefore tissue conductivity increases as temperature increases. The resistivity of saline with the same resistivity as that of cerebral cortex decreased by 1.3% per °C increase (Li et al, 1968). In the present study, under resting conditions with measurement in the scalp, impedance decreased by about 1.5% for an increase in scalp temperature of 1°C (Fig. 3.5). It therefore seemed possible that the impedance increases observed with scalp electrodes might be due to decreases in temperature in the cortex and extracerebral layers. In particular, the time course of the initial scalp impedance increase (which differed from that of the initial cortical impedance increase) appeared to have an inverse roughly linear relation to the scalp temperature decrease (Fig. 3.3). If the scalp impedance change was entirely due to temperature changes, this would have explained the discrepancy.

This was tested by a series of experiments in which scalp temperature was artificially varied by warming the scalp by a lamp or water jacket. The rationale for this was that some of the observed temperature decrease would have been due to diminished blood flow, so that the brain and scalp equilibrated with room air (at about 20 °C) at a greater rate. This could be eliminated or reversed by altering the external temperature to body temperature or above. The relative contribution of a decrease in metabolic activity during cerebral ischaemia is unclear; this would have been unaffected by this manoeuvre. However, if the external temperature was raised to above body temperature, the effect of diminished blood flow would result in an increase in temperature. By trial and error, therefore, it should be possible to keep scalp temperature during cerebral ischaemia constant by finding an external temperature at which an *increase* in scalp temperature due to diminished blood flow exactly counterbalanced a *decrease* due to impairment of metabolism.

In practice, it was not possible to keep the scalp temperature exactly constant, but a series of results were obtained in which scalp temperature at the end of 5 min of cerebral ischaemia was maintained to within 0.5 °C of the initial temperature (mean -0.26 ± 0.06 °C, 16 records in 8 animals). Significant

impedance increases of about 2.8% were still observed (Fig. 3.6). Although the mean temperature of the group differed significantly from zero, a mean impedance-temperature relation of -10.8% per °C would have been necessary to produce the results if temperature were the only factor. In other individual records (Fig. 3.7) impedance clearly increased during cerebral ischaemia when scalp temperature remained constant or increased. There are two possible explanations for this : 1) The observed scalp impedance change in temperature controlled records is not due to temperature changes, or 2) The temperature record (produced by a subcutaneous thermocouple on the other side of the head) was not an accurate index of the temperature changes of the tissue in which the impedance measuring current was passing. However, in 18 measurements in 6 rats, thermocouple measurements were made over the frontoparietal areas of the head bilaterally and varied by 0.1 ± 0.07 °C (section 2.1.5). It therefore is most unlikely that scalp temperature varied by the amount of about 2 °C which would have been needed to produce these impedance changes. It is likely that some of the applied electric current passed into the skull and brain (see section 4.3), and that the temperature of these tissues varied in a different way to that of the overlying scalp. Since the heat loss from these tissues would be determined by the temperature of the scalp, it is likely that their temperature change would have been decreased. Even if the cortical temperature decrease was unchanged at -0.8 °C (Table 3.2), given that only a fraction of the electric current would pass into it, and that the rest would pass into isothermic scalp, it is inconceivable that this could have caused the observed impedance changes recorded from the scalp.

In summary, it appears that temperature decreases of about one degree during cerebral ischaemia, when measured at a room temperature of about 20 °C, cause an impedance increase of about 1%. This forms a relatively insignificant proportion of measurements made with cortical electrodes, as the total impedance increase is 20-30% (depending on the duration of ischaemia). In contrast, this does form a significant proportion of impedance changes during cerebral ischaemia measured with scalp electrodes, which are about 5%. As both the temperature fall and total impedance change increase roughly in

a roughly linear fashion with time, the proportion of the total impedance increase due to the temperature is likely to remain constant for durations of cerebral ischaemia of up to 30 min. However, the studies in which temperature was controlled indicate that the major proportion of the scalp impedance changes cannot be attributed to temperature changes.

5.1.4. Role of local changes in scalp impedance in causing observed impedance changes.

The resistivity of the subcutaneous scalp has not specifically been measured, but it seems likely that it is similar to that of muscle (see section 4.3). The resistivity of blood is lower than this, so it seems possible that scalp impedance increases if scalp blood volume falls. This could arise during cerebral ischaemia induced by the "four vessel" method either as the result of impaired arterial supply or because of an increase in sympathetic activity consequent to carotid artery occlusion. It is possible that a component of the observed scalp impedance increases was due to this process, and it is also possible that, therefore, the contribution from this differed in experiments in which the common, as opposed to the internal carotid, artery were occluded. However, any effects on scalp impedance caused by the method of arterial occlusion were not significant for $\delta Z(5)$ in position 1 (Table 2.2b) and so it is assumed that, as for temperature effects, the contribution of any such changes was obscured by variability from other causes.

In order to eliminate any possible effect from local scalp changes, control experiments were performed in which the scalp was excised completely, and then stitched back into its former position so that there was electrical continuity but all vascular or nervous connections were interrupted. In these experiments, there was considerably greater baseline fluctuation (*e.g.* Fig. 3.9), but it was possible to assess the overall peak impedance change by pooling results from several experiments. When measured at ambient temperatures, there was no significant difference in $\delta Z(5)$ measured in normal or surgically isolated scalp (section 3.1.3). The mean temperatures fell, but did not differ

significantly between the two groups. The groups therefore appeared to be directly comparable, and this indicated that there was no effect on scalp impedance of local scalp changes. In individual records in surgically isolated scalp impedance clearly increased in a way that could not be explained by temperature changes. An example is shown in Fig. 3.8. Scalp temperature fell during cerebral artery occlusion by 1.4 °C, and then rose on reperfusion to 1.7 °C above its initial value, presumably due to a reactive hyperaemia. In contrast, impedance measured from position 1 increased by 5.5%, and then, on reperfusion, fell to about 2.9% below its original baseline value. Temperature was therefore clearly contributing to the changes, but could not explain all the observed changes as the scalp impedance increase during cerebral ischaemia was greater than its subsequent decrease, whereas the reverse was true for temperature.

The contribution of temperature was reduced by increasing scalp temperature with a lamp or water jacket, so that scalp temperature changes were reduced to less than 0.5°C. Then $\delta Z(5)$, measured in position 1 in surgically isolated scalp, was significantly greater than zero (Fig. 3.6 and section 3.1.4). The temperature in this group did not differ significantly from zero. In some experiments, the effects of temperature and any possible discrepancies due to thermocouple inaccuracy were controlled more tightly by recording from surgically isolated scalp on one side of the head, and from electrically isolated scalp on the other during the same episode of cerebral ischaemia, whilst temperature was controlled as above. "Electrically isolated" scalp was surgically excised and then replaced in its former position but on a thin but electrically insulating film. It was therefore in thermal but not electrical continuity with the underlying head. In these experiments, impedance measured in surgically isolated scalp increased significantly more (1.1%) than in electrically isolated scalp. This indicates that a residual increase in impedance can still be measured with scalp electrodes when the effects of both temperature and local scalp changes were eliminated.

However, when scalp temperature was controlled in this way, the changes in surgically isolated scalp were significantly less than the changes in

records made in normal scalp in different animals (Fig. 3.6) (1.5% compared to 2.8%). A direct comparison between normal and surgically isolated scalp in the same animals was not made, so it is unclear whether this difference was due to local changes in scalp impedance or to variability between animals.

The preponderance of the data therefore suggests that local changes in the scalp had a negligible effect on scalp impedance. The exception is the evidence in the above paragraph. In summary, it therefore appears that there was a substantial component of the impedance change which was not due to temperature effects or local changes in the scalp. The evidence is equivocal with regard to the possibility that four vessel occlusion might have caused an additional impedance increase due to ischaemia of the scalp. Further evidence with respect to this was obtained during EIT images recorded during cerebral ischaemia with scalp electrodes (see section 5.3). In these, a distinct peripheral impedance increase of about 3% was observed. The most likely explanation was that this was due to a local scalp impedance increase; it was not due to temperature increases, as temperature was held constant. A larger study with paired records in the same animal would be needed to assess the contribution, if any, of any local changes in scalp impedance to the impedance increase measured with scalp electrodes during cerebral ischaemia.

5.1.5. Possible role of changes in blood volume of the temporalis muscle in causing observed impedance changes.

The temporalis muscle is vascular, and lay under approximately three of the electrodes in position 1. It was conceivable that a change in its blood volume during cerebral ischaemia could have accounted for some of the impedance increases observed during cerebral ischaemia. The impedance increases during cerebral ischaemia were observed in all electrode positions (including those not over the temporalis or other muscles), and so changes in muscle blood volume could not have been entirely responsible for the observed impedance increases. However, the isolated scalp and temperature control studies were performed in position 1, in which the most lateral electrode

overlay the temporalis muscle. Loss of blood volume in this muscle did not appear to influence these results significantly, as no significant difference was observed in paired records in the same animal obtained from positions 1 and 9 (which overlay skull in the midline) (Fig. 3.8).

5.1.6. Probable explanation of impedance changes measured in the scalp during cerebral ischaemia.

It was possible to measure reproducible increases in impedance with scalp electrodes after the effects of temperature and any local scalp impedance changes had been removed. This section considers the possible origin of this change, which are termed "residual scalp impedance changes" to distinguish them from "scalp impedance changes", which were measurements made with intact scalp.

The qualitative correspondence of cortical and scalp impedance changes, and the fact that both were consistently in the same direction, strongly suggests that both were related to the procedure for causing cerebral ischaemia. Elements of the scalp impedance change were attributable to temperature changes and, possibly, to local scalp ischaemia. The important issue therefore is whether the residual scalp impedance changes were directly related to the cerebral impedance increase, or were an unrelated epiphenomenon which also resulted from the method of producing cerebral ischaemia.

The following considerations support the proposition that the residual scalp impedance changes were a result of cortical impedance changes : 1) The quantitative time courses of the cortical and scalp impedance changes corresponded in all respects except that the initial bipartite nature of cortical records was absent in scalp records. 2) This explanation is plausible on physical grounds for the simple case of electrode position 1, when current flow could be modelled for infinite planar layers (section 4.3). 3) The majority of the current in electrode position 1 would have flowed through the scalp, so this tissue would have been the principal candidate for an alternative explanation;

this was ruled out by the experiments in which the scalp was surgically isolated.

Measurements made simultaneously from electrode positions 1, 2 and 3 during cerebral ischaemia might have been able to differentiate mechanisms underlying the impedance changes (Table 3.2). The effects of two possible explanations could be predicted as follows. 1) If scalp electrodes were measuring cerebral changes due to anoxic depolarization. The proportion of current applied to scalp electrodes which flows through the brain as opposed to the scalp and skull has not been analyzed in the rat. However, it was estimated that 45% of current applied between electrodes placed on the frontal and occipital scalp in a model of the human skull passed into the cranial cavity (Rush and Driscoll, 1968). The proportions of a rat head are roughly similar, so it seems likely that more current would have passed into the brain in position 3 (electrode pairs 26 mm apart over contralateral parietal areas) than in position 1. δZ would therefore have been larger in position 3 than in 1. However, there are two complicating factors : i) The impedance change measured with cortical electrodes was lower (although not significantly) in position 3. If, as seems reasonable (see section 5.1.2), the intracerebral impedance change was lower in position 3, this would have offset the expected greater impedance increase in that position. ii) Temperature was not controlled in these measurements. It seems reasonable to expect that heat was lost to the exterior during cerebral ischaemia, so that central structures in the brain remained warmer than those at the periphery. This would have had the effect of a smaller average temperature drop in the tissues through which current was passing from electrodes in position 3, and so also resulted in a lesser impedance increase in this position. 2) If the observed scalp impedance changes were entirely due to local changes in the scalp or extracerebral tissues. If this was the case, the scalp impedance change should have been greatest in electrode position 1, less in position 2, and least in position 3 (electrode pairs respectively 2, 13, and 26 mm apart), because a lesser proportion of current would have flowed through the extracerebral tissues as electrodes were separated. In the event, the evidence is equivocal : There was no significant

difference in $\delta Z(5)$ measured in the scalp, compared between positions 1-3; $\delta Z(15)$ was significantly less in position 3 (3.9% compared to 5.9% in position 1), but cortical $\delta Z(15)$ was also less in position 3 (20.3% compared to 32.3% in position 1). A clearly greater impedance increase in position 3 than in position 1 would have supported the proposition that the changes were arising from brain. The equivocal similarity or decrease in position 3 compared to 1 does not distinguish either hypothesis. A larger study in which impedance was measured in various positions when temperature was controlled would be needed to elucidate this issue.

The main evidence which suggests that the observed scalp impedance changes during cerebral ischaemia were not due to intracerebral impedance changes is the difference in time course of the initial impedance increase in cortical, as opposed to scalp, records. This discrepancy is evident in records in which temperature was uncontrolled (Fig. 3.3) as well as those in which temperature was controlled (Fig. 3.7). In both these cases, the scalp was intact. This difference in time course also accounts for the discrepancy between scalp impedance changes in channels 1-3 expressed as a fraction of the cortical impedance changes measured at 5 or 15 min : (8.3-14.2% compared to 17.9-19.2% at 5 and 15 min after carotid artery occlusion respectively) (Table 3.2, section 5.1.2). This may be explained on the basis that the scalp records increased linearly ($\delta Z(15)$ was about three times greater than $\delta Z(5)$), whilst most of the increase in cortical records occurred in the first few minutes, so that $\delta Z(15)$ was not much greater than $\delta Z(5)$. The ratio of scalp to cortical impedance changes was therefore greater at 15 min than at 5 min after the onset of ischaemia.

There are several possible explanations for this discrepancy : 1) There may have been an underlying component due to anoxic depolarization, but the bipartite time course of this may be masked by additional impedance changes due to other causes. One of these might be local changes in scalp impedance due to ischaemia, which might be expected to be linear with respect to time. It should have been possible to test this by recording in temperature controlled isolated scalp preparations. Unfortunately, records made with isolated scalp

had greater baseline variability (*e.g.* Fig. 3.9), so it is not possible to assess definitely if a bipartite initial time course was present. 2) The latent period which occurred between carotid artery occlusion and the onset of the cerebral impedance increase may have varied at different cortical sites. The extracerebral layers act as a spatial filter, in the sense that impedance measurements made with scalp electrodes will record from a larger volume of brain than that recorded from with underlying cortical electrodes. If the time of onset of the impedance change did vary within the volume of brain sensed during scalp recording, this could have produced a more gradual initial impedance increase. This possibility was not specifically investigated. However, the bipartite time course was evident in records made during cerebral ischaemia with widely separated electrodes (Fig. 3.3), so it is unlikely that a variation in the onset of the impedance change due to current flow in subcortical structures could have explained the observed time courses. 3) There may also have been other causes of a gradual impedance increase following carotid artery occlusion, but it was not possible to investigate these in the time available. They include changes in skull impedance, meningeal blood volume, or volume of the cerebrospinal fluid.

Some further evidence was obtained with EIT images made during cerebral ischaemia (section 5.3). In these, the time course of the central impedance increase in EIT images collected with scalp electrodes appeared to have a bipartite time course, while the overall change did not. This was only observed in a small number of images, and needs to be replicated. It does, however, support the above explanation that the observed scalp impedance change contains a substantial element due to cerebral anoxic depolarization, but is accompanied by impedance increases due to other causes which increase linearly with respect to time.

In summary, the majority of the evidence suggests that the cerebral impedance changes are measured by scalp impedance recording, but the signal is attenuated by the skull and scalp which behave as passive resistances. The difference in the initial rate of impedance change is not explained on this basis. It may be explained by the contribution of impedance increases due to local

scalp ischaemia or other unknown processes in the extracerebral layers. This point would need to be clarified before scalp impedance measurement could definitely be said to be an index of intracerebral impedance changes in this experimental situation.

5.1.7. Implications for further research.

These results raise a number of issues which require clarification.

1) Experiments to elucidate the origin of the time course of the scalp impedance changes. When internal carotid artery occlusion was employed, the tie was placed around that portion of the artery visible after exposure of the carotid bifurcation. As a result, blood flow to the pterygopalatine artery (which probably supplies the anterior scalp and meninges (see section 5.1.3)) was stopped. The possible effects of changes in blood flow to these areas could be assessed by comparing impedance changes with bilateral occlusion of the internal carotid artery above the origin of the pterygopalatine artery with that of the common carotid artery. The former manoeuvre should selectively render only the brain ischaemic, whereas the latter should render meninges, skull and scalp ischaemic. An alternative would be to occlude solely the middle cerebral artery. This is a well established animal model of cerebral ischaemia (Bederson et al, 1986), which resembles the human condition more closely. Its disadvantages are that it is irreversible, so no impedance recovery data would be available, and only one episode could be produced in one animal. An alternative would be to use hypoglycaemia to cause anoxic depolarization (Pelligrino et al, 1981). In principle, this should not directly disturb the skull or scalp. However, their impedance, and displacement of the CSF, might be altered if the hypoglycaemia altered tissue blood volume by sympathetic action or changes in local vascular tone.

Another way to clarify this issue would be to make use of the frequency dependence of the grey matter impedance change during anoxic depolarization. The frequency dependence of the cerebral impedance change during cerebral ischaemia has not been investigated, but it is likely to be similar to that during

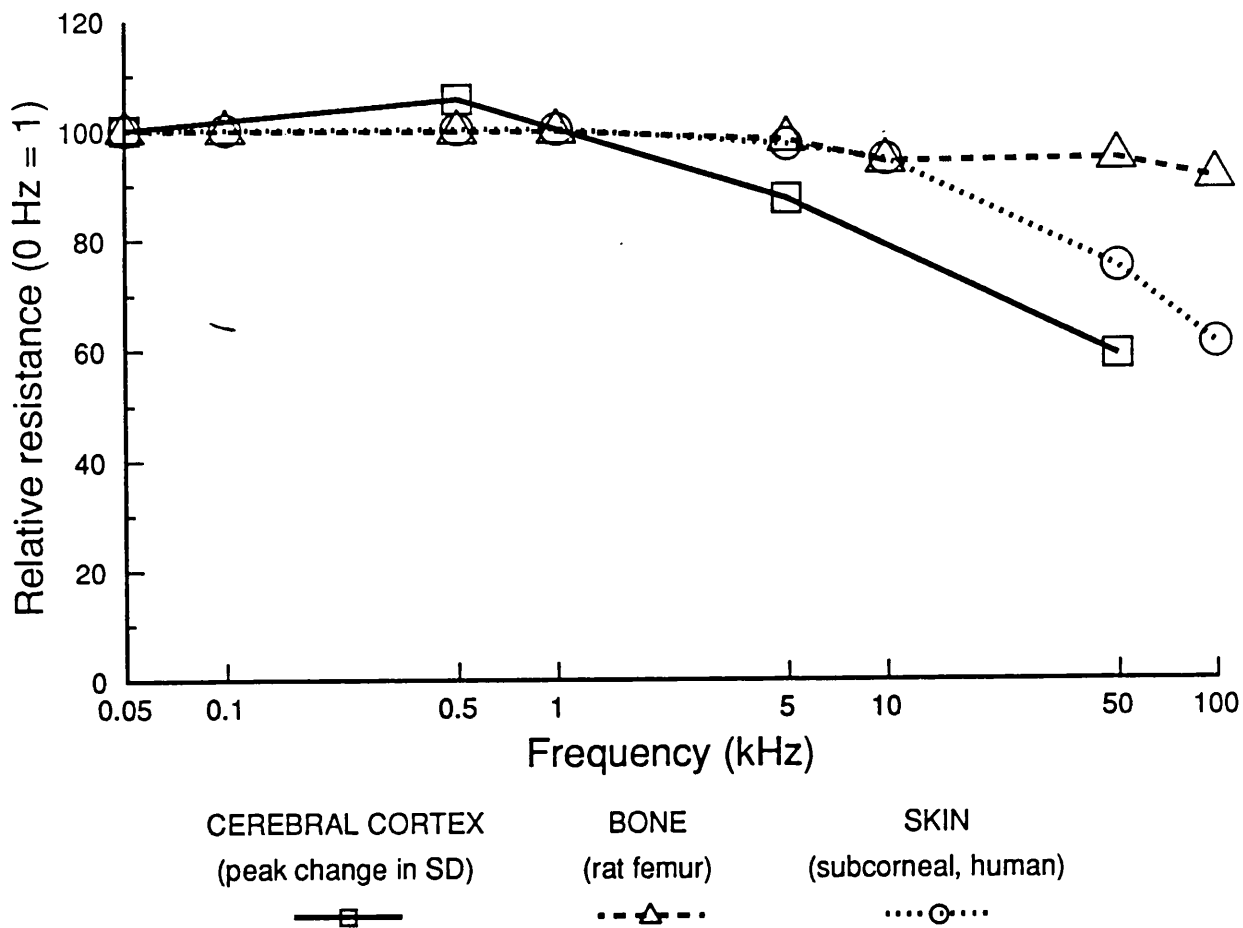


Figure 5.1. Comparison of the frequency dependence of the peak resistance change during CSD, and the resistances of bone or subcorneal tissues. The data has been redrawn from the following sources : The peak resistance increase during CSD was measured in rat cortex (Ranck, 1964, Fig. 2). The resting resistance of cortical bone was measured in the rat femur with two electrodes, placed in the central cavity and externally. Corrections were made which validated the use of a two electrode system (Kosterich et al, 1983, Fig. 5). The resting resistance of the human forearm was measured with electrodes 5 cm apart. The stratum corneum was stripped off with tape. This should resemble the scalp current path in the present study, as current would have flowed in the dermis and underlying soft tissues (Yamamoto and Yamamoto, 1976, Fig. 3).

CSD, which has been studied in detail (Ranck, 1964). A comparison of the frequency dependence of the peak resistance change during CSD, and that of the resting resistance of bone and subcorneal tissues (skin with the stratum corneum removed and underlying tissues) is shown in Fig. 5.1. The resistance increase during CSD increases by 70% as the frequency is reduced from 50 to 0.5 kHz (Ranck, 1964, (measured from Fig. 2)) (see section 1.3.3 for an explanation of this effect). In contrast, the resting resistance of bone increases by 5.7% (Kosterich et al, 1983, (measured from Fig.5)), and that of tissues below the stratum corneum increases by 34% (Yamamoto and Yamamoto, 1976 (measured from Fig.3)) over the same frequency range. The arachnoid membrane in the cat has been estimated to have a surface resistance of 50 - 100 $\Omega \cdot \text{cm}^2$ and capacitance of at least 30 $\mu\text{F} \cdot \text{cm}^2$ (Bennet, 1969). At frequencies above 500 Hz, the magnitude of its complex impedance will be about 10 $\Omega \cdot \text{cm}^2$ or less, so it is unlikely to be a significant factor. The effect of the dura mater is unclear, as no measurements of its resistance appear to be available. It is, however, a thin membrane like the arachnoid, and so probably would have little effect on the overall frequency dependence of the extracerebral layers. It therefore seems possible that this frequency dependence could be used to discriminate the site of origin of the impedance increase observed with scalp electrodes. It would first be necessary to confirm that the frequency dependences of the above factors in the same experimental situation in the rat were significantly different. A frequency range could be chosen which gave the greatest discriminative powers; in Fig. 5.1 it would probably be between 1 and 10 kHz.

2) Improvement of baseline variability. Signal detection is limited by the variability in the baseline impedance record. In the experiments on cerebral ischaemia, needle electrodes were used in the scalp. Even in an immobile anaesthetized animal, the baseline impedance varied by the order of 1% over a few minutes. In many experiments, this was superimposed on an approximately linear baseline drift, which could be corrected subsequently. In a clinical situation, even in an unconscious patient, any impedance changes would have to be identified against such a background. Further work is

needed to identify how best to improve it. The findings in section 3.2.2 suggest that firm pressure would be one possibility. Fluctuations in temperature would be another source of variation. Both these might be reduced by designing a rigid helmet which would be placed on the head. Electrodes would be held in place by a flexible rubber tube, which was inflated to a firm pressure with water heated to body temperature. Measurement at two frequencies might also be useful, providing a frequency range could be found over which the resting impedance of extracerebral tissues was constant but the impedance change of brain during cerebral ischaemia was not. It would also be necessary to record concurrently at the two frequencies. Since sampling is only needed for these changes every few seconds or so, it should be possible to achieve this by multiplexing between different applied frequencies. Then a disturbance, due to temperature or other factors, in the extracerebral layers would be equally mirrored in records made at both frequencies; subtraction of the record at one frequency from the other should lead to a cancellation or substantial reduction of the resistance change due to the disturbance. In contrast, the resistance change due to anoxic depolarization in the brain would still be evident after subtraction.

3) Clinical studies to detect cerebral ischaemia. No experiments were performed in conscious rats, but it is likely that movement would further worsen baseline variability. There are several clinical situations in which advance warning of cerebral impedance changes in an unconscious patient would be useful. These include anaesthetized patients in whom hypotension is induced deliberately to reduce haemorrhage, or unconscious patients in an intensive care unit following a head injury or subarachnoid haemorrhage. It seems advisable, however, to clarify the relationship between the scalp and cortical impedance changes further, and investigate ways of improving baseline variability, before proceeding to any clinical studies.

5.2. IMPEDANCE CHANGES DURING SPREADING DEPRESSION.

5.2.1. Technical manoeuvres to improve baseline variability.

With measurement with scalp electrodes, impedance changes during spreading depression were similar in magnitude to baseline variability in records made with freestanding needle electrodes. A small component of this variability appeared to be related to the pulse and respiration. In humans, Weindling et al (1982) observed that pulse related impedance changes measured with electrodes 2 cm apart on the scalp were abolished when scalp blood flow was occluded by a tourniquet. Impedance changes measured across the entire head remained largely unaffected. In this study, pulse related changes increased when a weight was placed on scalp needle electrodes spaced 1.5mm apart (Fig. 3.12). This suggests that intracerebral pulse related impedance changes were being detected. Respiration related impedance changes were much reduced by application of a weight, which suggests they were due to secondary electrode movement. Baseline variability of about 1% impedance change over minutes was reduced by the application of pressure, in the form of a weight placed on subcutaneous needle electrodes, or firm application of the araldite electrode array. Its cause was unclear; possibilities include movements of the electrodes or fluctuations in scalp resistance due to alterations in autonomic tone. The araldite electrode array was chosen for further scalp measurements, as it could also be simply applied to the cortex.

5.2.2. Comparison of impedance changes measured on the cortex and in the scalp at ambient temperatures.

Cortical impedance increased by about 40% during spreading depression. This is consistent with other published reports. In rat cerebral cortex, a resistance increase of about 34% and FWHM of about 1.5 min was measured with a two electrode arrangement operating at 1 kHz (Weiss et al, 1966). In rabbit cerebral cortex, resistance increased by about 43% with a FWHM of

about 1 min when measured with a four electrode system operating at 50 kHz (Ranck, 1964).

The finding of a decrease in impedance measured with scalp electrodes at room temperature was unexpected. All the available evidence suggested that it was directly linked to cortical SD in some way. Impedance was not measured concurrently on the cortex and overlying scalp, because to do so would have altered recording conditions. However, the scalp change occurred at the same time interval after initiation of CSD as did the cortical SD itself (*e.g.* Fig. 3.13). It also propagated with the same speed as cortical SD (Fig. 3.15). It could not be recorded contralaterally to the site of initiation, in the same way that CSD does not propagate across the midline (see Bures et al, 1974) (Fig. 3.13). When potassium chloride was applied to the cortex *post-mortem*, a cortical depolarization (due to glial cell uptake of potassium) but no scalp impedance decrease were observed.

In contrast, its duration was significantly greater than that of CSD (FWHM 2.0 min as opposed to 1.0 min, electrodes spaced 0.5 mm apart, Table 3.3). Similar changes were recorded with wider electrode spacing with the araldite electrode array, and with wire needle electrodes, both pressed firmly onto the scalp. When wire electrodes were used without a weight, a smaller impedance decrease was observed (Table 3.4). This suggested that close contact between the electrodes and skull was needed to maximize the change, but this did not assist in distinguishing between possible causes.

5.2.3. Role of temperature changes in scalp impedance records during CSD.

At the time of the experiments discussed above, temperature changes had not been identified as a possible cause of the scalp impedance change, and temperature was not measured. Cortical temperature increases of about 0.5°C during CSD have been recorded by other investigators (see section 1.3.3), so further measurements were therefore made to examine the possibility that the observed scalp impedance decreases were due to a rise in temperature. Epidural and scalp temperatures were recorded simultaneously.

Unfortunately, the thermocouple which recorded scalp temperature had to be displaced a few mm away from the site of impedance recording. This was because the araldite array was used, as it gave the least baseline deviation. The thermocouple had to be placed to one side of this. In contrast, the epidural thermocouple could be placed underneath the araldite probe. It was constructed from two strands of wire each 0.1 mm in diameter, so these should not have materially influenced recording conditions.

With this arrangement, impedance measured on the scalp decreased by about 0.4% for each rise of 1°C measured epidurally or on the scalp, when scalp temperature was varied by a lamp (under resting conditions). This ratio is less than that observed with needle scalp electrodes during experiments on cerebral ischaemia. It may be because the araldite probe sheltered underlying scalp from heating by the lamp. During CSD, a ratio nearer to that of -1.5%/°C would be more appropriate in estimating impedance changes due to temperature difference, as the heat source would be underneath the araldite electrode array.

In these records, an unexpected finding was that the resting scalp temperature, both when the external temperature was ambient, or the scalp was warmed, was half to one degree warmer than the epidural temperature (Fig. 3.16). It might have been expected that heat would be lost from the brain to the environment through the scalp, so the scalp would be cooler than the brain. This could have been due to a calibration error, but both thermocouples were calibrated against the same mercury thermometer over the range of 20 - 40 °C before each experiment, with an estimated accuracy of ± 0.1 °C. However, there is an alternative explanation : It is now generally accepted that the brain is cooled in most mammals by a countercurrent exchange system. Blood from the cerebral veins is cooled by its passage near the upper aerial pathways, mainly the nasopharynx. This then cools cerebral arterial blood in structures such as the cavernous sinus. Exchange is enhanced in species which have a rete mirabile (Baker, 1979). This is absent in the rat, but it is also absent in the rabbit, which has been shown to maintain a lower brain than core temperature, especially on exercise (Cabanac, 1986). This has not been

specifically investigated in the rat. However, LaManna et al (1987) measured the cortical temperature in rats in which the cortex was exposed and covered by a cup which contained a 5 mm depth of mineral oil. Temperature was measured 0.7 and 1.6 mm into the cortex, and was found to be 1.2 and 1.8 °C below core temperature at these two sites respectively. This suggests that the anaesthetized rat has a similar countercurrent mechanism which cools the brain. This explained why an increase in blood flow caused an increase in cortical temperature during CSD (see section 1.3.3). Since the scalp is highly vascular (Romanes, 1972), it is also possible that the scalp is supplied by central arterial blood which only loses a small amount of heat to the air and so is slightly warmer than underlying cortex. This consideration may be relevant to the design of any experiments in which brain temperature is artificially elevated so as to prevent an increase in temperature during SD (or cerebral ischaemia). In this study, the scalp was warmed by a lamp or water jacket, which might have led to a temperature gradient from the warmed cortex adjacent to the scalp across to deep areas cooled by incoming arterial blood. A more uniform increase in brain temperature might be produced if respired air is humidified and warmed to body temperature. In addition, it would be necessary to raise the scalp to *brain* rather than *core* temperature if temperature increases due to increased blood flow are to be prevented.

Using these thermocouples, a temperature increase of about 0.15 °C was observed at ambient temperatures during CSD with the epidural thermocouple. Its time course was very similar to the impedance change (Fig. 3.16). A biphasic temperature change was measured by the scalp thermocouple. Its predominant increase of about 0.15 °C occurred about 2 min after the scalp impedance change. Scalp temperature changes were not systematically investigated. It seems likely that the discrepancy could be attributed to the physical displacement of the thermocouple from the araldite probe. It seems reasonable to take the temperature measured by the epidural thermocouple as indicative of conditions in the vicinity of the impedance measuring electrodes. The relative magnitudes of the changes could be explained if the ratio of change in impedance to temperature was about 1%/°C, which is reasonable in

terms of the general relationship for tissues (see section 1.3.3).

In the introduction (section 1.3.3), evidence was presented which suggested that cortical impedance would *increase* during SD due to cell swelling; it would *decrease* due to a fall in membrane resistance, temperature increase, or blood flow increase. A temperature change appeared to be the most likely explanation of the scalp impedance changes : the temperature of the cortex involved in SD and adjacent tissues through which current passed would all be affected. This could cause an impedance decrease of a few tenths of one per cent. If the electrical properties of the extracerebral layers were such that the cortical impedance increase due to cell swelling could not be detected by scalp electrodes, this would result in a net impedance decrease. It is conceivable that a blood flow increase could also have been responsible, if the effect of scalp recording was to disperse current over a wide volume of cortex which had an increased blood flow, while the region of cell swelling was restricted. In contrast, the fall in cell membrane resistance would be likely to occupy the same region as cell swelling, and be dwarfed by the accompanying impedance increase.

This was tested by warming the scalp with a lamp, in order to remove the effects of temperature by maintaining epidural temperature to be constant (see section 1.3.3). In the event, it was difficult to adjust the lamp so that there was no significant temperature change in individual records. Records were therefore grouped into those with or without warming and averaged; no significant temperature change was observed in the warmed group. In this group, no significant impedance change was observed, so it is concluded that temperature changes were the cause of the scalp impedance decrease.

In the experiments in which temperature was measured, the impedance decrease during CSD was less than in those in which the impedance decreases were originally observed (-0.15% compared to a mean of -0.8%). The former experiments were carried out after an interval of two years, but recording conditions and apparatus were identical. Room temperature was not systematically measured; the former experiments were performed in September and October, whilst the latter were carried out in November and December.

The rooms were centrally heated, so it is unlikely that ambient temperature differences could explain the discrepancy. The explanation is therefore unclear ; there may have been differences between the animal strains used. The conclusion that temperature explained the impedance decrease in the animals in whom temperature was measured still seems valid. It seems probable that it also explained the larger decreases in the earlier group, as it is the most plausible explanation on physical grounds. However, this cannot definitely be asserted unless further temperature controlled studies can be performed in animals which exhibit a similar magnitude of scalp temperature decrease during CSD.

5.2.4. Probable explanation of observed impedance changes.

It therefore appeared that the observed impedance changes measured on the scalp at ambient temperatures were a result of changes in temperature. It follows that, with the electrode spacing used of 0.5 mm, no impedance change greater than baseline variability of about 0.1% could be detected.

The physical basis for this was examined with the finite element model (section 4.3). Parameters for this were chosen from the literature, and consideration of the measurements made in this study. The depth of cortex disturbed was obtained from studies in which the slow potential change or local impedance changes had been found to occur in all layers of the cortex (section 4.2). These were supported by the analysis in section 4.2. The magnitude of the impedance disturbance of the cortex was calculated from experimental results in this study, which agreed with most other published results (section 1.3.3). Hoffman et al (1973) measured local impedance changes with a microelectrode in the cortex during SD. Their recordings were claimed to be of small volumes of cortex, but were an order of magnitude larger than other measurements. The reason for this is unclear. No other attempt was made to alter the variables in order to agree with the experimental findings.

The magnitude of the impedance changes measured on the scalp predicted by the finite element model during CSD was less than 0.2%, and so

was consistent with the (negative) experimental observations made when scalp temperature was controlled. It therefore seems that the relatively small volume of cortex whose impedance changes during SD only slightly perturbs surface potentials if the temperature is held constant. Even with the improved baseline variability achieved by pressure on electrodes, the resulting impedance change could not be discerned from background variability of about $\pm 0.1\%$.

5.2.5. Implications for further experiments.

1) Further impedance measurements with scalp electrodes spaced more widely during CSD in the rat. The spacing of 0.5 mm of the impedance measuring electrodes was chosen in advance, before any quantitative analyses had been performed. In view of the negative findings (with controlled scalp temperature), the finite element model was used to predict if a larger scalp impedance signal might be expected with wider electrode spacings. The model had agreed with experimental observations in both cerebral ischaemia and CSD. It seemed to be a fair representation of the real situation, providing the approximation to planar layers was appropriate. Results were obtained with drive electrodes spaced up to 10 mm apart, the greatest distance at which the planar approximation could be justified (section 4.3.6, Fig. 4.4). This suggested that the scalp impedance increase during CSD would increase up to this electrode separation; with drive electrodes 10 mm apart, an impedance increase of over 1% might be expected.

Rush and Driscoll (1968) measured current densities in the cranium when constant current was applied to two electrodes on the scalp in a physical model of a human skull in a tank of saline, and compared the results with a mathematical model. They found that current density in the cortex was greatest when the current electrodes were 5 cm apart. This is roughly equivalent to an electrode spacing of 6 mm in the rat. A priority in further studies into this condition would therefore be to repeat the experiments with various electrode spacings. For EIT, it would be preferable to have the electrodes equally spaced, but better discrimination may be achieved by placing

the recording electrodes close to the drive electrodes. These issues could usefully be refined with the aid of the finite element model. If such changes are found, then there will be a trade-off between the impedance *increase* due to cortical anoxic depolarization and the *decrease* due to temperature. It may then be desirable to control temperature in the way proposed above.

2) Use of temperature changes to detect CSD. One purpose of these experiments was to determine if CSD could be detected during migraine in human subjects. The temperature change during CSD has a characteristic time course and spatial distribution, so it might be possible to try to detect this rather than (or as well as) an impedance change. It might be possible to achieve this by thermal imaging (Shevelev et al, 1986) which has a temporal resolution of a few seconds, or by recording from multiple thermocouples placed over suspected regions. However, scalp impedance measurement (with closely placed electrodes) could also be used specifically in order to detect the local temperature changes. The main problem is likely to be whether such small changes could be detected against background variability in a clinical subject.

3) Improvement of background variability. Experiments in this work were performed in immobile anaesthetized animals. Any experiments in humans would probably be in conscious mobile subjects, who might be in pain during an episode of migraine. The sought changes in impedance are small, and it would be essential to reduce baseline variability. The proposals for use of a warmed helmet or measurement at two frequencies (section 5.1.7) apply equally to this situation.

5.3. EIT IMAGES TAKEN DURING CEREBRAL ISCHAEMIA.

5.3.1. Method of illustration of EIT images.

Reconstructed images, such as those obtained with X-ray computed tomography or PET, are generally represented as contour maps viewed from above, in which areas of different values are represented by different shades of grey or colours. This presentation is useful for visualizing disturbances.

Sophisticated computer programs have recently become available which can generate pictures of a surface, as if viewed from an angle in three dimensions. The advantage of these is that it is easier to form an impression of the gradients and contours of the surface. From the point of view of assessing EIT, the critical factor is the degree to which impedance disturbances are blurred when represented in an image. In the author's opinion, this could be more easily judged in surface maps. All the EIT images have therefore been shown in this way. The disadvantage of this is that some of the data remains hidden. To circumvent this, conventional contour maps have also been included for the EIT images in Fig. 3.26.

5.3.2. Calibration of the Sheffield EIT system.

From an understanding of the data collection procedure and algorithm employed by the Sheffield EIT system (section 1.2), it is possible to anticipate limitations in its imaging abilities. A full calibration study was beyond the scope of this work; the limited situations in which the system was assessed were intended to give a semi-quantitative estimate of its accuracy and limitations.

1) Baseline shift. Baseline variability was noted in measurements made with single channel impedance measurements *in vivo*. It was likely that measurement with 16 electrodes would increase this effect, as different variabilities at each electrode might be expected to summate. The effect of this would vary from pixel to pixel, which could increase or decrease in impedance with time. This was assessed in the saline tanks and *in vivo* by calculating the standard deviation of pixels 10 min after a reference frame (Table 3.9). This gives an indication of the variability within one image and so is more important than the mean change in impedance, which indicates a common drift in all pixels. The standard deviation *in vivo* was about ten times greater than that in the tanks.

The cause of the variation in tanks was not specifically investigated. A variation in temperatures of the saline or local impedance conditions at the

electrodes were probably important. Although each impedance was measured with a four electrode system, the data collection as a whole was probably more prone to errors due to variations in electrode impedance. This would have been because the phase of the phase sensitive detector was common to all 16 electrodes. This was necessarily the case because the input signal was serially multiplexed. However, individual variations would have caused the phase selection to be slightly inaccurate in different channels. As a result, the impedance could have been sensitive to capacitative currents passing through the electrodes as a result of stray capacitance between the leads. The magnitude of any capacitative current passing through the tissue from the recording leads would then have been influenced by electrode impedance. The following steps were taken to reduce any such effects to a minimum : i) All leads were bundled together and were not moved throughout the course of an experiment. ii) Some test EIT images were made in tanks filled with saline whose resistivities covered the ranges expected in experiments. The phase was then set to the value which gave the least variation in image pixels. Inter-pixel variation could be reduced to a standard error of less than 0.3% in this way for resistivities corresponding to 50 - 300% relative to brain resistivity (Fig. 3.18). iii) Electrodes were chlorided before each experiment and left to stand, connected together, for 12 hours or so. This decreases variations in impedance between electrodes, as well as allowing a stable chemical equilibrium to develop (Ferris, 1974). In this way, variation in images made in tanks could be reduced to insignificant proportions.

In contrast, there was substantial variation in images *in vivo*, which affected the interpretation of results. This was presumably due to variations in tissue impedance around the electrodes. In addition, the silver chloride was friable, and it was possible that it was disturbed as the electrodes were applied, particularly in the case of the needle electrodes used in the scalp. This drift was corrected empirically. It was found that the variation in any individual pixel of the reconstructed image was linear with respect to time (section 3.3.1), so each pixel in images *in vivo* or *post-mortem* was corrected for the gradient of the linear regression of its values over a resting period. In

practice, this gave reasonably level corrected baselines (see Fig. 3.19, 3.26).

2) Spatial resolution in the electrode plane in conditions of initially uniform resistivity. Spatial resolution is likely to be best in these circumstances. The limiting factors are then the crude nature of the algorithm, and the physical limitation that current density is least in the centre of the image. Unfortunately, it is difficult to produce a test object which has a resistivity different from the initial conditions by the same amount likely to be encountered in a physiological situation. Agar containing saline of different resistivities may be used, but the test and background solutions tend to mix. Therefore the test object was a plastic rod, which has a very high resistance. The reconstruction algorithm assumes that there is a linear relation between the impedance disturbance and the potential difference change measured on the boundary (Barber and Seagar, 1987); this is only true for relatively small disturbances. The spatial resolution in practice in a biological subject with similar conditions is therefore likely to be better than that observed with a plastic object.

The immediately evident effect of a sub-optimal reconstruction algorithm is that a point impedance increase appears as a distributed disturbance in the EIT image; the degree of spread dictates the ability of the system to resolve two adjacent objects. The FWHM for a polythene rod 10% of the array diameter in the cylindrical tank varied from about 15% at the edge to about 25% in the centre (Fig. 3.21). These figures are similar to those found by Eyuboglu et al (1989) for similar conditions with a polythene ball (section 1.2.4). This indicates that, as expected, spatial resolution is least in the centre of the image, because current density is least there. This would affect the ability of the system to discriminate two objects in the centre; the centres of two similar rods had to be more than 32% apart to be discriminated at the centre of the tank (Fig. 3.22). However, the localization of the centre of a *single* object is unaffected by the degree of lateral spread of the impedance signal in the image. Spatial resolution is then determined by the pixel size, which is about 10% of the image diameter for 16 electrodes (section 1.2.4). A polythene rod in the cylindrical tank could be well localized to about 5% of its

true position on average.

The data collection hardware is sensitive to small changes in impedance. Changes of 0.1% could be measured with a cardiac gated system and averaging (McArdle et al, 1989). Small central impedance increases of 5-20% could be detected clearly. The image impedance increase bore a significant linear relation to the actual impedance increase, but the correspondence was not 1 : 1 (Fig. 3.24). Although the test hole was about 10% of the diameter of the test tank, it might have straddled more than one pixel. Representation of the actual impedance change as a lesser amount in the image may have been due to a partial volume effect or because sensitivity was less in the centre of the image.

Errors in representation may occur as a result of the reconstruction algorithm and filtering methods. When two or more resistive test objects were employed, as in Fig. 3.28, it was possible to obtain a "shadow" in the image which represented an opposite impedance change. This might be the explanation of the central impedance increase seen in Fig. 3.20 in the rat *in vivo* after scalp warming.

3) Distortion of the image by a non-circular electrode array. The software available for the Sheffield system assumed that the electrode array was circular. This was not possible for the planned experiments, and two test tanks were constructed, which had the approximate elliptical proportions of the cortical or scalp electrode arrays used *in vivo*. The image was distorted, but this appeared to be in a straightforward fashion. For instance, the actual relative dimensions of the cortical electrode array were 1.6:1; the ratio of the axes of the FWHM of the circular polythene rods was 1.3:1 (Fig. 3.21).

4) Degradation of spatial resolution by non-uniform initial resistivity. Several measurements were made in order to assess the spatial resolution of intracranial contents when recording was performed with scalp electrodes in rats. *A priori*, it seemed likely that spatial resolution would be substantially degraded, as the reconstruction algorithm assumed uniform initial resistivity in the subject. In all measurements in which test objects were placed in the cranial cavity, the rat lay supine, and all surgery or interference with the

cranial contents was performed from the ventral aspect. This was done so that the scalp electrodes were not disturbed. A problem arose, because contraction of the scalp *post-mortem* tended to lead to movement of the electrodes into a smaller ring over the vertex. This effect was minimized by placing the rat, prior to sacrifice, in a dental acrylic mould which preserved the cervical lordosis.

The simplest case was examined by making a reference image in a rat *post-mortem*, whose cranial contents had been replaced by physiological saline. The test image was made when the saline was replaced by air (Fig. 3.21). The cranial cavity in the image was represented by a disturbance whose FWHM was 28% of the image diameter; the real dimensions of the cranial cavity compared to the electrode positions was about 80%. This supports the findings of McArdle et al (1989) (see section 1.3.4), that the skull is represented as a wide ring; representation of the cranial contents is compressed into a small central area. Unfortunately, application of current from only two electrodes at a time is likely to worsen this effect. Even in a medium of constant resistivity, current density will be least in the centre of the subject. Shunting through the scalp and obstruction of current flow by the skull is likely to make this much worse, so it might be expected that spatial resolution of objects in the cranial cavity was degraded. Greater separation of drive electrodes would not improve this : the Sheffield system collects a complete data set from which the current distribution resulting from any two drive electrodes may be calculated by superimposition. It would be necessary to drive currents from multiple electrodes in order to optimize current density in the centre of an image. This is theoretically possible, but has not yet been implemented in practice because of greater technical problems (see Webster, 1990).

The presence of a single polythene rod in the cranial cavity of a rat *post-mortem* could be detected on an EIT image. It was not possible to distinguish it from a second rod, placed about 25% of the electrode array diameter away in a coronal direction (Fig. 3.23). This is not surprising, as two rods could only be distinguished in a tank of saline when their centres were about 30% apart. In the rat *post-mortem*, it was unfortunately not possible to produce a greater

separation because rod placement was limited by the lateral limits of the skull. However, inspection of the transverse decay of the impedance disturbance in Fig. 3.23 suggests that spatial resolution would not have been better than about 50% of the electrode array diameter.

For comparison, an experiment was designed in which it was intended that the resistance of the scalp alone was altered. This was attempted by placing a lamp over the scalp of an anaesthetized rat. The rationale was that the scalp would warm up first, and it should have been possible to distinguish the resulting impedance change in consecutive images. A definite impedance decrease may be seen in the EIT image collected 3 min after the lamp was switched on, when scalp temperature had risen by 5 °C (Fig. 3.20). It forms a ring around the periphery, is about 15% of the image diameter wide, and is about -3% in amplitude. In subsequent images collected while the lamp remained it deepens, reaching an impedance decrease of about 6% when scalp temperature had increased by 7 °C. This ratio is reasonably consistent with the ratio of -1.3% per °C observed for warming of saline (section 1.3.3). The peripheral change reversed to a large extent on scalp cooling. In the later images, a central impedance increase was observed in the EIT images. It is unclear whether this was a result of "shadowing" produced by the algorithm, or represented a cooling of the brain. Overall, it seems probable that the peripheral decrease represents scalp warming, though the precise contribution of warming of the skull or underlying brain is uncertain.

5. Contribution of off-plane impedance changes. Applied current will travel in three dimensions. Inclusion of off-plane impedance changes will therefore be a problem for all EIT systems imaging with a 2-dimensional electrode array. Because current will spread most in the centre of the image, it would be expected that sensitivity to off-plane impedance changes is greatest if they are central to the electrode ring. This is illustrated in Fig. 3.25. For large impedance changes, a more complex toroidal disturbance was seen. This indicates that care must be exercised in interpreting EIT images. Localization of an impedance disturbance in the plane of an image can only be justified if it is known to be restricted to the image plane, or is symmetrical about it (*e.g.*

a plastic rod held perpendicular to the image plane).

In summary, the calibration studies have indicated that single impedance disturbances can be localized accurately. Blurring of the profiles of objects occurs, so multiple objects can only be distinguished if they are 20% of the array diameter or more apart in a uniform medium. Limitations in the algorithm may produce "shadow" artefacts. Off-plane impedance disturbances are included, and intracranial resolution is substantially degraded by measuring through the skull with scalp electrodes. On the other hand, images may be collected in a fraction of one second, the system is tolerant to inaccuracies in electrode placement that are inevitable in physiological applications (section 1.2), and it should be possible to distinguish impedance changes in the scalp from those in deeper layers in the head.

5.3.3. Comparison of EIT images recorded with cortical and scalp electrodes during cerebral ischaemia and *post-mortem*.

The EIT images collected in rats should therefore be interpreted with caution. In images collected with cortical electrodes, the assumption of initial uniform resistivity is met to a large degree. It is reasonable to assume that current flow will have been restricted to the brain, and a negligible amount will have entered the skull or other extracerebral tissues. Off-plane impedance changes will have distorted the image, but it is reasonable to assume that any peripheral changes are likely to be fairly accurately localized. In images localized with scalp electrodes, intracranial changes are likely to be compressed into a central space, but, again, it should be possible to localize peripheral changes in the scalp fairly accurately.

1) Images collected during cerebral ischaemia *in vivo*. During measurement with cortical electrodes, impedance increased reversibly in two major areas near the midline of the frontoparietal and occipital areas (Fig. 3.26a). The frontoparietal central peak is unlikely to reflect the actual profile of impedance changes across the brain. While there might be minor differences

in different regions of grey matter, it would be expected that the impedance increase in cortex should be roughly similar to that elsewhere. The central peak is most likely to be due to off-plane impedance increases both above and below the plane of the electrode ring. The large impedance increase observed in the occipital region was surprising, in view of previous studies with other methods which did not record a substantial difference in blood flow in posterior areas of the brain (see section 5.1.1). The electrode ring was of fixed diameter. Although no separation of brain from electrodes was apparent by eye, one possibility is that the posterior impedance change was due to movement of the electrode-tissue interface as a result of the cerebral ischaemia.

During measurement with scalp electrodes, impedance increased reversibly, mainly over one central area (Fig. 3.26b). The position of the peak was near the midline, between the peaks recorded with cortical electrodes. It is probable that this central area includes on- and off- plane impedance changes from the brain, but all changes have been blurred together as one peak. It may also include off-plane impedance changes from the scalp overlying central regions. It seems unlikely that this will be a large contribution, because it is likely to be smaller than the 3% increase seen at the periphery after 15 min, which probably represents scalp impedance changes (see below). The volume under each main peak (defined as in section 2.4.2.3) is also plotted (Fig. 3.26b, lower left). Only one main peak is apparent; it includes about one half of the total volume of the impedance change, and represents the central main peak. It may be seen that its increase is bipartite, with a more rapid increase over the first 4-5 min. In this respect, it resembles the bipartite impedance increase recorded with cortical electrodes. Around this central area is a ring of intermediate impedance increase, which probably represents the skull. It is unclear why the impedance of this region is increased. Possibilities include that there was an increase in skull impedance, or, more probably, that this is blurring secondary to the central impedance peak. Around the edge of the image there is a small impedance increase of about 3%. This could also be secondary to the central impedance increase. However, it appears to be a discrete plateau, and so probably represents a true

impedance increase of the scalp.

2) Images collected *post-mortem*. The images collected with cortical electrodes were similar to those seen during cerebral ischaemia *in vivo*, except that the changes did not reverse and were larger (Fig. 3.26b). *Post-mortem* impedance changes have been investigated with applied current at 1 kHz in rabbit cerebral cortex (Van Harreveld and Ochs, 1956). A resistance increase of 155% was observed 25 min *post-mortem*. The impedance changes were attributed to anoxic depolarization, cooling, draining of fluids such as the cerebrospinal fluid, and emptying of blood vessels. These processes probably caused the increased amplitude of the impedance changes seen in this study.

The EIT images collected with scalp electrodes show an irregular impedance increase after 15 min, which is roughly uniform over the whole image (Fig. 3.26d). During these recordings, unlike those during cerebral ischaemia, scalp temperature was not controlled. At 15 min, it had fallen by about 3 °C. This is likely to have caused a scalp impedance increase of about 4%. The peripheral impedance increase is about 10% after 15 min. Allowing for the temperature effect, this suggests that scalp impedance increased by about 6% as a result of other causes. This is greater than that observed during cerebral ischaemia *in vivo*. However, blood will have drained from the scalp, which may account for the difference. The central impedance changes are irregular and bear no clear resemblance to the *post-mortem* cortical changes. The cause of the irregularity compared to the *in vivo* scalp records is unclear; it may have been due to electrode movement or off-plane substantial scalp impedance changes.

5.3.4. Implications regarding the origin of the impedance changes.

In the EIT images obtained during cerebral ischaemia with scalp electrodes, a peripheral impedance increase is present. Its distribution resembles that obtained when the scalp was warmed by a lamp (Fig. 3.20), and such a peripheral increase is largely absent in the images made *post-mortem* when the impedance of the cranial cavity was altered (Fig. 3.19 and 3.23). It

therefore probably represents scalp. In these images, scalp temperature was kept almost constant, so this suggests that an impedance increase does occur in the scalp as a result of occlusion of the common carotid arteries. The larger peripheral impedance increase in the *post-mortem* record suggests that a temperature change and drainage of blood from the scalp can cause larger impedance increases. A clear and substantially larger change was present centrally, whose initial time course resembled the bipartite nature of the cortical impedance increases.

These observations are made in a small number of preliminary images, and so require validation from a larger study. They suggest that the impedance change recorded from scalp electrodes during cerebral ischaemia will reflect cerebral impedance increases in a central area. They will also reflect impedance increases in the scalp as a peripheral change. The observed changes may explain the absence of a clear bipartite time course in the single channel impedance changes recorded with scalp electrodes, if they include a significant element from the scalp which has a linear time course.

5.3.5. Implications for the clinical use of EIT in detecting cerebral ischaemia non-invasively.

One of the reasons for performing these experiments was to assess if the Sheffield EIT system in its present form appeared suitable for detecting cerebral ischaemia in clinical subjects with scalp electrodes. The calibration results suggest that the brain is represented by a small central area into which any regional changes will be blurred together. It therefore seems most unlikely that this could provide any more information capable of localizing an ischaemic area within the brain than single channel impedance measurement.

5.3.6. Implications for further research.

The main clinical use of EIT would be in non-invasive recording with scalp electrodes. A priority in research is to improve the algorithm so that

images could be collected with satisfactory spatial resolution of intracranial contents. There are several ways in which this could be achieved : 1) Compensation for non-uniform initial conditions could be introduced into a simple algorithm like the one used by the Sheffield system. This could be achieved by inserting prior knowledge of conditions into the algorithm, but this would be inaccurate if these conditions varied in different subjects. The Sheffield algorithm only employs a single iteration. Successive iterations, with progressive adjustment of the equipotential lines might, in theory, produce better spatial resolution. This was observed with a computer phantom (Yorkey and Webster, 1987). 2) The principal problem with any system which introduces current from two electrodes is that central spatial resolution will be worse than at the edges. This may be overcome by injecting currents from multiple electrodes (see Webster, 1990). 3) Various algorithms are available for reconstruction. An analysis of these is outside the scope of this discussion. Yorkey and Webster (1987) compared the performance of six different algorithms using a computer phantom, and concluded that the Newton-Raphson method was superior to the weighted back-projection one used by the Sheffield system. This is an adaptive method, which employs successive iterations to form closer approximations to the object resistivity distribution. 4) The spatial resolution is ultimately limited by the number of independent measurements made from the electrodes. Resolution may therefore, in principle, be increased by increasing the number of electrodes. Barber and Brown (1984) estimated that a maximum spatial resolution of 1% of the electrode diameter could be achieved with the use of 128 electrodes.

The results from this study indicate that, at present, EIT would have the greatest application in localizing single, rapid impedance changes in a homogeneous medium. In the clinical sphere, these conditions would be met if EIT were used with intracranial electrodes to localize an epileptic focus in patients being assessed for curative surgery. For physiological studies in experimental animals, recording with cortical electrodes should be technically feasible. It would be important to develop a reliable means of producing electrode contact with the brain which eliminated movement artefacts, but did

not damage cortex in the process. This may be possible with spring mounted electrodes.

5.4. POSSIBLE APPLICATIONS OF EIT IN NEUROSCIENCE.

The results in the present work have all addressed the possibility of imaging anoxic depolarization. This is a suitable area for initiating an assessment of the use of EIT in neuroimaging, because the impedance changes in brain tissue are large and well characterized and there should be considerable clinical and scientific dividends if EIT could be successfully used to detect anoxic depolarization in the conditions in which it occurs. These include epilepsy and hypoglycaemia, as well as the two conditions used as models in this study.

There are, however, several other physiological and pathological conditions to which EIT might be applied. For these, as for anoxic depolarization, it would be desirable to be able to image non-invasively with scalp electrodes. The present study therefore had a secondary purpose in attempting to estimate how large such other intracranial impedance changes would have to be in order to produce a measurable and reliable signal when recorded with scalp electrodes.

An impedance decrease of about 50% would be expected in intracranial haemorrhage, as the resistivity of blood is about half that of brain (see sections 1.3.2 and 1.3.3). Patients suffering from cerebrovascular disease are at risk from this as well as cerebral ischaemia. EIT could play a useful role in continuous monitoring for both these conditions in the same patient, and should be able to discriminate between them. This could be of particular value in situations when cerebral infarction is secondary to an embolus arising from an extracranial source, such as a diseased heart valve. If the result is ischaemic infarction, then anticoagulation of the blood is needed, in order to prevent further embolus formation; if the result is haemorrhagic, then anticoagulation is contraindicated (Drug & Therapeutics Bulletin, 1983). Premature babies have a high risk of a related and potentially fatal condition,

intraventricular haemorrhage, in which an impedance increase would be expected to occur as cerebrospinal fluid is replaced by blood (Murphy et al, 1987). Early warning of this could alter management. In addition, the neonatal skull is not calcified and has a lower resistivity (see McArdle et al, 1988), so spatial resolution of EIT images should be less affected by recording with scalp electrodes.

In principle, EIT could be used to detect any intracranial pathology whose impedance is different to that of the surrounding brain. This cannot be achieved by the present Sheffield EIT system, as it can only produce comparative images; pathology could only be detected if conditions change during the course of a recording. One way to overcome this problem would be to gate the EIT images to the pulse. The minimum time needed to acquire a minimum data set is 40 msec; two such images corresponding to peak diastole and peak systole can give an index of blood flow. This facility is available with current Sheffield EIT systems, and has been used to produce preliminary images with scalp electrodes in adult human subjects (McArdle et al, 1989). Unfortunately, the impedance changes are at the limit of contrast resolution of the Sheffield system, and it is likely that regional changes would have to be gross before they could be detected against background variation. In the future, it should become possible to produce static images, either with improved hardware and reconstruction algorithms, or by imaging with two frequencies with systems similar to the Sheffield system (Griffiths and Ahmed, 1987). However, it seems unlikely that EIT is ever likely to become a routine tool of clinical investigation of slowly developing intracranial pathologies, because spatial resolution will always be worse than that of X-ray CT scanning or MRI. It may turn out to have an ancillary place if a reasonable spatial resolution could be achieved with measurement with scalp electrodes, and such a system cost substantially less than other imaging methods.

Impedance decreases of a few per cent lasting several seconds have been recorded with deep intracerebral electrodes in the limbic system after physiological stimuli (Adey et al, 1962). Their origin is unclear, but, given their time course, it seems likely that they were related to metabolic recovery

processes, possibly blood flow changes in particular. Measurement of such changes would primarily be of physiological interest, but might provide a means of imaging cerebral activity in much the same way as measurements of blood flow with PET (see Jolles et al, 1989).

In all the above possible applications, the advantages of EIT would be primarily practical. All the changes, or similar closely related ones, may be imaged with greater spatial resolution by other methods. The advantages of EIT would be that it is non-invasive, inexpensive, portable, and could be left in position for repeated measurements over long periods. It also has a greater temporal resolution. Extensive testing in the future will be the only way to determine if these advantages will outweigh its disadvantages of poor spatial resolution, especially if imaging is to be performed with scalp electrodes.

However, there is one potential use for EIT in which it would have a unique advantage over other methods. It is well known that the impedance of neuronal membranes falls substantially during the action potential (Cole and Curtis, 1939). It is therefore likely that the impedance of white or grey matter in the brain will fall during nervous activity, and that this could be imaged by EIT (Holder, 1987). The magnitude of such changes is uncertain. Impedance decreases of about 0.01% which do not appear to be artefactual have been recorded at 1 kHz during auditory evoked responses in the cat (Klivington and Galambos, 1968). Any such changes might be expected to be frequency dependent. No change greater than noise of 0.02% could be recorded at 50 kHz during action potentials in crab nerve (Holder, 1989b). However, a predominant impedance decrease of about 0.2% could be recorded with a steady measuring current when electrodes were placed transversely across the nerve. The changes did not appear to be caused by technical artefacts or latency changes resulting from the measuring current. The advantage of EIT in measuring changes such as these is that it could achieve a temporal resolution of milliseconds. This could be achieved if recordings were made by averaging after a repeated stimulus, in the same way as for conventional visual or somatosensory evoked responses. Each individual data point can be collected in 380 μ sec, so these could be placed in memory "bins" and collected together

as a complete data set after completion of the averaging sequence. This could yield images of functional nervous activity with a temporal resolution which is not available with any other method (see Holder, 1987).

In summary, possible useful applications of EIT in the brain may be classed as follows (approximate impedance changes in the brain follow in parentheses) : 1) Anoxic depolarization or haemorrhage ($\approx 50\%$), 2) Impedance changes related to functional activity with a time course of seconds ($\approx 2\%$), 3) Impedance changes related to depolarization of neuronal membranes during functional activity ($\approx 0.01\%$, possibly $\approx 0.2\%$ if recording with DC is technically possible).

The contrast resolution of the Sheffield EIT system is about 0.1% (Brown et al, 1985). Intracranial recording is likely to be of use only for research purposes in animals, or in exceptional circumstances in humans, when the use of intracranial electrodes can be justified. An example of this is in epileptic patients awaiting surgery, in whom intracranial electrodes have been inserted in order to record the EEG. The boundary potentials generated from cerebral impedance changes will be a complex function of their local amplitude, volume of origin, and the resistivity of intervening tissues. Taking into account the local changes listed for each category of event and the sensitivity of impedance measurement, it seems probable that reasonable EIT images could be produced with intracranial electrodes of anoxic depolarization above with relatively little modification of the Sheffield system. They should have a spatial resolution of the same order - about 20% of the electrode array diameter - as images made in conditions of initially uniform resistivity in this study. Off-plane impedance changes would, of course, contribute to the images and it would be an empirical matter to judge if these images could provide useful information in a given situation. Detection of changes in categories 2 or 3 with intracranial electrodes will depend on the contrast resolution of the imaging system. If the local impedance change is only 2% , then it would have to occupy a relatively large volume of tissue to generate sufficiently large boundary potentials to be reliably measured. Neuronal depolarization could clearly not be imaged with

the present Sheffield EIT system which operates at 50 kHz. However, individual impedance measurements can be made with greater accuracy : with averaging, and AC coupling when measurements were made over tens of milliseconds, baseline noise in recordings at 50 kHz could be reduced to 0.005% or less (Holder, 1989a). If it is possible to increase signal amplitude by recording at lower frequencies, and low noise recording can be achieved by averaging, it is conceivable that images of volley discharges in the CNS might be produced with intracranial electrodes.

The results of this study indicate that no useful imaging with scalp electrodes of intracranial impedance changes, irrespective of size, could be accomplished with the Sheffield system in its present form. If the reconstruction algorithm could be improved to overcome the problem of imaging through the scalp, then the following considerations would apply. This study suggests that an intracerebral signal will be attenuated when measured on the scalp according to the known resistivities of the skull and scalp. If 16 electrodes are equally spaced around the head, the resulting signal will be of the order of 5% if there is a global cerebral impedance increase of about 50% (from experimental results), or 1% if there is a local impedance increase of the same amplitude in adjacent cortex (estimated by the finite element model for SD). These signals will have to be discriminated from a baseline whose variability in anaesthetized animals is about 0.1% over a few minutes under ideal conditions. Movement, changes in local scalp blood flow and temperature, if not controlled, will worsen baseline variability. It may be possible to improve this further by the use of recording at two frequencies. It therefore seems that it might be possible to image changes related to anoxic depolarization or haemorrhage, but it is unlikely that the other smaller changes could be usefully imaged in the near future with scalp electrodes.

5.5. CONCLUSIONS.

1. During global cerebral ischaemia or CSD in the anaesthetized rat, reproducible impedance changes of one to several per cent could be recorded

with scalp electrodes.

2. These changes could be reliably distinguished from baseline variability, which could be reduced to about $\pm 0.1\%$ by the application of pressure and control of temperature.

3. Such changes recorded at ambient temperatures were caused in part by temperature fluctuations in the scalp and adjacent tissues. The relationship was about -1.3% impedance change for a 1°C temperature increase.

4. These changes recorded during global cerebral ischaemia produced by occlusion of the vertebral and common or internal carotid arteries were probably caused in part by impedance changes in the scalp due to local ischaemia.

5. The contribution of cerebral impedance changes caused by cell swelling during anoxic depolarization to impedance measurements on the scalp will depend on electrode spacing. An exact assessment of the contribution of such changes to experimentally observed results was not possible : During CSD, no scalp impedance change was observed when temperature was controlled. This may be attributed to electrode spacing of 0.5 mm. During cerebral ischaemia, scalp impedance increases of several percent were still present when temperature and local scalp effects were removed. The origin of these could not be determined from the experimental data. Results from a finite element model, and their qualitative temporal correspondence with cerebral impedance changes, supported the view that they were due to cell swelling in the brain, but the contribution of impedance changes due to other causes, such as alterations in the skull, meninges, or cerebrospinal fluid, could not be excluded.

6. For repeated episodes of four vessel cerebral ischaemia in the anaesthetized rat, inspired halothane and neuromuscular blockade with artificial ventilation produced better animal survival and blood pressure than halothane alone,

intravenous alphadolone/alphaxolone, or intraperitoneal urethane, all with spontaneous ventilation.

7. The "Sheffield" EIT system is unsuitable for imaging intracranial impedance changes with scalp electrodes. It should be able to provide useful information on the regional distribution of intracerebral events if imaging is performed with cortical electrodes. Spatial resolution will then worsen towards the centre of the image, and off-plane impedance changes may complicate the localization of events.

8. A finite element model in which the brain, skull and scalp were represented as infinite planar layers was consistent with experimental data obtained during cerebral ischaemia or CSD. It predicted that CSD could be detected in the rat if impedance was measured with scalp electrodes spaced 3mm apart.

9. EIT has the practical advantages that it is inexpensive, portable and has a high temporal resolution. Improvements to the reconstruction algorithm used in the Sheffield system are needed if non-invasive imaging of intracranial impedance changes is to be performed with scalp electrodes.

REFERENCES.

Adey W R, Kado R T and Didio J 1962 Impedance measurements in brain tissue of animals using microvolt signals *Exptl. Neurol.* 5 47-66

Altura B M and Weinberg J 1979 Urethane and contraction of vascular smooth muscle *Br. J. Pharmacol.* 67 255-263

Baker M A 1979 A brain-cooling system in mammals *Sci. Am.* 240 114-122

Barber D C and Brown B H 1984 Applied potential tomography *J. Phys. E : Sci. Instrum.* 17 723-733

Barber D C and Brown B H 1988 Errors in reconstruction of resistivity images using a linear reconstruction technique *Clin. Phys. Physiol. Meas.* 9 Suppl. A 101-104

Barber D C and Seagar 1987 Fast reconstruction of impedance images *Clin. Phys. Physiol. Meas.* 8 Suppl. A 47-54

Bederson J B, Pitts L H, Tsuji M, Nishimura M C, Davis R L and Bartkowski H 1986 Rat middle cerebral artery occlusion : evaluation of the model and development of a neurologic examination *Stroke* 17 472-476

Bennet M V L 1969 Electrical impedance of brain surfaces *Brain Res.* 15 584-590

Bostem F, Thibaut A and Hanton J 1982 Rheoencephalography : clinical and neuroradiological correlations *EEG Clin. Neurophysiol.* 35 307-316

British Standard 5724 (Part 1) 1979 Safety of medical electrical equipment (British Standards Institution : London)

Brown B H 1983 Tissue impedance methods *in* Imaging with non-ionizing radiations ed D F Jackson (Surrey University Press) pp 85-110.

Brown B H, Barber D C and Jossinet J (ed) 1988 Electrical impedance tomography - applied potential tomography Clin. Phys. Physiol. Meas. 9 Suppl. A

Brown B H, Barber D C and Tarassenko L (ed) 1987 Electrical impedance tomography - applied potential tomography Clin. Phys. Physiol. Meas. 8 Suppl. A

Brown B H, Barber D C and Seagar A D 1985 Applied potential tomography: possible clinical applications Clin. Phys. Physiol. Meas. 6 109-121

Brown B H and Seagar A D 1987 The Sheffield data collection system Clin. Phys. Physiol. Meas. 8 Suppl. A 91-98

Buelke-Sam J, Holsen J F, Bazare J and Young J F 1978 Comparative stability of physiological parameters during sustained anaesthesia in rats Laboratory Animal Science 28 157-162

Bures J, Buresova O and Krivanek J 1974 The mechanism and applications of Leao's spreading depression of electroencephalographic activity (Academic Press : New York)

Cabanac M 1986 Keeping a cool head N.I.P.S. 1 41-44

Capdeville C, Pruneau D, Allix M, Plotkine M and Boulu R G 1986 Model of global forebrain ischemia in the unanaesthetized rat J. Pharmacol. (Paris) 17 553-560

Carruba M O, Bondiolotti G, Picotti G B, Catteruccia N and Da Prada M 1987

Effects of diethyl ether, halothane, ketamine and urethane on sympathetic activity in the rat *Eur. J. Pharmacol.* 134 15-24

Chapman R W, Santiago T V & Edelman N H 1979 Effects of graded reduction of blood flow on ventilation in unanaesthetized goats *J. Appl. Physiol. : Resp. Environ. Exercise Physiol.* 47 104-111

Child K J, Currie J P, Davis B, Dodds M G, Pearce D R and Twissell D J 1971 The pharmacological properties of CT1341 - a new steroid anaesthetic agent *Br. J. Anaesth.* 43 2-13

Cole K S and Curtis H J 1936 Electric impedance of nerve and muscle *Cold Spring Harb. Symp.* 4 73-89

Cole K S and Curtis H J 1939 Electric impedance of the squid giant axon during activity *J. Gen. Physiol.* 22 649-670

Coombs J S, Eccles J C and Fatt P 1955 The electrical properties of the motoneurone membrane *J. Physiol.* 130 291-

Cuffin N B and Cohen D 1979 Comparison of the MEG and EEG *EEG Clin. Neurophysiol.* 47 132-146

Drug and Therapeutics Bulletin 1983 Treatment in the first 12 hours of stroke 21 21-24

Edelberg R 1971 Electrical properties of skin *in* *Biophysical properties of the skin* ed H R Elden (Wiley-Interscience : New York)

Eisenberg R S and Johnson E A 1970 Three-dimensional field problems in physiology *Prog. Biophys. Molec. Biol.* 20 1-65

Eyuboglu B M, Brown B H, Barber D C and Seagar A D 1987 Localisation of cardiac related impedance changes in the thorax *Clin. Phys. Physiol. Meas.* 8 Suppl. A 1987

Eyuboglu B M and Brown B H 1988 Methods of cardiac gating applied potential tomography *Clin. Phys. Physiol. Meas.* 9 Suppl. A 43-48

Eyuboglu B M, Brown B H and Barber D C 1989 Limitations to SV determination from APT images *IEEE Eng. Med. Biol. Soc. 11th Ann. Int. Conf.* 442-443

Ferris C D 1974 *Introduction to bioelectrodes* (Plenum Publ. Corp. : New York)

Flecknell P A 1987 *Laboratory animal anaesthesia* (Academic Press : London)

Freygang W H and Landau W M 1955 Some relations between resistivity and electrical activity in the cerebral cortex of the cat *J. Cell. Comp. Physiol.* 45 377-392

Furlow T W 1982 Cerebral ischaemia produced by four-vessel occlusion in the rat: a quantitative evaluation of cerebral blood flow *Stroke* 13 852-855

Gamache F W, Dold G M and Myers R E 1975 Changes in cortical impedance and EEG activity induced by profound hypotension *Am. J. Physiol.* 228 1914-1920

Gardner-Medwin A R and Mutch W A C 1984 Experiments on spreading depression in relation to migraine and neurosurgery *An. Acad. Brasil. Cienc.* 56 423-430

Geddes L A and Baker L E 1967 *The specific resistance of biological material - a compendium of data for the biomedical engineer and physiologist* *Med. Biol.*

Eng. 5 271-293

Geddes L A and Baker L E 1968 Principles of applied biomedical instrumentation (John Wiley and Sons : New York) pp. 155-161, 206-239

Green C J, Halsey M J, Precious S and Wardley-Smith B 1978 Alphaxolone-alphadolone anaesthesia in laboratory animals *Laboratory Animals* 12 85-89

Greene E C 1963 Anatomy of the rat (Hafner Publ. Co. : New York)

Griffiths H and Ahmed A (1987) A dual-frequency applied potential tomography technique: computer simulations *Clin. Phys. Physiol. Meas.* 8 Suppl. A 103-107

Hansen J H and Olsen C E 1980 Brain extracellular space during spreading depression and ischemia *Acta. Physiol. Scand.* 108 355-365

Harris N D, Suggett A J, Barber D C and Brown B H 1987 Applications of applied potential tomography (APT) in respiratory medicine *Clin. Phys. Physiol. Meas.* 8 Suppl. A 155-165

Harris N D, Suggett A J, Barber D C and Brown B H 1988 Applied potential tomography : a new technique for monitoring pulmonary function *Clin. Phys. Physiol. Meas.* 9 Suppl. A 79-85

Hayashi F, Yoshida A, Fukuda Y & Honda Y 1983 The ventilatory response to hypoxia in the anesthetized rat *Pflügers Archiv.* 396 121-127

Hodgkin A L 1947 The membrane resistance of a non-medullated nerve fibre *J. Physiol.* 106 305-318

Hodgkin A L and Rushton W A H 1946 The electrical constants of a crustacean

nerve fibre Proc. Roy. Soc. Lond. B 133 444-479

Hoffman C J, Clark F J and Ochs S 1973 Intracortical impedance changes during spreading depression J. Neurobiol. 4 471-486

Holder D S 1987 Feasibility of developing a method of imaging neuronal activity in the human brain: a theoretical review Med. Biol. Eng. Comput. 25 2-11

Holder D S 1989a Impedance changes during evoked nervous activity in human subjects : implications for the application of applied potential tomography (APT) to imaging neuronal discharge Clin. Phys. Physiol. Meas. 10 267-274

Holder D S 1989b Changes in impedance during the action potential in isolated crab nerve : implications for applied potential tomography (APT) of neuronal discharge J. Physiol. 415 56P

Hosek R S, Sances A, Jodat R W, Larson S J 1978 The contributions of intracerebral currents to the EEG and evoked potentials IEEE Trans. Biomed. Eng. BME-25 405-413

Hossman K 1971 Cortical steady potential, impedance and excitability changes during and after total ischaemia of cat brain Exp. Neurol. 32 163-175

Jenkner F L 1962 Rheoencephalography (Charles C Thomas : Springfield, Illinois)

Jolles P R, Chapman P R and Alavi A 1989 PET, CT , and MRI in the evaluation of neuropsychiatric disorders : current applications J Nucl. Med. 30 1589-1606

Jorgensen M B and Diemer N H 1982 Selective neuron loss after cerebral

ischemia in the rat: possible role of transmitter glutamate *Acta Neurol. Scand.* 66 536-546

Klivington K A and Galambos R 1968 Rapid resistance shifts in cat cortex during click-evoked responses *J. Neurophysiol.* 31 565-573

Kosterich J D, Foster K R and Pollack S R 1983 Dielectric permittivity and electric conductivity of fluid saturated bone *IEEE Trans. Biomed. Eng. BME* 30 81-86

Kuffler S W and Potter D D 1964 Glia in the leech central nervous system : physiological properties and neuron-glia relationship *J. Neurophysiol.* 27 290-320

Kulkarni V, Hutchison J M S, Ritchie I K and Mallard J R 1990 Impedance imaging in upper arm fractures *J. Biomed. Eng.* 12 219-227

LaManna J C, McCracken K A, Patil M and Prohaska O 1987 Brain tissue temperature: activation-induced changes determined with a new multisensor probe *Adv. Exp. Med. Biol.* 222 383-389

Lamont G L, Wright J W, Evans D F and Kapila L A 1988 An evaluation of applied potential tomography in the diagnosis of infantile hypertrophic pyloric stenosis *Clin. Phys. Physiol. Meas.* 9 Suppl. A 65-70

Lauritzen M 1987 Cerebral blood flow and cortical spreading depression *Acta. Neurol. Scand.* 76 (Suppl. 113) 9-40

Lauritzen M and Olesen J 1987 Leao's spreading depression in Migraine : Clinical, therapeutic, conceptual and research aspects ed J N Blau (Chapman and Hall : London)

Li C, Bak A F and Parker L O 1968 Specific resistivity of the cerebral cortex and white matter *Exp. Neurol.* 20, 544-557

Liu W P, Hua P and Webster J G 1988 Three dimensional reconstruction in electrical impedance tomography *Clin. Phys. Physiol. Meas.* 9 Suppl. A 131-136

MacKnight A D and Leaf A 1977 Regulation of cellular volume *Physiol. Rev.* 57 510-573

Mangnall Y F, Baxter A J, Avill R, Bird N C, Brown B H, Barber D C, Seagar A D, Johnson A G and Read N W 1987 Applied potential tomography : a new non-invasive technique for assessing gastric function *Clin. Phys. Physiol. Meas.* 8 Suppl. A, 119-130

Matsuoka Y and Hossman K 1982 Cortical impedance and extracellular volume changes following middle cerebral artery occlusion in cats *J. Cereb. Bl. Flow Metab.* 2 466-474

McArdle F J, Brown B H Pearse R G and Barber D C 1988 The effect of the skull of low-birthweight neonates on applied potential tomography imaging of centralised resistivity changes *Clin. Phys. Physiol. Meas.* 9 Suppl. A 55-60

McArdle F J, Brown B H and Angel A 1989 Imaging resistivity changes of the adult brain during the cardiac cycle *IEEE Eng. in Med. Biol.* 11th Ann. Int. Conf. 480-481

Monakhov K K, Fifkova E and Bures J 1962 Vertical distribution of the slow potential change of spreading depression in the cerebral cortex of the rat *Physiol. Bohemoslov.* 11 269-276

Murphy D, Burton P, Coombs R, Tarassenko L and Rolfe P 1987 Impedance imaging in the newborn *Clin. Phys. Physiol. Meas.* 8 Suppl. A 131-140

Nair V, Palm D and Roth L J 1960 Relative vascularity of certain anatomical areas of the brain and other organs of the rat *Nature* 188 497-498

Nedergaard M 1988 Mechanisms of brain damage in focal cerebral ischaemia *Acta. Neurol. Scand.* 77 81-101

Nedergaard M and Hansen A J 1988 Spreading depression is not associated with neuronal injury in the normal brain *Brain Res.* 449 395-398

Nicholson P W 1965 Specific impedance of cerebral white matter *Exp. Neurol.* 13 386-401

Paxinos G and Watson C 1982 *The rat brain in stereotaxic coordinates* (Academic Press : Sydney)

Pelligrino D, Almqvist L and Siesjö B K 1981 Effects of insulin-induced hypoglycaemia on intracellular pH and impedance in the cerebral cortex of the rat *Brain Res.* 221 129-147

Prys-Roberts C, Gersh B J, Baker A B and Reuben S R 1972 The effects of halothane on the interactions between myocardial contractility, aortic impedance, and left ventricular performance 1 : Theoretical considerations and results *Br. J. Anaesth.* 44 634-649

Pulsinelli W A and Brierly J B 1979 A new model of bilateral hemisphere ischaemia in the unanaesthetized rat *Stroke* 10 267-272

Pulsinelli W A and Buchan A M 1988 The four vessel occlusion rat model : method for complete occlusion of vertebral arteries and collateral circulation *Stroke* 19 913-914

Ranck J B 1963a Specific impedance of rabbit cerebral cortex *Exp. Neurol.*

7 144-152

Ranck J B 1963b Analysis of specific impedance of rabbit cerebral cortex *Exp. Neurol.* 7 153-174

Ranck J B 1964 Specific impedance of cerebral cortex during spreading depression and an analysis of neuronal, neuroglial and interstitial contributions *Exp. Neurol.* 9 1-16

Rayport M, Sandler B and Katzman R 1966 Observations on the passive electrical properties of cat brain *EEG Clin. Neurophysiol.* 20 513-519

Romanes G J (ed.) 1973 *Cunninghams's textbook of anatomy* 11th ed. (OUP: London)

Rush S and Driscoll D A 1968 Current distribution in the brain from surface electrodes *Anaesth. Analg.* 47 717-723

Shevelev I A, Kuznetsova G D, Gulyaev Y V, Godik E E, Petrov A V, Taratorin A M, Tsykalov E N, Koroleva V I, Budko K P and Gorbach A M 1986 Dynamic thermal mapping of rat brain during sensory stimulation and spreading depression *Neirofiziologiya* 18 26-35

Siesjö B K 1990 Calcium, excitotoxins, and brain damage *N.I.P.S.* 5 120-125

Todd N V, Picozzi P, Crockard A and Ross Russell R 1986 Reperfusion after cerebral ischaemia : influence of duration of ischaemia *Stroke* 17 460-466

Tropp J S, Sugiura S, Derby K A, Suzuki Y, Hawryszko C, Yamagata H, Klein J E, Ortendahl D A, Kaufman L and Acosta G F 1988 Characterization of MR spectroscopic imaging of the human head and limb at 2.0 T. *Radiology* 169 207-212

Van der Meer C, Versluys-Broers J A M, Tuynman H A R E and Buur V A J 1975 The effect of ethylurethane on haematocrit, blood pressure and plasma glucose Arch. Int. Pharmacodyn. 217 257-275

Van Harreveld A 1972 The extracellular space in the vertebrate nervous system *in* The structure and function of nervous tissue Vol 4 ed G H Bourne (Academic Press : New York) pp 449-511

Van Harreveld A and Ochs S 1956 Cerebral impedance changes after circulatory arrest Amer. J. Physiol. 187 180-192

Van Harreveld A and Ochs S 1957 Electrical and vascular concomitants of spreading depression Amer. J. Physiol. 189 159-166

Van Harreveld A and Schadé J P 1962 Changes in the electrical conductivity of cerebral cortex during seizure activity Exp. Neurol. 5 383-400

Von Hanwehr R, Smith M and Siesjö B K 1986 Extra- and intracellular pH during near-complete forebrain ischaemia in the rat J. Neurochem. 46 331-339

Vickers M D, Wood-Smith F G and Stewart H C 1983 Drugs in anaesthetic practice, 5th ed. (Butterworths : London) pp. 44-46

Webster J G Electrical 1990 Impedance Tomography (Adam Hilger : Bristol)

Weindling A M, Murdoch N and Rolfe P 1982 Effect of electrode size on the contributions of intracranial and extracranial blood flow to the cerebral impedance plethysmogram Med. Biol. Eng. Comput. 20 545-549

Weiss T R, Kado R T and Adey W R 1966 Impedance and DC potential shifts during cortical spreading depression Activ. Nerv. Sup. 8 194-195

Yamamoto T and Yamamoto Y 1976 Electrical properties of the epidermal stratum corneum *Med. Biol. Eng. Comput.* 14 151-158

Yorkey T J and Webster J G 1987 A comparison of impedance tomographic reconstruction algorithms *Clin. Phys. Physiol. Meas.* 8 Suppl. A 55-62

GLOSSARY OF ABBREVIATIONS

The following abbreviations have been used in more than one section in the text.

AC	Alternating current
CSD	Cortical spreading depression
CT	X-ray computerised tomography
δZ	Impedance change
D1 and 2	Two electrodes used for measuring impedance through which constant current is passed.
DC	Direct current
EIT	Electrical impedance tomography
FWHM	Full width at half maximum
NMR	Nuclear magnetic resonance
MRI	Magnetic resonance imaging
PD	Potential difference
PET	Positron emission tomography
R1 and 2	Two electrodes used for recording potential during impedance measurement
SD	Spreading depression. The term "standard deviation" is used occasionally. To avoid confusion, it is spelt in full or the abbreviation "S.D." in a table or figure is defined in adjacent text.
SE	Standard error of the mean
SPECT	Single photon emission computed tomography

All results are presented as mean \pm SE.